NATIONAL ENERGY TECHNOLOGY LABORATORY

COOLED GAS TURBINE AND COMBINED CYCLE ANALYSIS FOR NH_3-CH_4 FUEL MIXES (UP TO 100% NH_3)



October 30, 2024

DOE/NETL-2024/4522

Disclaimer

This project was funded by the United States Department of Energy, National Energy Technology Laboratory, in part, through a site support contract. Neither the United States Government nor any agency thereof, nor any of their employees, nor the support contractor, nor any of their employees, makes any warranty, express or implied, or assumes any legal liability or responsibility for the accuracy, completeness, or usefulness of any information, apparatus, product, or process disclosed, or represents that its use would not infringe privately owned rights. Reference herein to any specific commercial product, process, or service by trade name, trademark, manufacturer, or otherwise does not necessarily constitute or imply its endorsement, recommendation, or favoring by the United States Government or any agency thereof. The views and opinions of authors expressed herein do not necessarily state or reflect those of the United States Government or any agency thereof.

All images in this report were created by NETL, unless otherwise noted.

Selcuk Can Uysal[1,2]*: Methodology, Software, Validation, Formal Analysis, Investigation, Data Curation, Writing – Original Draft, Writing – Review & Edit, Visualization;* ***Sandeep Pidaparti***[1,2]*: Formal Analysis, Validation, Writing – Original Draft, Writing – Review & Edit;* ***Charles W. White***[1,2]*: Validation;* ***Mark C. Woods***[1,2]*: Supervision, Resources;* ***Travis R. Shultz***[2]*: Conceptualization, Resources,* ***Robert W. Stevens***[2*]*: Supervision, Project Administration, Funding Acquisition*

[1]National Energy Technology Laboratory (NETL) support contractor
[2]NETL
*Corresponding contact: Robert.Stevens@netl.doe.gov, 304.285.4305

Suggested Citation:
Uysal S.C., "Cooled Gas Turbine and Combined Cycle Analysis for NH_3-CH_4 Fuel Mixes (up to 100% NH_3)," National Energy Technology Laboratory, Pittsburgh, 2024.

This page intentionally left blank.

TABLE OF CONTENTS

ACRONYMS AND ABBREVIATIONS III
EXECUTIVE SUMMARY V
1 INTRODUCTION 1
2 AMMONIA COMBUSTION AND COMBUSTOR TYPE FOR LOW NOX 4
2.1 Combustion Kinetics for Low NOx Ammonia Oxidation 4
2.2 NOx emissions Abatement for Ammonia Fuel Combustion 5
2.3 Two-Stage Combustion for Low NOx Ammonia Combustors 6
2.4 Preliminary Combustion Analysis and Fuel Mixtures 7
3 AMMONIA FUEL GAS TURBINE DESIGN 12
3.1 Analysis Tool 12
3.2 Design Point Analysis 12
3.3 Turbomachinery Design 13
3.3.1 Flexible Fuel Operation Strategy 13
3.3.2 Component Designs 14
3.4 Turbine Cooling Design 21
3.4.1 Coatings 21
3.4.2 Internal Cooling Effectiveness 23
3.4.3 Film Cooling Effectiveness 23
3.4.4 Turbine Cooling Configuration 24
3.5 Cooled Gas Turbine Performance and Sensitivity Analysis 24
3.5.1 Cooled Gas Turbine Performance 24
3.5.2 Sensitivity Analysis 27
4 AMMONIA FUEL COMBINED CYCLE PERFORMANCE ANALYSIS 34
4.1 Steam Cycle Design 34
4.2 Ammonia Fuel Combined Cycle Performance Results 35
5 COST ANALYSIS FOR AMMONIA FUEL COMBINED CYCLE 42
5.1 Ammonia Fuel Cost 42
5.2 Ammonia Fuel Combined Cycle Capital Costs Calculation 44
5.3 Levelized Cost of Electricity, Owner's Costs and Operating Costs 45
5.4 Levelized Cost of Electricity Sensitivity Analysis 49
5.4.1 Ammonia Fuel Cost Sensitivity 49
5.4.2 Capacity Factor Sensitivity 50
6 CONCLUSION 52
7 REFERENCES 54
APPENDIX A: STREAM TABLE FOR 100% AMMONIA FUEL CASE 57
APPENDIX B: CAPITAL COSTS FOR AMMONIA COMBINED CYCLE 60

ACRONYMS AND ABBREVIATIONS

°F	Degrees Fahrenheit
K	Degrees Kelvin
°R	Degrees Rankine
AFCC/ACC	Ammonia fuel combined cycle
AFGT	Ammonia fuel gas turbine
AGR	Acid gas removal
AIST	The National Institute of Advanced Industrial Science and Technology
atm	Atmospheres
Bi	Biot number
BOP	Balance of plant
Btu	British thermal unit
CC	Combined cycle
CCS	Carbon capture and storage
CFD	Computational fluid dynamics
CGTM	Cooled Gas Turbine Model
CH_4	Methane
CMSX	Canon-Muskegan
CO	Carbon monoxide
CO_2	Carbon dioxide
DLN	Dry low NOx
DOE	Department of Energy
EBC	Environmental barrier coating
Eng'g CM	
H.O.& Fee	Engineering construction management, home office, and fees
FEB	Fossil Energy Baseline
AFGT	Ammonia fuel gas turbine
FM	Fuel Mixture
GE	General Electric
GJ	Gigajoules
gpm	Gallons per minute
GT	Gas turbine
GW	Gigawatt
h, hr	Hour
H_2	Hydrogen
HCC	Hydrogen combined cycle
HHV	Higher heating value
HRSG	Heat recovery steam generator
IGV	Inlet guide vanes
kg	Kilogram
kJ	Kilojoule
kW, kWe	Kilowatt electric
kWh	Kilowatt-hour
kWt	Kilowatt thermal
lb	pound
lbm	Pound-mass
LCOE	Levelized cost of electricity
LHV	Lower heating value
m	Meter
m^3/min	Cubic meter per minute
MM	Million
MMBtu	Million Btu
MW, MWe	Megawatt electric
MWh	Megawatt-hour
N_2	Nitrogen
NETL	National Energy Technology Laboratory
NG	Natural gas
NGCC	Natural gas combined cycle
NH_3	Ammonia
NO	Nitric oxide
NOx	Oxides of nitrogen
O_2	Oxygen
OGV	Outlet guide vanes
ORNL	Oak Ridge National Laboratory
ppm	Parts per million
ppmvd	Parts per million by volume-dry
PR	Pressure ratio
psi	Pounds per square inch
psia	Pound per square inch absolute
QGESS	Quality Guidelines for Energy System Studies
rpm	Revolutions per minute
RQL	Rich-Quick Mix-Lean
s	Second
SCR	Selective catalytic reduction
ST	Steam turbine
T&S	transport and storage
TASC	Total as-spent costs
TBC	Thermal barrier coating

TOC	Total overnight costs	UK	United Kingdom
Ton	1000 kg	U.S.	United States
TPC	Total Plant Cost	USA	United States of America
UC Berkeley	University of California Berkeley		

EXECUTIVE SUMMARY

In this study, a cooled gas turbine (GT) analysis was conducted for varying levels of ammonia (NH_3) blends with methane. The ultimate goal is to have a gas turbine design that can be used for all the fuel blends (including 100% NH_3) without any changes to the system. The technological developments in the cooling system, gas turbine design, and materials that will be required for NH_3 combustion were identified and analyzed in this study to develop an advanced gas turbine design for NH_3 fuels. The study includes a combined cycle performance analysis with the NH_3 fuel blends using the advanced gas turbine design developed in this study. A techno-economic analysis was conducted for analyzing the impact of the NH_3 fuels on the levelized cost of electricity and cost sensitivities to fuel price and capacity factor.

A two-stage combustor design was selected for the gas turbine design for ammonia fuels, to have minimum oxides of nitrogen (NOx) and higher combustion efficiency. A combustion analysis was performed using an in-house analysis software for two-stage combustors [17] to determine NOx amounts at the combustor outlet, combustor design specifics, and combustor exhaust compositions for different fuel mixtures and equivalence ratios. For all ammonia fuel mixtures, selected combustor design gives less than 20 parts per million (ppm) NOx (at 15% oxygen [O_2]) at the combustor outlet.

Composition of fuel mixtures considered in this study are listed in Exhibit ES-1. Mix 1 corresponds to the lowest amount of ammonia mixing. Mix 5 is the 100 percent ammonia fuel case by fuel mass fraction. The two-stage combustor technology does not require diluents to reduce the combustor exit NOx emissions, therefore no diluent mixing is considered.

Exhibit ES-1. Fuel mixtures determined for the study (molar fractions are given)

Mixture Name	NH_3%	CH_4 %
Mix 1	20%	80%
Mix 2	40%	60%
Mix 3	60%	40%
Mix 4	80%	20%
Mix 5	100%	0%

The Cooled Gas Turbine Model (CGTM) was used in this study to design and do a performance analysis for a gas turbine that supports all of the fuel mixes identified for this study. Single gas turbine design is aimed to support all of the fuel mixes and is referred to as ammonia fuel gas turbine (AFGT). The design point of this engine was selected to be very similar to current H-Class natural gas fuel using engines, because NH_3 fuel does not need higher firing temperatures than natural gas firing temperature for low NOx and high efficiency, and to have similar engine size with current levels for reducing manufacturing costs and complexity.

The design point of the AFGT design is presented in Exhibit ES-2. A turbomachinery design analysis was conducted, and the design details are also presented in Exhibit ES-2.

Exhibit ES-2. Design point and turbomachinery design details of compressor and turbine for AFGT designs

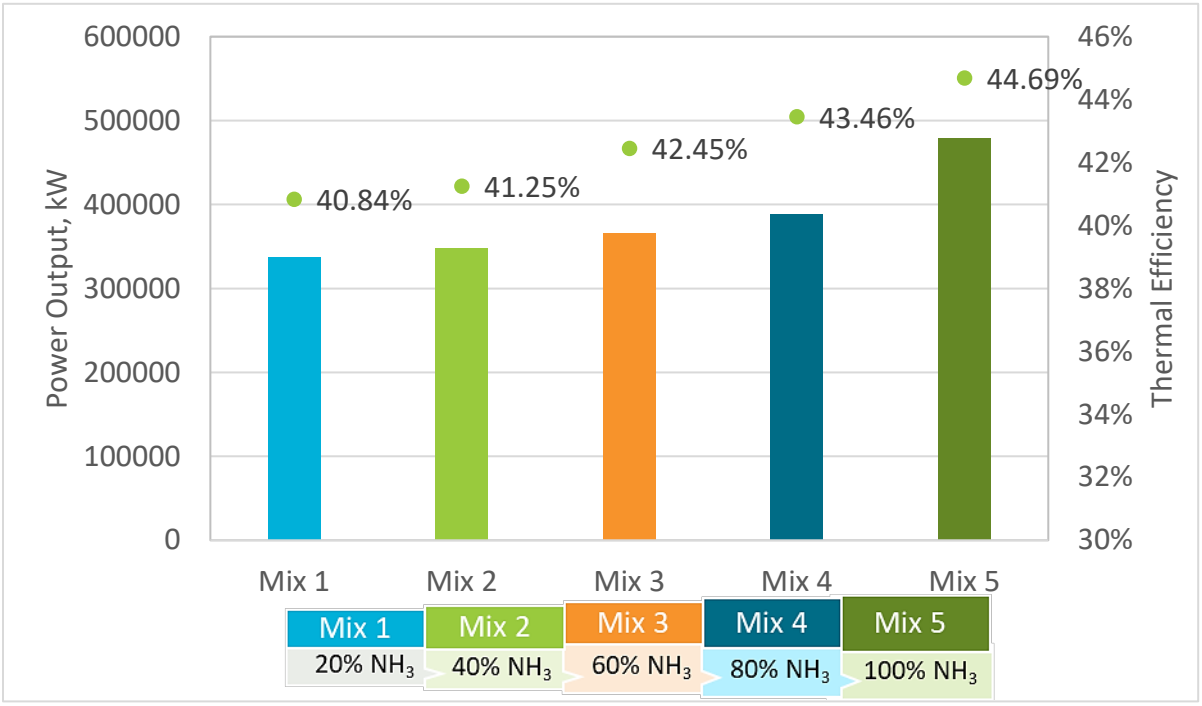
Parameter	Value
Engine Inlet Flowrate	1523 lbm/s
Compressor	
Pressure Ratio	23.1
Blade Material	INCOLOY-909
Disk Material	UDIMET-720
Diffusion Factor	0.5
Blade Turning Angle	16.8°
Efficiency	86.4%
Number of Stages	14
Turbine	
Inlet Temperature	3260 °R (2800 °F)
Stage Loading	1.2
Degree of Reaction	0.499
Flow Turning Angle	27.5°
Blade Material	CMSX-7
Disk Material	UDIMET-720
Number of Stages	5

Similar to F- and H-Class gas turbines, shaft and disk cooling will be needed for AFGT design. The gas turbine design was made for 100 percent ammonia fuel case, and other fuel mixture cases are turn down cases for the gas turbine. Therefore, a single inlet air flowrate (1523 lbm/s) is used in AFGT for all fuel mixture cases. Presence of steam in the turbine flow path increases corrosion and oxidation risks, which requires the use of advanced coatings. For the fuel mixtures containing methane, the turbine inlet flow density does not change significantly from 100 percent ammonia fuel case, which makes it possible to use compressor outlet guide vanes to adjust the necessary flow speed changes for the turbine section.

After finalizing the turbomachinery design, the cooled gas turbine performance of AFGT was calculated using CGTM. Properties of the selected materials from turbomachinery design were used from their manufacturer's datasheets. The Biot numbers of the blade metal and thermal barrier coating (TBC) were calculated by using empirical formulas. Internal cooling and film cooling effectiveness values were based on the performance data of the advanced cooling features from previous modelling data [19] and advanced gas turbine literature [21,22]. The cooling configuration is based on the current H-Class gas turbine technology.

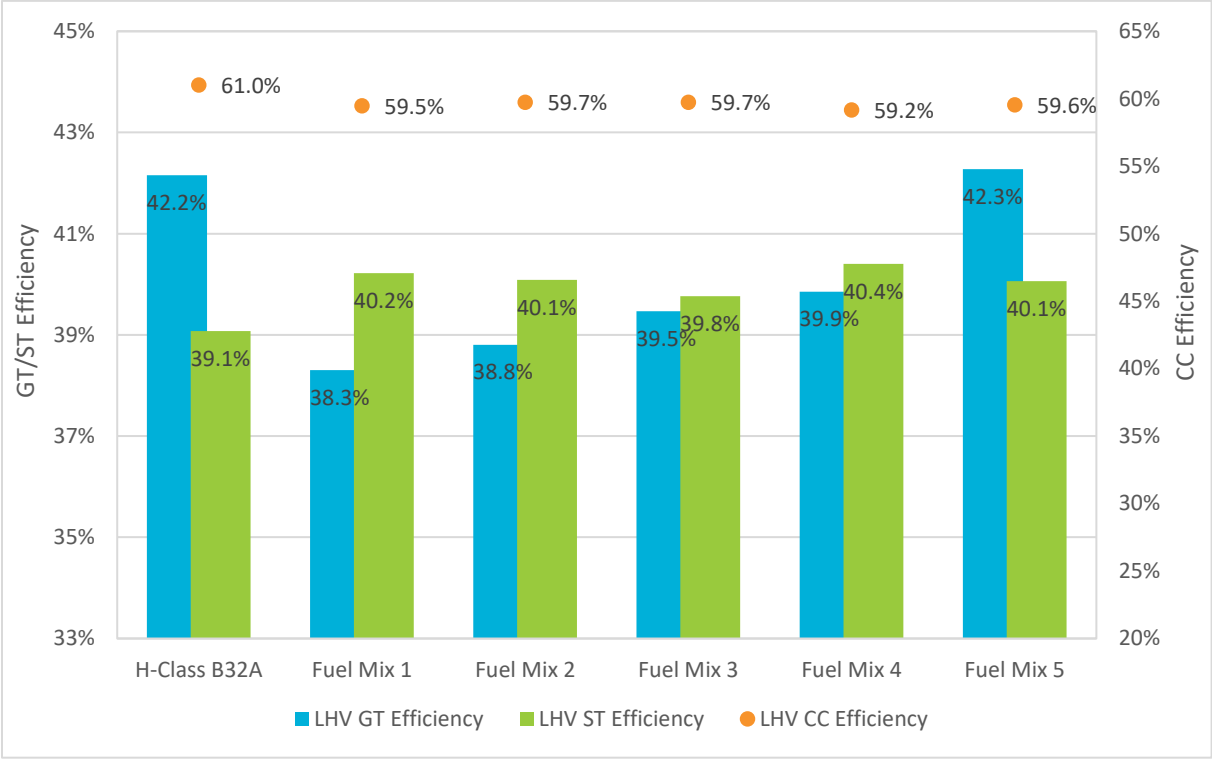
Key gas turbine performance metrics such as power output, thermal efficiency, and heat rate are calculated for AFGT. For all fuel mixture cases, the cooled performance of AFGT is comparable to current F- and H-Class natural gas fuel engines. For AFGT design, power output and thermal efficiency are calculated and compared for each fuel mixture case in Exhibit ES-3.

Exhibit ES-3. Cooled Gas Turbine Performance results of AFGT



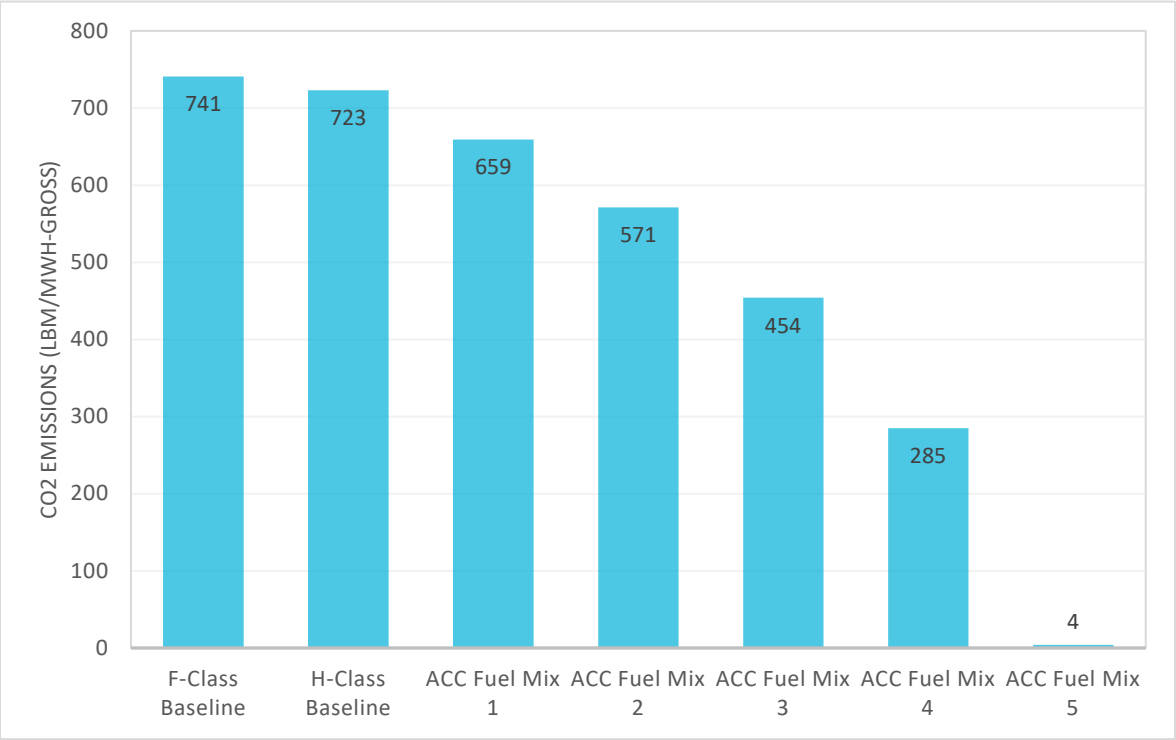
For the ammonia combined cycle analysis, natural gas combined cycle (NGCC) revision 4 B32A ASPEN Plus model [31] was used. The gas turbine inside this model was modified to match the AFGT design specifications. The lower heating value (LHV) cycle efficiency outputs from the ammonia combined cycle cases are compared with each other and to B32A NGCC levels in Exhibit ES-4.

Exhibit ES-4. Ammonia Combined Cycle efficiency comparison with B32A levels



The carbon dioxide (CO_2) emissions of the ammonia combined cycle are compared for each fuel mix case and to NETL baseline H- and F-Class values in Exhibit ES-5.

Exhibit ES-5.Carbondioxide emissions from AFCC cycles with H-Class and F-Class levels



The advantage of using ammonia in the fuel mix shows clearly for all of the ammonia fuel combined cycle (AFCC) cases. For the case with 100 percent NH_3 fuel, the carbon dioxide emissions are negligible, and comparable with NGCC with carbon capture systems.

A preliminary techno-economic analysis was conducted for AFCC cases for calculating the levelized cost of electricity (LCOE), owner's costs, operating costs, and cost sensitivities on ammonia fuel price and capacity factor. The LCOE values calculated for ammonia combined cycle cases are compared with each other and to F- and H-Class NETL baseline values (without CCS) in Exhibit ES-6. Exhibit ES-7 compares the 100% NH_3-fired AFCC case with H-Class NGCC plants with 90%, 95% and 97% CO_2 capture. For these cases, NH_3 fuel price is assumed to be \$0.39/kg (\$0.3/kg for NH_3 production + \$0.09/kg for NH_3 transportation) and the natural gas fuel price for all the cases is \$4.42/MMBtu. The LCOE of 100% NH_3 case is ~2x the LCOE of H-class NGCC plant with 97% CO_2 capture. One of the major outcomes is that the advanced AFCC design considered in this study can be cost competitive with state-of-the-art H-class NGCC plants with carbon capture, if NH_3 fuel cost is lower than 4.31 \$/MMBtu (about \$83/ton). Significant research and development (R&D) is needed to bring the ammonia fuel cost down from today's price levels (19.7 \$/MMBtu) to make ammonia an alternative fuel for gas turbines for power generation.

Exhibit ES-6. LCOE comparison of AFCC cases with NGCC without CCS for ammonia fuel cost of 0.39 $/kg (includes 0.3 $/kg of production cost + 0.09 $/kg of transportation cost)

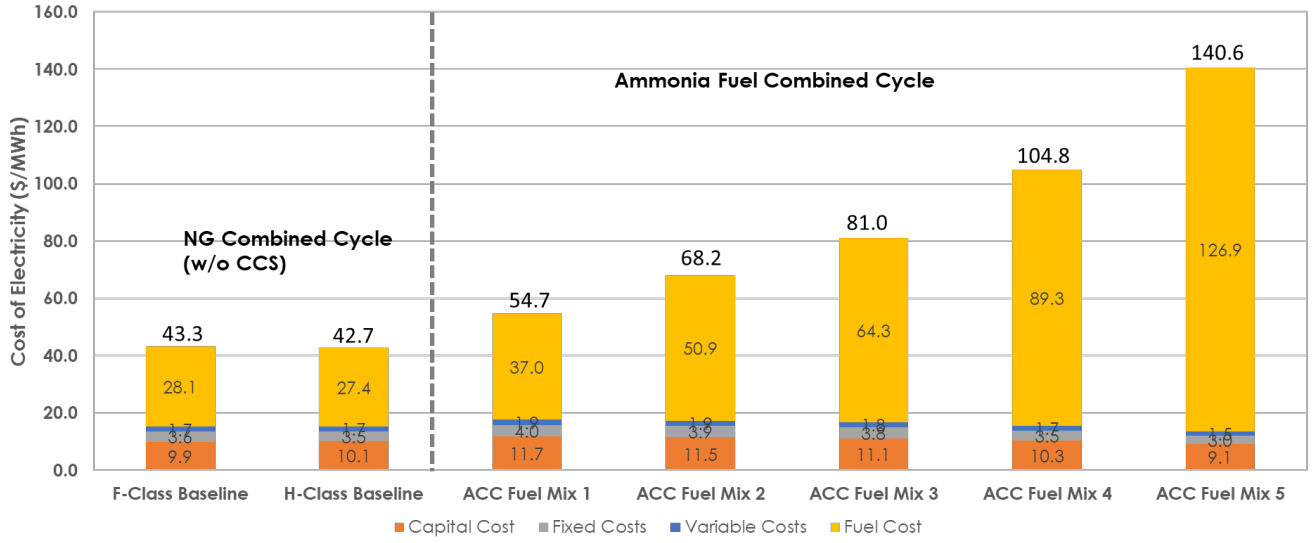
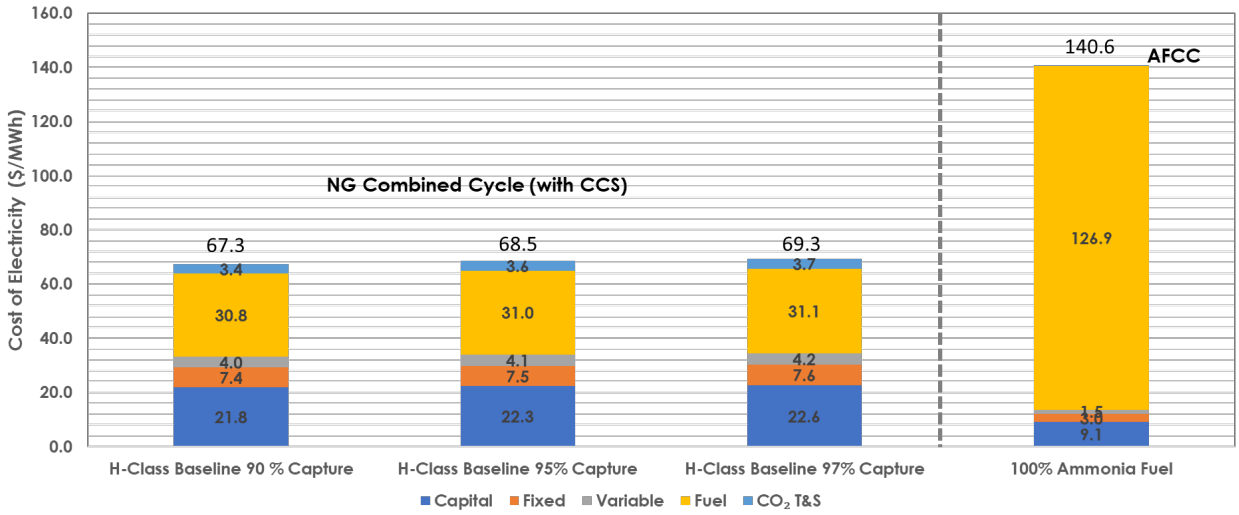


Exhibit ES-7. LCOE comparison of AFCC cases with NGCC with CCS for ammonia fuel cost of 0.39 $/kg (includes 0.3 $/kg of production cost + 0.09 $/kg of transportation cost)



1 INTRODUCTION

Ammonia has recently been reconsidered as a gas turbine fuel. Ammonia is considered an alternative fuel for reducing carbon emissions because the combustion of ammonia produces zero carbon emissions. The current production methods used for ammonia, however, are not carbon free. The Haber-Bosch process emits carbon emissions but efforts to reduce the emissions of the production methodologies are also underway [1]. Overall, ammonia is considered a good initial alternative to molecular hydrogen because of its availability, lower costs associated with production (traditional methods) and transportation, and for being a hydrogen carrier.

One of the benefits of ammonia over hydrogen is that its production and transportation infrastructure already exists, because ammonia is extensively used in the fertilizer industry. For instance, ammonia pipeline infrastructure already exists in the United States (U.S.), which primarily covers the Midwest and East Coast [2].

One of the biggest advantages of ammonia fuel over hydrogen or natural gas is that it can be stored as liquid at ambient temperature, without needing excessive pressurization (~200 psia is needed) [1]. It can be transported through pipelines, railroads, ships, and trucks with easier and cheaper storage technologies. Compared to natural gas, the compression and refrigeration costs are lower. Aside from its cost, the main reason for considering ammonia over hydrogen is the extensive knowledgebase in production, transportation, storage, safe handling, and emergency procedures.

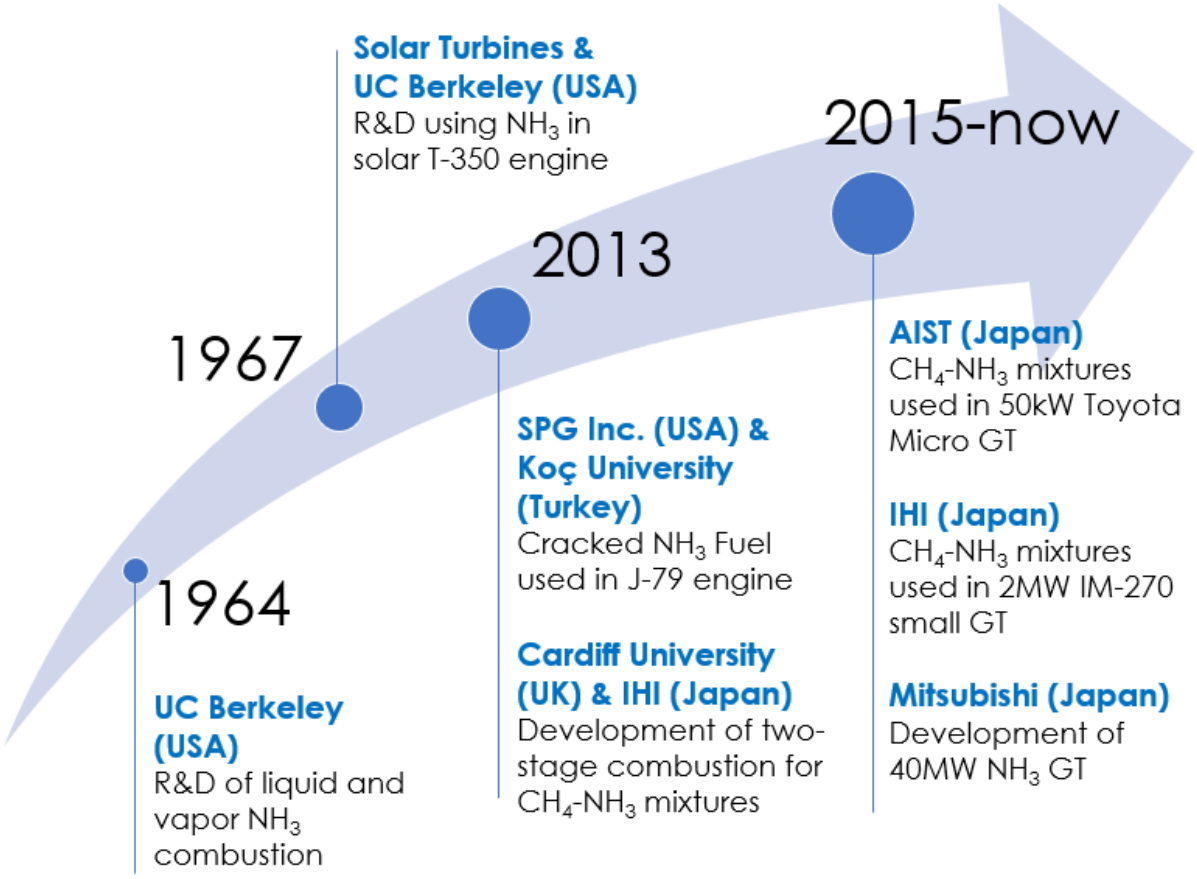
Aside from being a promising carbon-free fuel, ammonia has several challenges. Pure ammonia-air combustion has low flame velocity, which inhibits flame stability and leads to low combustion efficiency. Combustion also yields high nitrogen oxides (NOx) emissions in lean fuel conditions and unstable combustion regimes exist that make combustor efficiency low and operation difficult [3]. The laminar burning velocity of pure-ammonia air combustion is much lower than conventional fuels [4]. Knowledge gaps for ammonia combustion research are identified as follows [5]:

- Develop burner designs to achieve stable flames
- Reduction of NOx emissions
- Reduction of unburned ammonia

Eliminating the unburned ammonia from gas turbine exhaust is very important because it poses a toxicity risk.

The chronology of ammonia gas turbine developments in the open literature are schematized in Exhibit 1-1.

Exhibit 1-1. Schematization of ammonia gas turbine developments



In 1964, research and development of liquid and vapor ammonia combustion was done at the University of California (UC) Berkeley. In 1967, a Solar Turbines T-350 engine was used for the experimental analysis of ammonia in a gas turbine. Low combustion efficiencies and high NOx emissions caused the technology to be abandoned [6]. In 2013, with the increased need for reducing carbon emissions from several agencies and governments, ammonia fuel got reconsideration. SPG Inc. in the United States and Koc University in Turkey used cracked ammonia fuel in J-79 turbojet engine [1]. Also, during 2013, Cardiff University in the United Kingdom (UK) and IHI in Japan developed a two-stage combustor technology for ammonia-methane fuel mixtures [7]. In recent years, the National Institute of Advanced Industrial Science and Technology (AIST), in Japan, used ammonia-methane fuel mixtures in a micro gas turbine rated for 50 kW. The operation was successful, and it proved there was potential, but to reduce the NOx emissions, large selective catalytic reduction (SCR) systems were required [8]. IHI in Japan also demonstrated a successful operation of ammonia-methane fuel mixture in a 2MW small gas turbine. Similarly, large-scale SCR systems were needed to reduce the exhaust NOx to permissible levels [9]. Mitsubishi is currently working to develop a 40 MW scale ammonia gas turbine [10].

NETL funded several external projects for ammonia combustion analysis. The first NETL funded project is from Creative Power Solutions in Arizona and was completed in 2020 [11]. An ongoing

study funded by NETL, the "Investigation of Ammonia Combustion for Turbines," is carried out by the Gas Turbine Institute. The second recent project is "Low-NOx Operable Ammonia Combustor Development for Zero Carbon Power" and is carried out by Raytheon [12]. Phase reports and presentations from these projects were used in the combustion analysis section of this study.

Ammonia as a gas turbine fuel was first studied in 1964, and early experiments showed that liquid ammonia combustion has unacceptably low efficiency due to its low flame speed. The experiments continued with vapor ammonia, which yielded higher combustion efficiency compared to the liquid form. The tests were made in UC Berkeley and used a turbojet engine. One of the outcomes of early studies was to mix ammonia with methane to increase the combustion efficiency [6].

Due to the low combustion efficiencies and lower fossil fuel costs at the time, the idea of using ammonia as a gas turbine fuel was abandoned until 2013. In recent studies, ammonia cracking is used to further enhance combustion efficiency. However, cracking systems use electrolyzers with Nickel based catalysts, which are expensive even for small scale gas turbines. Cracking also requires low flowrates that are not suitable for gas turbines [1]. In later years, a two-stage combustor technology was developed in which the ammonia is partially cracked in the first stage. Two-stage combustors use a fuel-rich mixture for initial combustion, and the products are re-combusted with a fuel lean mixture on the second stage [8].

The adiabatic flame temperature of ammonia is about 300 °F lower than natural gas, which brings several advantages in terms of gas turbine design. Firing temperatures used in current gas turbines will be adequate for ammonia-methane fuel mixtures, therefore changes to turbine cooling and the design changes from current technology levels will be minimal. The biggest design challenge for the ammonia gas turbine is to have low exhaust NOx emissions, because these will be higher than conventional gas turbines unless special combustors and capturing techniques are employed. The test results made with a micro gas turbine using a conventional combustor showed around 200 ppm (at 16% oxygen [O_2]) NOx at exhaust [8], and the tests with a small gas turbine with stock combustor showed 500 ppm (at 16% O_2) NOx at the exhaust. [9] Both are in the limits of current SCR technologies; however, special combustor technologies are required for ammonia fuel to be a feasible option for large frame gas turbines.

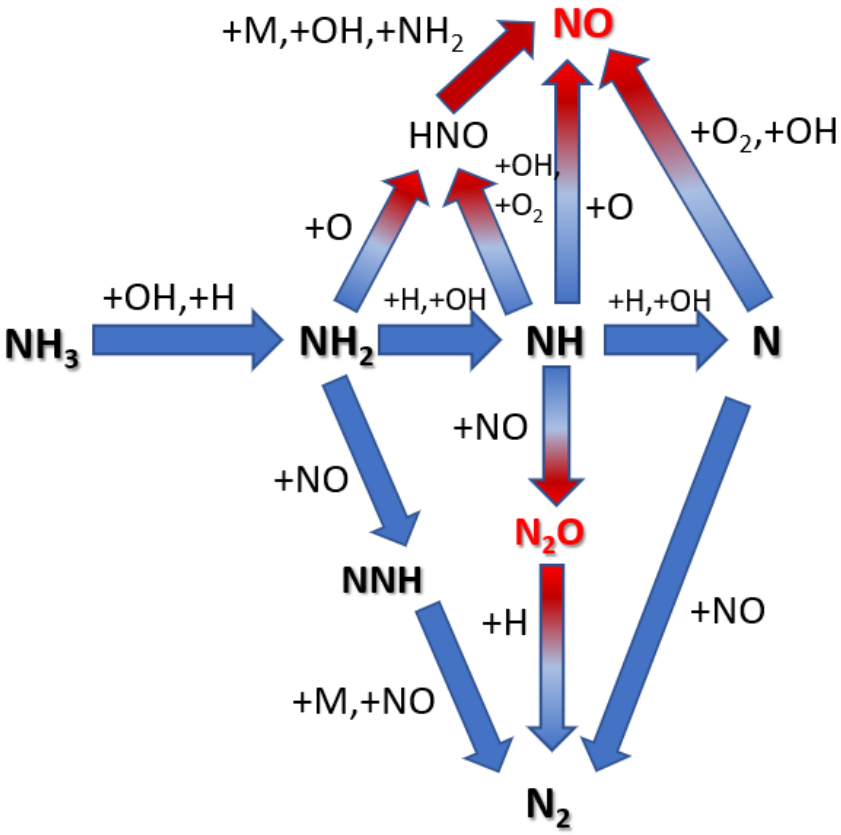
In this study, the cooled gas turbine analysis was made for varying levels of ammonia blends with methane. The technological developments in the cooling system, gas turbine design, and materials that are required for ammonia combustion were identified and analyzed in this study to develop an advanced gas turbine design. The combined cycle performance with the ammonia fuel blends using the advanced gas turbine design was performed next. The study concluded with a techno-economic analysis including the impact of using ammonia fuel on the levelized cost of electricity. This report includes the details of each part of the ammonia gas turbine and combined cycle analysis.

2 AMMONIA COMBUSTION AND COMBUSTOR TYPE FOR LOW NOX

2.1 COMBUSTION KINETICS FOR LOW NOX AMMONIA OXIDATION

The most critical components in ammonia combustion are the NOx elements, and the combustion systems using ammonia fuels should be designed to minimize the NOx amounts from the combustion. The ammonia oxidation pathway is schematized in Exhibit 2-1.

Exhibit 2-1. Ammonia oxidation pathway schematization; +M represent metal catalysts



Lean ammonia flames have high nitric oxide (NO) concentration, which peaks around equivalence ratio of 0.9, due to the abundant O and H radicals. Addition of carbon monoxide (CO) (through the combustion of methane or natural gas in the fuel mixture), to lean ammonia (NH_3), NO, O_2, and nitrogen (N_2) mixture results in an increase in NO production, because of increased O and H radicals in the combustion (via HNO route). However, addition of carbon dioxide (CO_2) to stoichiometric ammonia-methane-air flames results in a significant decrease in NO production due to the depletion of the O and H radicals as the CO_2 is consumed to form CO [13,14].

Under all conditions, the HNO intermediate channel is the dominant NO production path in ammonia-air flames. Lower concentration of O and H in rich flames, leads to lower NO

production. The O and H radical concentration decreases as the flame becomes richer, but the relative concentration of H in the O/H radical pool in the flame increases. This increases the tendency for NH_2 and NH_3 to be oxidized through reactions with H atoms, leading to substantial hydrogen (H_2) production mainly from NH_2, and ultimately to the production of N atoms. Relative abundance of N atoms in rich flames promotes the set of reactions known as "extended Zeldovich Mechanism." This mechanism is also known as thermal-NO production and involves the reactions in Equation (1).

$$\begin{aligned} &N_2 + O \leftrightharpoons NO + N \\ &N + O_2 \leftrightharpoons NO + O \\ &N + OH \leftrightharpoons NO + H \end{aligned} \qquad (1)$$

In ammonia flames, the extended Zeldovich mechanism is active even at low temperatures, as opposed to hydro-carbon fuel combustion. The reaction of NO with NH, NH_2, and NH_3 leads to the reduction of NO to N_2. These reduction reactions are promoted under rich flame conditions and certain temperature range and O_2 concentrations (thermal de-NOx) [14].

The primary consumption step of ammonia remains essentially unaltered as pressure increases, even though the O and H radicals are depleted with an increase in pressure. As combustor pressure is increased, NO reduction mechanism is increased, yielding to lower NOx [14].

2.2 NOx emissions Abatement for Ammonia Fuel Combustion

In hydrocarbon combustion, the use of lean pre-mixed flames is one of the most promising gas turbine combustion techniques to meet the strict legislative limits on combustion pollutant emissions.

Lean turbulent premixed flames burn at lower temperature and have lower velocity than stoichiometric flames, which leads to combustion instability. To stabilize lean premixed flames, swirling is used in gas turbine combustors to create an inner recirculation with a low velocity zone and thus enhances flame anchoring. Recent numerical and experimental studies showed that recirculating flow upstream of the combustor results in more stable combustion of ammonia-air flames under high turbulence intensity and pressure [14].

For ammonia combustion, fuel NO generation can be significantly reduced when using rich flames at high pressure. Studies showed that there is a specific equivalence ratio in rich equivalence ratio (for every pressure condition) at which NO and unburned NH_3 emissions are at minimum. For combustor inlet temperature of 500K, the specific equivalence ratio (Φ_{sp}) for minimum NOx is 1.2, and for inlet temperature of 300K the specific equivalence ratio for minimum NOx is 1.05. Therefore, for an H-Class gas turbines combustor inlet conditions, this specific equivalence ratio is estimated to be 1.1.

The effect of pressure on unburned ammonia emission is also significant; at a specific equivalence ratio of 1.2, an increase in pressure from 0.1 to 0.5 MPa leads to a reduction in the ammonia emission from 700 ppm to 200 ppm (mole fraction) [14].

Experimental studies showed that ammonia-air flames can be stabilized over a wide range of inlet flow speeds and equivalence ratios, without the need for additives or diluents [15].

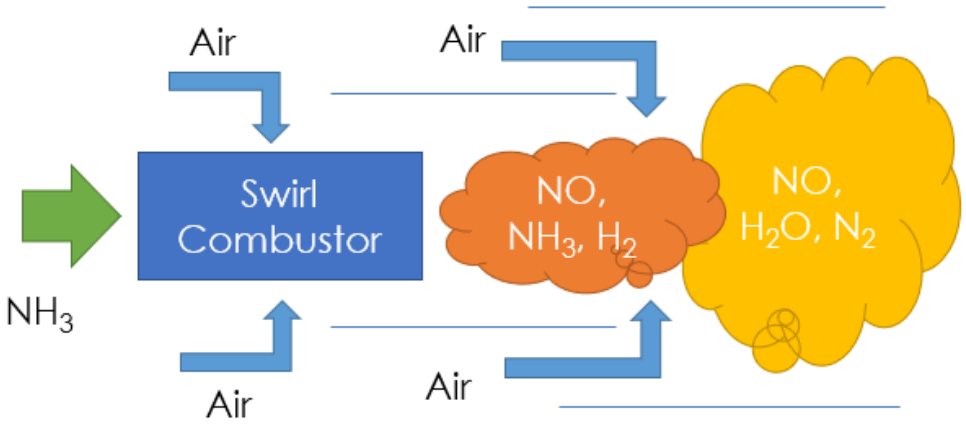
2.3 Two-Stage Combustion for Low NOx Ammonia Combustors

A combustor type that can satisfy the combustion stability, low NOx and unburned NH_3 at the exhaust and higher combustion efficiency is sought by researchers. Rich burn conditions are advantageous for ammonia combustion for the combustion stability and low NOx (see Sections 2.1 and 2.2). Rich burn of ammonia promotes ammonia cracking, where hydrogen is generated as a product (Equation (2)).

$$2NH_3 \rightarrow N_2 + 3H_2 \qquad (2)$$

To take advantage of the generated hydrogen, a secondary combustion zone is needed. This zone can be run with lean ammonia fuel, as the primary purpose of this section would be to use the generated hydrogen and reduce the NO emissions further. A swirl combustor needs to be used in the first stage to increase combustion stability and enhance flame holding. The concept of two-stage combustors for ammonia fuels is schematized in Exhibit 2-2.

Exhibit 2-2. Two-stage combustion concept for ammonia fuel



In the two-stage combustor, the equivalence ratio of the first stage (primary zone) should be equal to the specific equivalence ratio, Φ_{sp} from the previous section to have minimal NO and unburned NH_3. Under rich fuel conditions, the exhaust of the primary zone contains unburned ammonia. When the unburned ammonia from the primary zone enters into the second stage (secondary zone), additional NO formation occurs but the unburned ammonia is consumed entirely.

Two-stage combustors are a type of Rich-Quick Mix-Lean (RQL) combustors, which were specifically developed in the 1980's for low NOx emissions from aircraft engines [16]. These combustors use a fuel rich mixture for initial combustion, and the products are re-combusted with lean fuel mixture on the second stage. Using such combustors for ammonia fuel will crack

the ammonia partially in the first stage, which increases the combustion efficiency and reduces the NOx formation.

An experimental combustor was developed in AIST that uses a modified RQL combustor for ammonia combustion analyses [8]. In the experimental combustor, the circumference of the liner base plate is corrugated, creating gaps between the liner and the base plate. Air injection holes in the circumference allow for air injection to the primary and secondary zones. In the experiments, significantly lower NOx at exhaust is observed when the swirler area is partially closed, there is avoidance of any sort of air dilution in primary zone, and fuel-air mixing is enhanced by use of inclined fuel injection. Reported combustor efficiency for the two-stage combustor is 99.5%, when the primary zone equivalence ratio is 1.1 and at combustor pressure ratio of 0.3 MPa. Reported NOx emissions from this experiment were 42 ppm (at 16% O_2).

The advantages of the two-stage combustors can be listed as follows: it's a proven technology that was used in aircrafts and it supports ammonia combustion per the experimental studies made with small gas turbines in Japan [8]. These combustors can reduce NOx amounts significantly, especially in gas turbine combustor inlet conditions. These combustors do not need diluents to reduce NOx, which reduces the complexity of the gas turbine and steam cycle design. The disadvantages of this technology are the requirement for advanced cooling and coatings materials and combustor length is longer than typical natural gas burning combustors for land-based applications.

2.4 PRELIMINARY COMBUSTION ANALYSIS AND FUEL MIXTURES

For the ammonia fuel gas turbine of this study, two-staged combustor technology is selected due to its stability, reducing the NOx emissions satisfactorily and ease of operation for ammonia fuels. Another motivation in selecting this technology is that it does not need diluents to reduce the NOx emissions. A combustion analysis program for two-stage combustors using ammonia-methane fuel mixtures was developed at NETL [17]. The program uses chemical analysis library CANTARA with a Python code interface. The program was validated with experimental data from Li et al. [18].

The analysis code has two versions. The first version finds the optimum rich zone equivalence ratio for the lowest NOx emissions, and the second version calculates the exhaust compositions for a given equivalence ratio, inflow conditions and exhaust temperature. Program inputs are listed as follows:

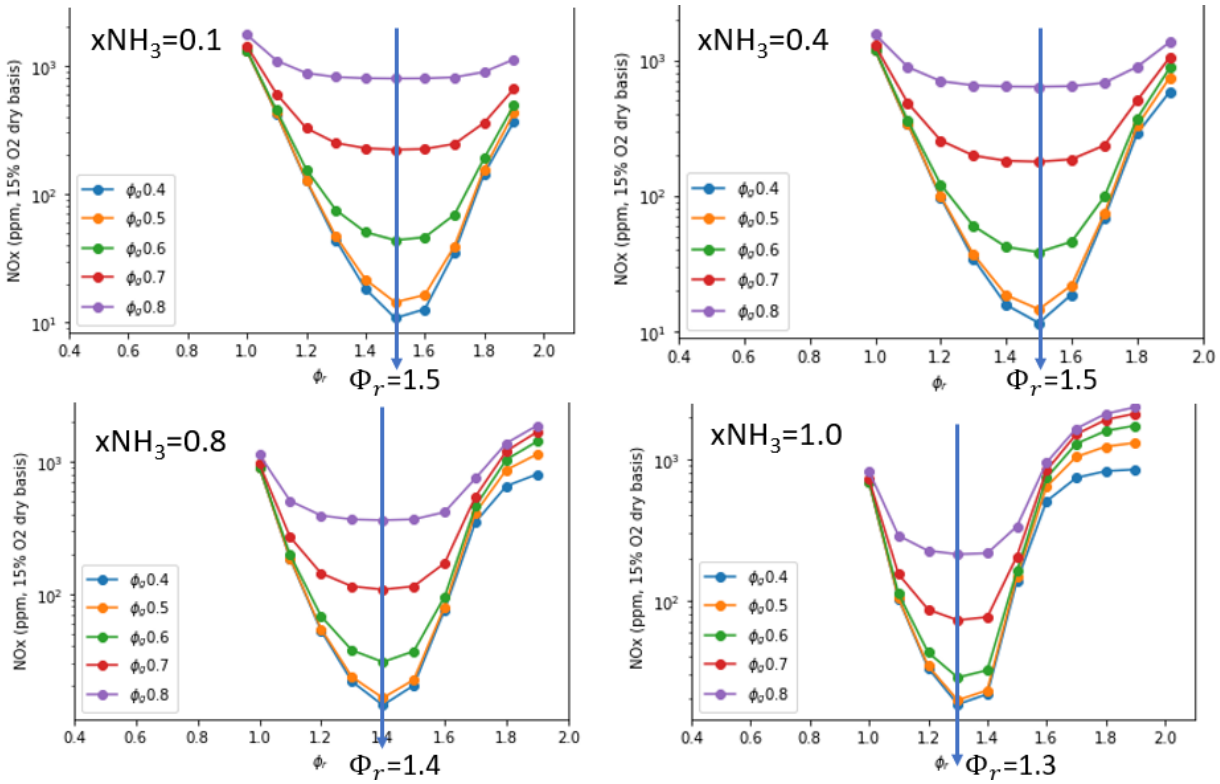
- Inlet air temperature and pressure
- Global equivalence ratio
- Rich stage equivalence ratio
- Methane (CH_4) or H_2 mole fractions in NH_3 fuel mixture
- Plug flow area
- Rich stage recirculating flame zone and post flame zone residence times
- Lean stage post flame residence time

The combustion analysis was performed by finding the optimum rich stage equivalence ratio for different ammonia fractions in methane fuel. Equivalence ratio is the fraction of the used fuel-to-air ratio to stoichiometric value. In the analysis, combustor inlet conditions are used as 794 K and 24 atm, which are representative of H-Class gas turbine compressor exit conditions. The first version of the combustion analysis program was used for various ammonia fractions from 10 percent to 100 percent, to find each cases optimum equivalence ratios. Then for each ammonia fraction, the second version of the program was used with the optimum equivalence ratio to generate the combustor exit flow compositions. Exit flow compositions are first checked for NOx emission amounts and then used to generate thermodynamic property datasets that will be used in Cooled Gas Turbine Model (CGTM) and ASPEN Plus combined cycle model.

Other program inputs such as the plug flow area and residence times are used from the experimental study configuration in AIST [8] and from the program defaults [17]. Plug flow area is used as 2.5E-3 m^2, rich stage recirculating flame zone residence time is used as 1.4E-2 seconds, post flame zone residence time is used as 1E-3 seconds, and lean stage post flame residence time is used as 2E-3 seconds in the analysis.

Calculated optimum rich stage equivalence ratios for minimum NOx emissions are shown in Exhibit 2-3 for selected ammonia fractions in methane fuel for different overall equivalence ratios.

Exhibit 2-3. Optimum rich stage equivalence ratios (Φ_r) found for different overall equivalence ratios (Φ_o)



The overall equivalence ratio is the arithmetic average of the rich and lean stage combustion zones equivalence ratios. As the ammonia fraction is increased in the methane fuel, optimum rich stage equivalence ratio for minimum NOx reduces. However, stoichiometric fuel to air ratio for ammonia fuel mixtures increases as the ammonia fraction is increased in the mixture.

Based on combustion analysis and NOx performances, the fuel mix cases were identified as presented in Exhibit 2-4. Mix 1 corresponds to the lowest amount of ammonia mixing and consists of 21 percent ammonia by mass. The fraction of ammonia is increased by 20 percent for each consequent mixture case. Mix 5 is the 100 percent ammonia fuel case.

Exhibit 2-4. Compositions of the identified fuel mixtures for the study (molar fractions are given)

Mixture Name	NH_3%	CH_4 %
Mix 1	20%	80%
Mix 2	40%	60%
Mix 3	60%	40%
Mix 4	80%	20%
Mix 5	100%	0%

For identified fuel mixture cases, the optimum combustor design conditions and corresponding NOx emissions for each case are calculated and presented in Exhibit 2-5.

Exhibit 2-5. Combustor design conditions for different fuel mixture cases

	Rich Stage Equivalence Ratio	Combustor Exit Temperature [F]	Secondary Air to Primary Air Ratio	Stoichiometric Fuel-to-Air Ratio (Mass basis)	NOx [ppm]	NOx [ppmvd]
Mix 1	1.5	2800	2.04	0.068	12.0	13.4
Mix 2	1.5		1.99	0.080	12.6	13.9
Mix 3	1.5		1.92	0.097	14.6	15.8
Mix 4	1.4		1.66	0.123	15.5	16.4
Mix 5	1.3		1.39	0.165	19.6	20.3

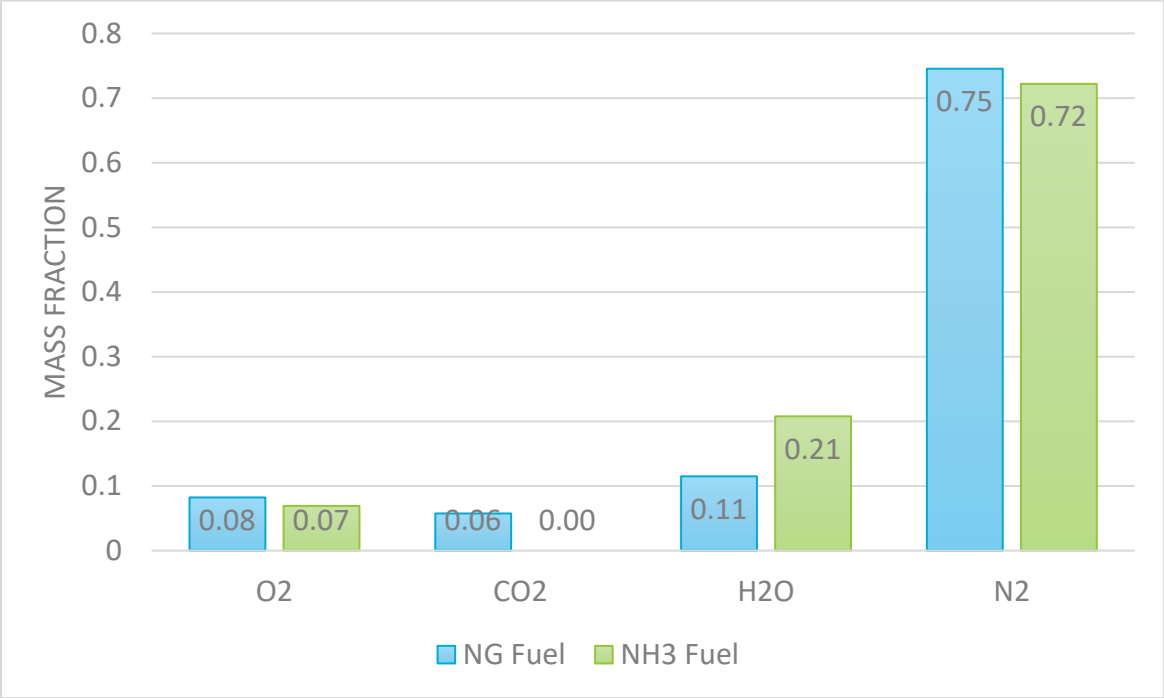
As the ammonia fraction is increased in the fuel, the stoichiometric fuel to air ratio increases, which translates to increasing fuel flowrate as the ammonia fraction is increased. The combustor exit temperature is the same as current H-Class gas turbine levels. The NOx emissions calculated for each case are within the current SCR technology limitations. As the ammonia fraction is increased in the mixture, the NOx emissions increase from 12 to 20 ppm.

The Cooled Gas Turbine Model is used in the gas turbine design and performance analysis. This program is developed for natural gas fuel gas turbine analysis and validated with public engine data [19]. CGTM requires some thermodynamic properties such as enthalpy, entropy, heat

capacity, specific heats ratio, and speed of sound for the combustion exhaust gases to perform the analysis. Aspen Properties Desktop was used with "IDEAL" property method for property analysis. ASPEN Properties is run for each fuel mix combustion exit composition.

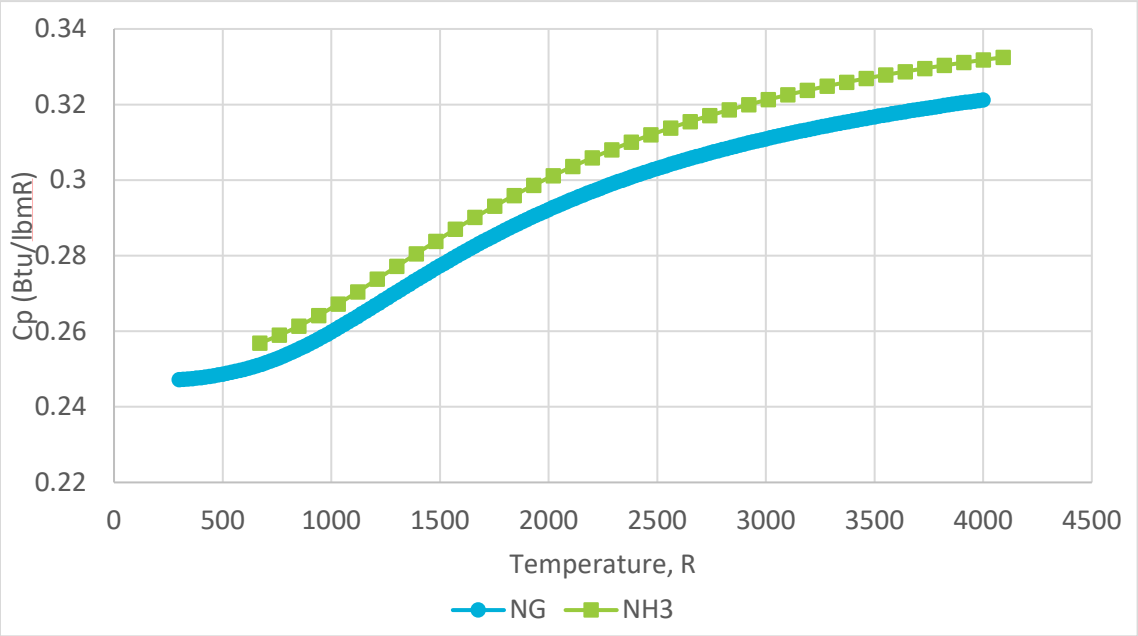
The combustor exhaust compositions are compared for natural gas and 100 percent ammonia fuel in Exhibit 2-6. High fractions of ammonia fuel mixtures combustion produce significantly lower CO and CO_2.

Exhibit 2-6. Selected combustor exhaust components comparison for different fuel mixture cases at GT exhaust conditions made for natural gas and ammonia fuel



Higher water content in the exhaust composition causes higher heat transfer coefficients and eventually higher heat transfer rates at the turbine. The impact of the higher water content can be seen in the comparison made for specific heat capacities calculated for natural gas and 100 percent ammonia fuel cases in Exhibit 2-7.

Exhibit 2-7. Specific heat capacities at constant pressure are compared for natural gas and 100% ammonia fuel cases for combustor exhaust



3 AMMONIA FUEL GAS TURBINE DESIGN

In this part of the study, the design point of the ammonia fuel gas turbine (AFGT) was determined, turbomachinery design of the engine was performed, the cooling design of the engine was made, and the cooled performance was calculated. Finally, a sensitivity analysis was conducted to investigate the impact of various cooling parameters on gas turbine performance metrics. The details of the design study are presented in the following subsections.

3.1 ANALYSIS TOOL

CGTM was used in this study to design and complete a performance analysis for a gas turbine that supports all of the fuel mixes identified for this study. CGTM was developed for natural gas fuel gas turbines and has the following features [19]:

- On-design and off-design gas turbine performance calculations
- Turbomachinery design section to perform a mean-line turbomachinery design
- Cooled turbine model that can calculate the impacts of cooling-related turbine losses in performance calculations
- Compressor model with coolant extraction losses

CGTM requires thermodynamic properties for the combustion exhaust gases to perform the analysis. ASPEN Properties is run for each fuel mix combustion exit composition. The exit compositions are taken from the two-stage combustor analysis program [17] results for the combustion analysis (see Section 2).

Ammonia fuel gas turbine data for large-frame gas turbines do not exist in the literature; microturbine lab-scale data are not representative for large gas turbine (GT) conditions. Therefore, a side-to-side comparison of CGTM's results with ammonia fuel mixtures is not currently possible.

3.2 DESIGN POINT ANALYSIS

In this study, the single gas turbine design is aimed to support all of the fuel mixes identified in the previous parts of this study.

Selecting a design point involves selecting the compressor pressure ratio, turbine inlet temperature, and engine inlet flowrate to find the optimums for the power output, thermal efficiency, and exhaust temperature.

The design point of the AFGT is selected to be similar to current H-Class natural gas fuel gas turbines. The reasonings for this selection are as follows:

- NH_3 fuel does not need higher firing temperatures than natural gas firing temperatures for low NOx and high efficiency
- Similar engine size with current levels would reduce manufacturing costs and complexity

- Minimizing the changes from the current technologies would reduce the engine's capital cost and maintenance costs, which increases the engine's market acceptance

Features of this design include having similar turbine inlet temperature with H-Class gas turbine levels (2800 °F); therefore, minimal to no changes to turbine cooling technologies will be needed from H-Class levels. However, some changes will be needed in the turbomachinery design of the turbine section.

The specifics of the design point of this engine are listed in Exhibit 3-1.

Exhibit 3-1. AFGT engine design point specifications

Design Specs	Value				
	Mix 1	Mix 2	Mix 3	Mix 4	Mix 5
Compressor PR	23.1				
Inlet Flowrate	1523 lbm/s				
Compressor Temperature Ratio	6.18				
Fuel-to-Air Ratio	0.03	0.04	0.05	0.06	0.08
Turbine Inlet Temperature	2800 °F (3260 °R)				
Turbine Pressure Ratio	0.0492				
Turbine Exit Temperature	1240 °F	1238 °F	1233 °F	1231 °F	1207 °F

3.3 TURBOMACHINERY DESIGN

3.3.1 Flexible Fuel Operation Strategy

Having a single gas turbine design for various fuels is a common application, but typical flex fuels for natural gas engines are diesel, kerosene, and syngas. The fuel options of this study have very similar lower heating values and densities. The operation strategies for flexible fuel operation are listed as follows [20]:

- Change the engine speed
- Adjust the inlet flowrate by compressor inlet guide vanes (IGVs) or outlet guide vanes (OGV)
- Change the firing temperature

In this study, the firing temperature and engine inflow rate were constrained, to ensure the maximum power output and efficiency for all fuel mixture cases. This operation preference leaves two operation options: changing the engine speed or changing the turbine inflow speed and direction.

Analyses made showed that the required turbine inlet flowrate change is not very high such as in the hydrogen gas turbine. Ammonia gas turbine can use compressor outlet guide vanes to handle the required flow changes to the turbine when the fuel mixture is changed. The rpm change is also not considered, since the OGV operation can easily handle the required flow changes. The reason for avoiding the engine speed change is to minimize the generator transmission losses, which would be higher if the gas turbine is run at a different speed than 3600 rpm.

3.3.2 Component Designs

3.3.2.1 Compressor Design

The turbomachinery design process started with the compressor design. AFGT requires the same compression ratio as a typical H-Class gas turbine. When switching between different fuel mixtures, the AFGT turbine section requires the flow speed to change slightly due to the changes in the flow composition and heat transfer rates. The required flow speed Mach number change is 0.005, which can easily be handled with current compressor outlet guide vane technology. The mass flowrate for AFGT is similar to H-Class gas turbine levels; therefore, blade heights will be similar to H-Class compressors.

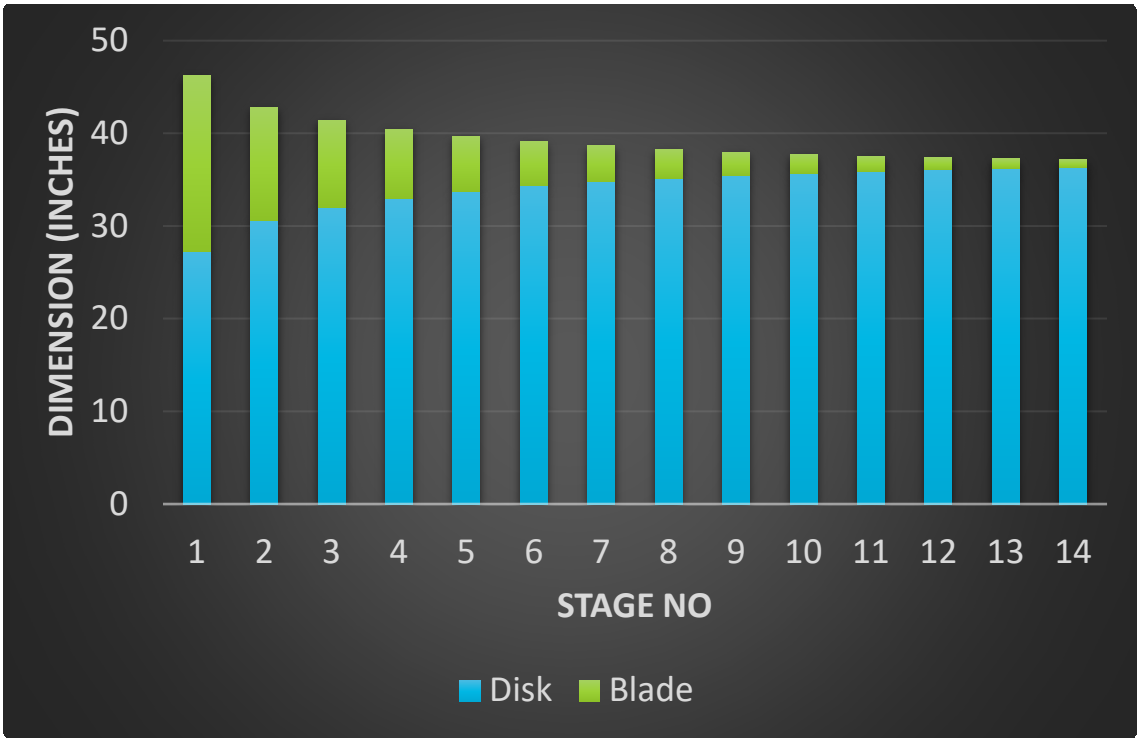
The critical material properties that were considered in material selection to reduce the listed issues in new compressor design for AFGT are as follows:

- Maximum metal temperature, density
- High cycle fatigue resistance
- 1 percent creep rupture strength at 1000 h
- Ultimate tensile strength
- Corrosion resistance
- Available as forged stock bar

Nickel alloys were selected over stainless-steel alloy materials to support future engine growth requiring higher inlet flowrates and to have higher stress and heat resistance. Stainless-steels have a limitation on use for high mass flowrates, which comes from the stress limits being exceeded when the blades get longer. This practical limit for the mass flowrate is around 1540 pound-mass per second, which can be reached easily when the engine is upgraded later per customer needs.

The turbomachinery design section of the CGTM was used to perform the mean-line design of the compressors for each engine. The compressor design for AFGT is presented in Exhibit 3-2.

Exhibit 3-2. Compressor design of AFGT



Some of the design specifics of the compressor are listed in Exhibit 3-3.

Exhibit 3-3. AFGT engine compressor design specifics

Parameter	Value
Pressure Ratio	23.1
Blade Material	INCOLOY-909
Disk Material	UDIMET-720
Diffusion Factor	0.5
Blade Loss Coefficient	0.05
Blade Turning Angle	16.8°
Efficiency	86.4%

The design isentropic compressor efficiency is 86 percent, which is on the same level as the compressors used in F- and H-Class engines. When the compressor blade and disk sizes are compared with an H-Class gas turbines compressor section of similar compression ratio, it is observed that the blade heights and dimensions are very similar. This is mostly because of the design engine inlet flowrate and stage compression ratios being very similar.

3.3.2.2 Shaft (Rotor) and Disks

It is expected that the shaft bending loads will be higher in AFGT than a standard gas turbine, due to combustor section being longer. Due to the higher fuel mass flowrate than natural gas turbines, high mass flowrates will require longer blades for later stage turbine blades, which results in higher centrifugal forces applied to turbine disks. Listed material properties were considered in selecting the shaft and disk material of the AFGT designs:

- Young's Modulus, thermal expansion coefficient, density
- Ultimate tensile strength, 0.2 percent yield strength
- Fracture toughness
- Low and high cycle fatigue properties
- Creep rupture limits
- Should be available as forged stock bar

Mechanical and thermal loading on the shafts and disks is expected to be higher on the turbine side due to the higher heat transfer rate from the exhaust gases than for a typical natural gas fuel turbine.

3.3.2.3 Turbine Design

AFGT has a similar firing temperature with H-Class gas turbines, but the higher steam presence in the gas path flow increases corrosion and oxidation risks. Higher steam presence in the hot section also increases the heat transfer rate to the blades. Therefore, advanced materials, good coating performance, and good cooling performance are necessary for ammonia gas turbines. Unburned ammonia is not expected to be present in the exhaust flow; therefore, no special coatings are needed for ammonia specific protection.

For AFGT designs, the listed material properties were considered in selecting the turbine blade materials:

- 1 percent creep rupture strength at 1000 hr
- Ultimate tensile stress
- Density, Young's Modulus, and thermal expansion coefficient
- Low cycle fatigue properties
- Maximum operating temperature
- Oxidation resistance
- Corrosion resistance
- Availability as forged stock bar

Among the listed properties, creep rupture strength and maximum operating temperature are the most important metrics in the selection, because of the higher firing temperatures used.

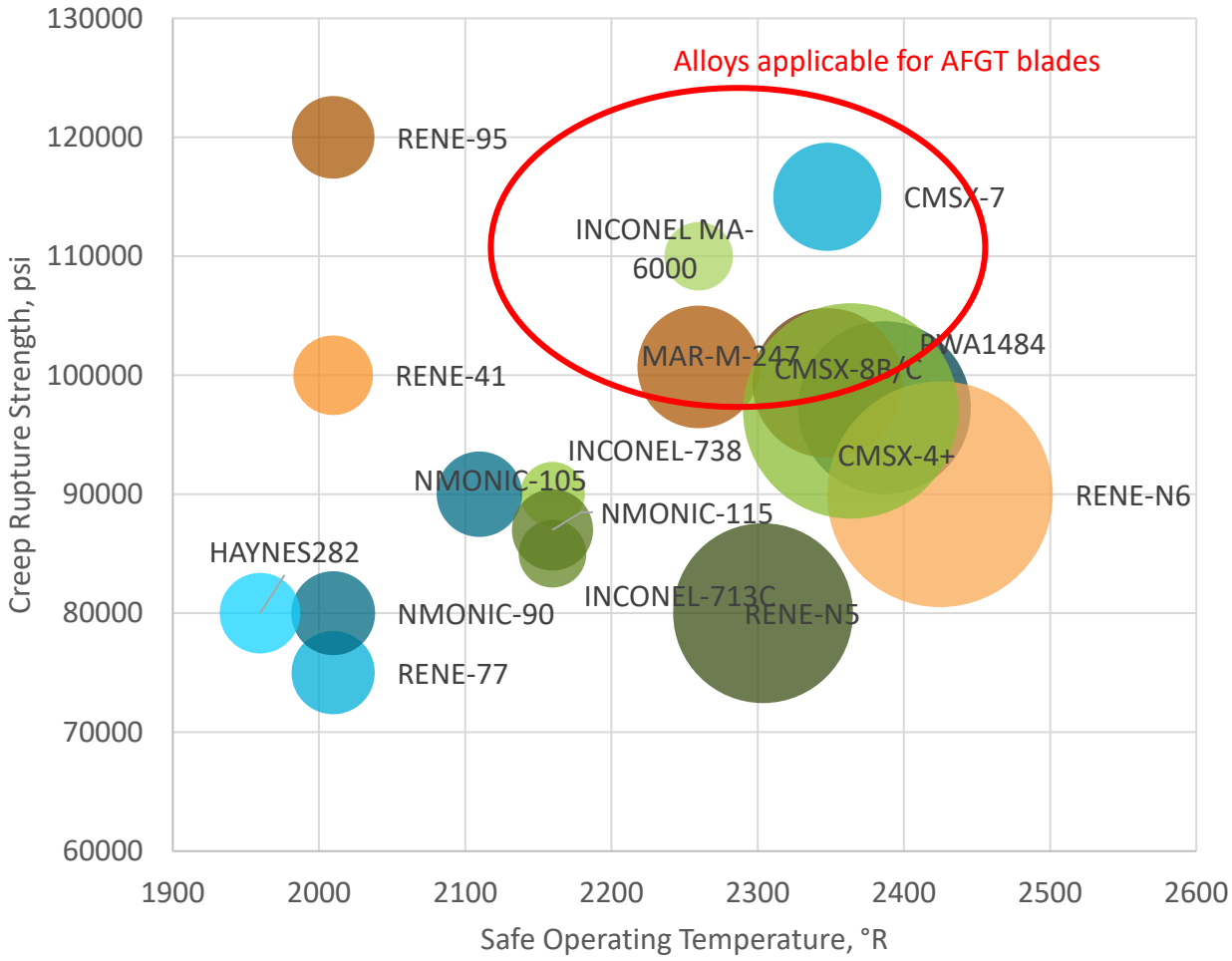
The following coating properties are considered for the thermal barrier coating (TBC) selection:

- Thermal conductivity and thermal expansion coefficient
- Phase stability
- Corrosion resistance
- Oxidation resistance
- Cracking, chipping, and delamination resistance

AFGT required more turbine stages than the comparable natural gas fuel gas turbine. In particular, AFGT design has 5 stages, where a typical H-Class turbine has 4 stages. The reasoning for having more stages in the ammonia case is mainly because of having a higher heat transfer rate, while having a similar compression ratio with the H-Class machine. Another reason for more stages is design consideration. Forcing the design to have 4 stages is possible if the design stage loading is used higher. However, this would yield extremely long blades at the last stage, which would create manufacturability problems and it increases the fir tree attachment design complexity. Current manufacturing techniques and materials can be used to manufacture AFGT turbine blades.

Based on the literature review on applicable materials for current advanced gas turbines, a list of materials was prepared for AFGT gas turbine design. Exhibit 3-4 shows the creep rupture strength of common and advanced alloys that can be used for gas turbine blades. The bubble sizes represent the relative price of each alloy.

Exhibit 3-4. Potential materials for the turbine blades of AFGT

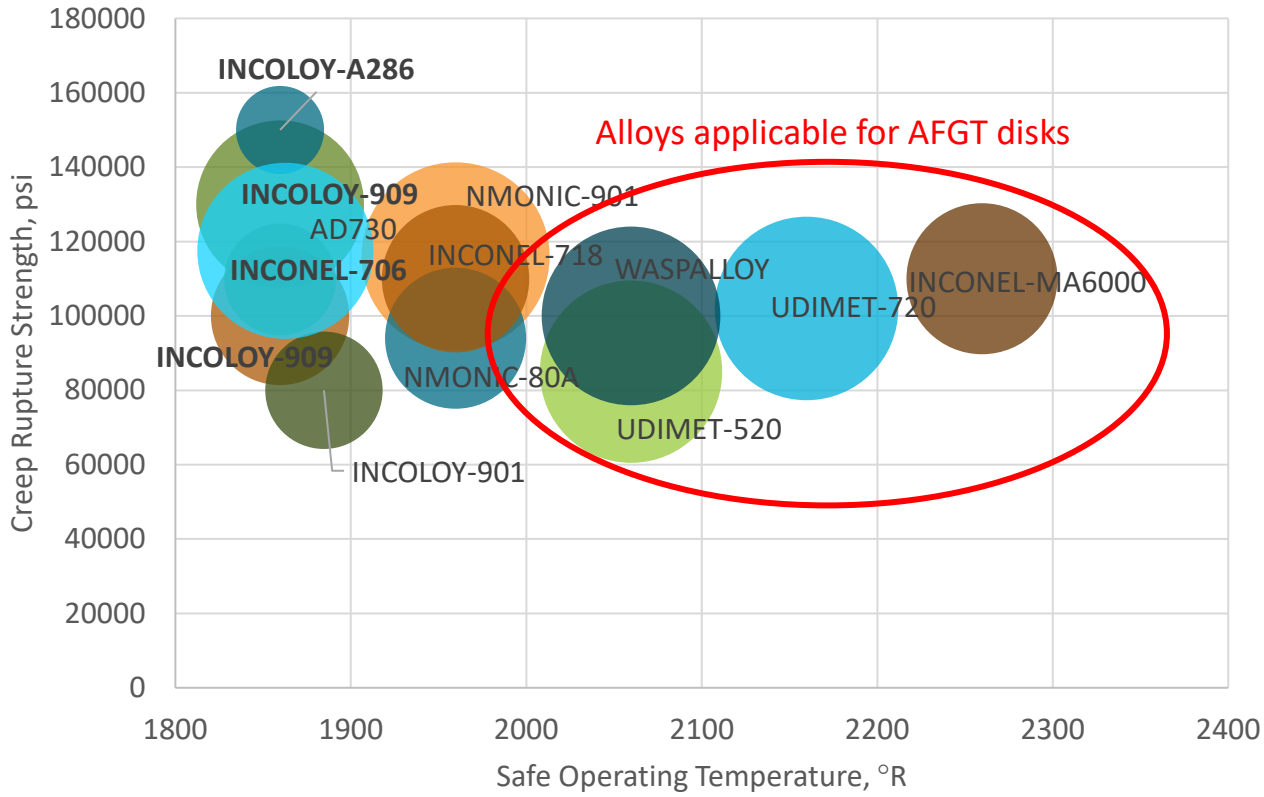


In Exhibit 3-4, advanced alloys are grouped in the upper right corner, indicating higher strength and higher operating temperature. Among these options, alloys applicable for AFGT designs are shown inside the red circle.

Possible materials selected for AFGT turbine blades are recent advanced alloys that are used in land-based gas turbines. CMSX alloys such as CMSX-8B/C, CMSX-7, and CMSX-4+ are the best candidates among the possible options. The reasons for this selection are their safe maximum operating temperature, creep rupture strength, cost, and current availability.

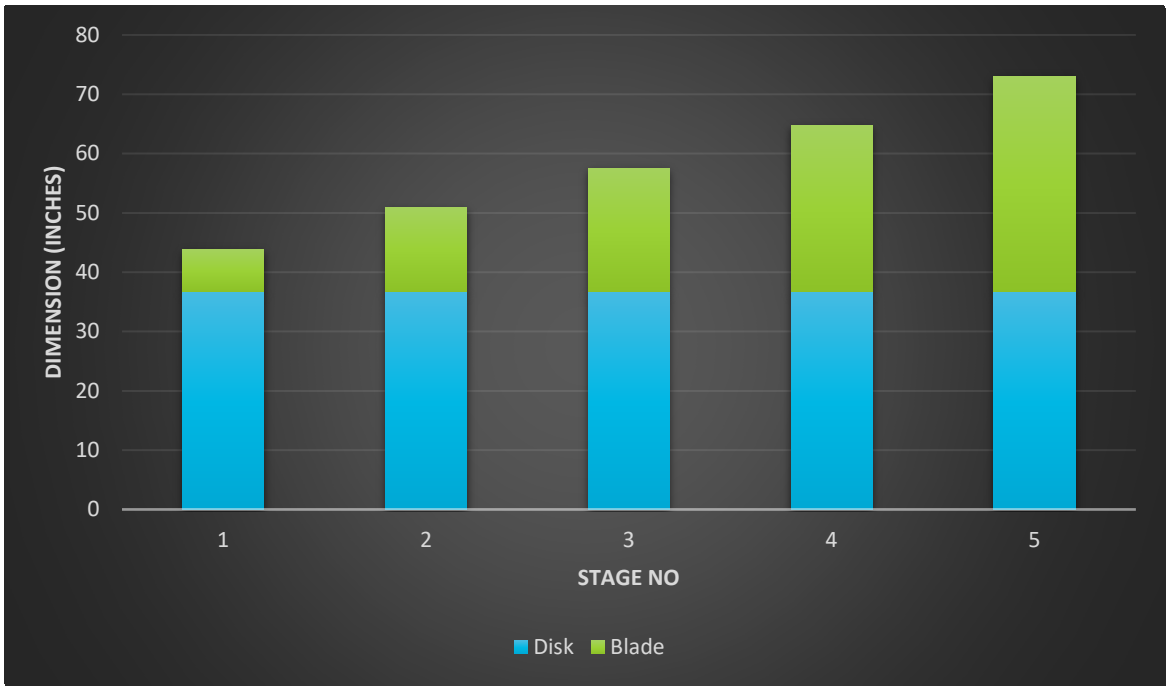
A list of applicable disk materials was prepared for the AFGT. Exhibit 3-5 shows the creep rupture strength of common and advanced alloys that can be used for the disks. The bubble sizes represent the relative price of each alloy.

Exhibit 3-5. Potential materials for the disks of AFGT



The selected group of materials were tried in turbine design. Some of the materials yield unsatisfactory designs, such as having longer blades, lower turbine stage efficiency, or impulse turbine designs for the 100 percent ammonia fuel case. The turbomachinery design section of the CGTM was used to perform the mean-line design of the turbines for each engine. It should be noted that 100 percent ammonia fuel case is used as the basis case for designing the turbomachinery of the AFGT, because this is the case where the turbine will have the highest mass inflow rate. For other fuel mixture operations, compressor outlet guide vanes will be used so that the existing turbine geometry can be used with minimal blade losses. The disk and blade heights of the turbine design made for the AFGT are presented in Exhibit 3-6.

Exhibit 3-6. Turbine design of AFGT



The turbine has 5 stages, with 93.6 percent isentropic efficiency. The flow coefficient, degree of reaction and flow turning angle are selected for highest efficiency and their values are shown along with other turbine parameters in Exhibit 3-7.

Exhibit 3-7. AFGT engine turbine design specifics

Parameter	Value
Stage Loading	1.2
Degree of Reaction	0.499
Flow Turning Angle	27.5°
Flow Coefficient	0.68
Isentropic Efficiency	93.6%
Blade Material	CMSX-7
Disk Material	UDIMET-720

The flow turning angle is generally high for ammonia gas turbine compared to natural gas turbines because of the higher temperature gradients, but it is similar to the hydrogen gas turbine design. The gas turbine blade material is a current level high end alloy that is extensively used in various land-based gas turbines.

The turbine designs were made and optimized primarily for 100 percent ammonia fuel because that is the ultimate design goal of the AFGT and also this is the case that will have the highest power output and efficiency compared to other cases involving natural gas fuel in the mixture.

Although having more stages, AFGT turbine blade sizes are similar to natural gas fuel turbines. Having similar materials and engine design with current H-Class gas turbines will increase customer acceptance of AFGT and reduce manufacturing and maintenance costs.

3.4 TURBINE COOLING DESIGN

After finalizing the turbomachinery design, the cooled performance of the engine is calculated. The cooled turbine model in CGTM uses the following information for cooling analysis:

- Metal and TBC Biot numbers (Bi)
- Internal cooling effectiveness value
- Film cooling effectiveness value
- Purge cooling flow fractions
- Cooling configuration information

Properties of the selected materials from the turbomachinery design were used from their manufacturer's datasheets. The Biot numbers of the blade metal and TBC are calculated using empirical formulas. Internal cooling effectiveness is used from the current level H-Class gas turbine technologies. Film cooling effectiveness values are used from the performance data of the advanced film cooling holes from open literature and previous experience.

3.4.1 Coatings

The coatings play an important role in ammonia gas turbines, as the hot gas flow through the turbine is more corrosive than a natural gas turbine due to having more steam content. The development of coatings for advanced gas turbines is mostly focused on bond coat and TBC layer improvements. [21-23].

The TBC on a gas turbine blade is made of three main layers: bond coat, TBC, and an environmental barrier coating (EBC). The bond coat is the first layer, and it mainly provides dense alumina scale for adherence of the outer layers to the blade metal wall, as well as an oxidation protection for the metal in the event of a TBC spall. TBC is the main protection layer that protects the blade from thermal gradients, oxidation, and corrosion. EBC protects the TBC and is applied with a silicon carbide bond coat to TBC. [24] In some recent studies by Oak Ridge National Laboratory (ORNL), EBC was infused into TBC for better coating protection and performance [25].

The Biot numbers of the coating and the metal wall are used in the cooled turbine model and are calculated using Equation (3).

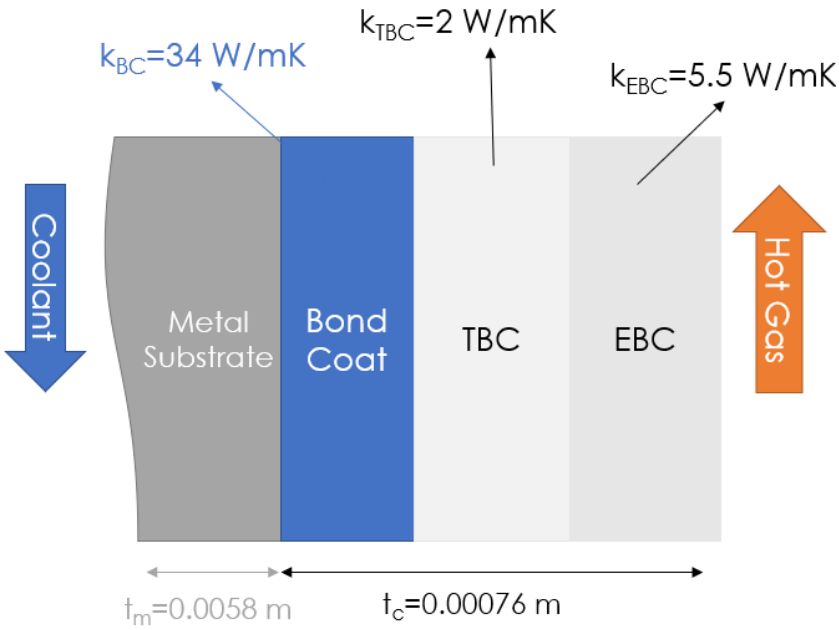
$$Bi_{m/c} = \frac{\alpha_g t_{m/c}}{k_{m/c}} \qquad (3)$$

In Equation (3), t is the thickness of the blade metal wall (m) or coating (c) and k is the coefficient of thermal conductivity of the blade metal wall (m) or the coating material (c). The convection heat transfer coefficient for hot gas, α_g is calculated with the empirical formula in Equation (4) [26].

$$\alpha_g = 0.285 \frac{(\rho_g V_g)^{0.63} c_{p,g}^{1/3} k_g^{2/3}}{D^{0.37} \mu^{0.7}} \qquad (4)$$

In Equation (4), ρ is the hot gas flow density (kg/m^3), V is the flow speed of the gas (m/s), D is the blade height (m), and μ is the viscosity of the hot gas (Pa-s). Flow properties including the density, heat capacity, and viscosity of hot gas flow for each fuel mix cases exhaust composition are calculated using ASPEN Properties software. [27] TBC, bond coat, and EBC conductivity values are used from the typical values for gas turbines. For the AFGT turbine blade coating, the coating properties used for cooling analysis are shown in Exhibit 3-8.

Exhibit 3-8. Coating property values used for Biot number calculations



The coating is a hybrid wall system involving different conductivity layers with known thicknesses. Therefore, the overall Biot number of the coating is calculated by using Equations (3) and (5).

$$\frac{t_c}{k_c} = \frac{t_{BC}}{k_{BC}} + \frac{t_{TBC}}{k_{TBC}} + \frac{t_{EBC}}{k_{EBC}} \qquad (5)$$

Metal conductivities are used from datasheets of the selected blade material. [28] Blade metal wall thickness is used as an average value from typical gas turbine blade values (0.23 inches). Coating thickness is used from typical coating thickness values from the literature. [29] With the

conductivity, thickness, and calculated convection heat transfer coefficients, the Biot numbers for the coating and the blade metal wall are calculated as presented in Exhibit 3-9.

Exhibit 3-9. Biot number calculations for the metal wall and coatings of AFGT

Parameter	Mix 1	Mix 2	Mix 3	Mix 4	Mix 5
α_g	779 W/m-K	780 W/m-K	782 W/m-K	783 W/m-K	784 W/m-K
Bi_c	0.421	0.422	0.423	0.423	0.424
Bi_m	0.188	0.189	0.189	0.189	0.189

3.4.2 Internal Cooling Effectiveness

For the internal cooling effectiveness values to be used in AFGT cooling analysis, a Siemens study on developing hydrogen gas turbines [21] and current natural gas turbine literature was used as references. The Siemens study includes the results for computational fluid dynamics (CFD) analyses of different internal cooling techniques applied to various turbine blades for different turbine stages.

The internal cooling effectiveness, which is used in CGTM, is defined as in Equation (6).

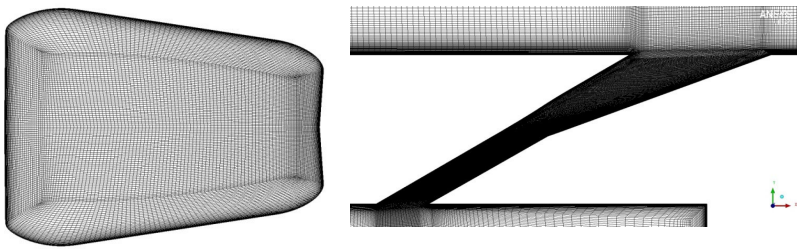
$$\varepsilon_c = \frac{T_{t,cl\ exit} - T_{t,cl\ in}}{T_{t,mw} - T_{t,\ cl\ in}} \qquad (6)$$

In Equation (6), $T_{t,cl\ exit}$ is the coolant flow temperature leaving the internal cooling channels, $T_{t,cl\ in}$ is the coolant flow temperature entering to the blade, and $T_{t,\ mw}$ is the blade metal wall temperature. The coolant temperatures and local blade metal wall temperatures are used from the contour plots from Siemens study for similar heat flux values [21] and then scaled to the ammonia gas turbine conditions. The average internal cooling effectiveness value for all blades is then calculated as 0.64. This value is in line with current-to-advanced internal cooling technologies.

3.4.3 Film Cooling Effectiveness

Advanced film cooling holes such as fan-shaped holes are expected to be used in the AFGT's first stages, such as the one shown in Exhibit 3-10.

Exhibit 3-10. Fan-shaped film cooling hole design used in GE hydrogen gas turbine study [22]



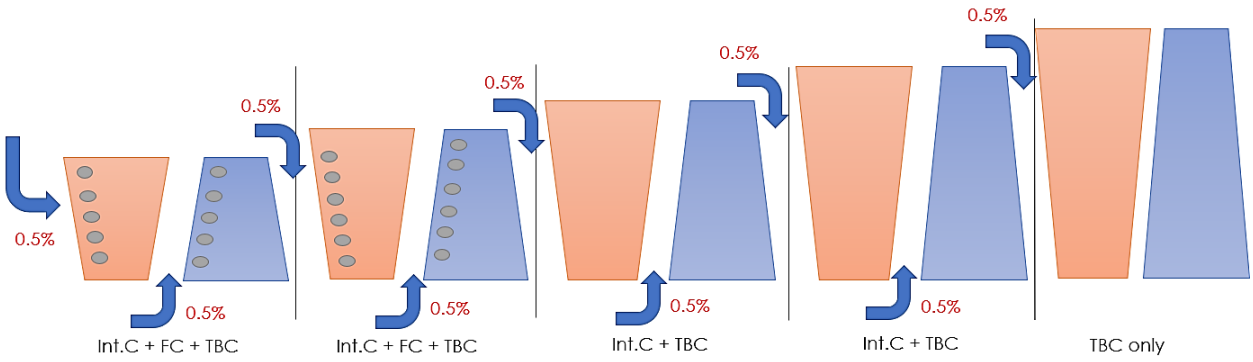
Fan shaped or 7-7-7 design type film cooling holes are shown to have good coolant coverage compared to simpler cylindrical holes. Advanced holes are used in the first couple of stages,

where the flow temperatures are higher. In the later stages, in order to reduce manufacturing costs, conventional film cooling holes are typically used. Effectiveness values of the fan-shaped holes are obtained from literature and are about 0.32–0.35. Particularly for ammonia gas turbines, advanced cooling features must exist even in the later stages due to having higher gas path temperatures. Exotic film cooling techniques such as hybrid film cooling or triple holes were not considered for this study.

3.4.4 Turbine Cooling Configuration

The cooling configuration of AFGT is based on typical H-class GT cooling configurations. The purge cooling flowrate is 0.5 percent of the mainstream flowrate, which is similar to typical H-class cooling technology levels. Internal cooling is used in every stage, except for the fifth stage. TBC is used in every stage. The configuration is determined using cooled turbine model in the CGTM to minimize cooling-related losses. The cooling configuration for AFGT is illustrated in Exhibit 3-11.

Exhibit 3-11. Turbine cooling configuration for AFGT design



3.5 Cooled Gas Turbine Performance and Sensitivity Analysis

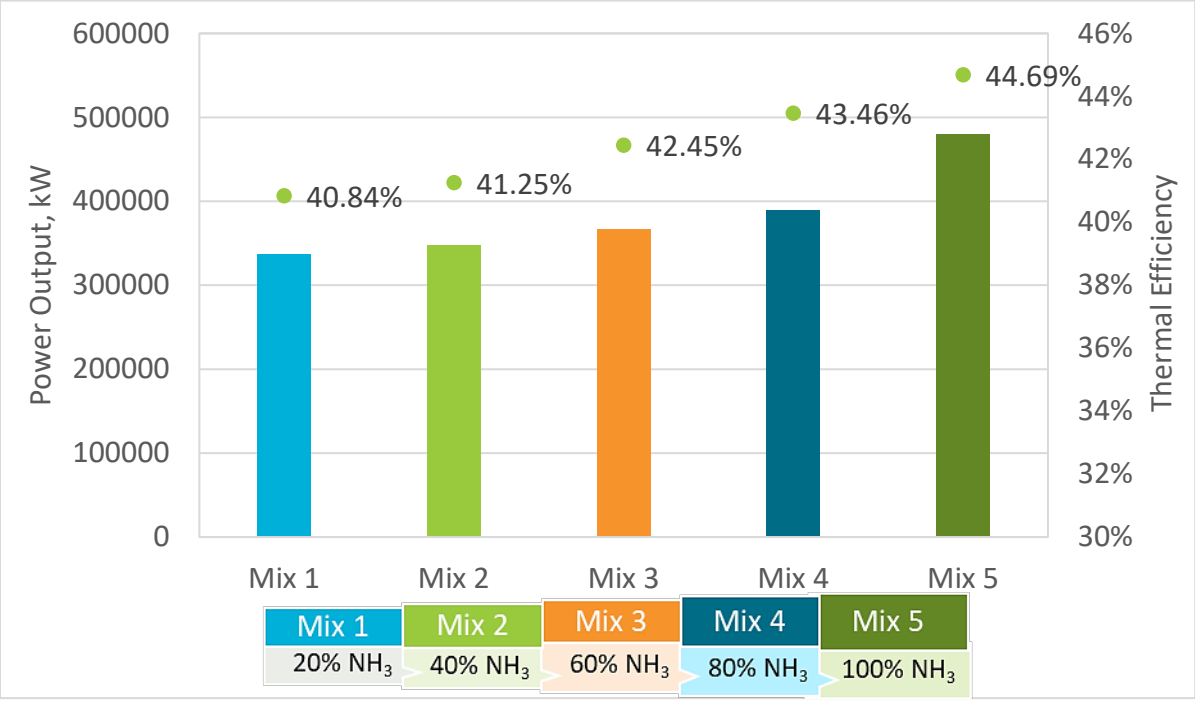
With the indicated cooling parameters and the determined cooling configuration, the cooled performances of the AFGT design options were calculated with CGTM. A sensitivity analysis for turbine cooling parameters impact on the gas turbine performance was made. The details of these are presented in the following subsections.

3.5.1 Cooled Gas Turbine Performance

CGTM was used to perform the cooled gas turbine performance analysis. Key gas turbine performance metrics such as power output, thermal efficiency, and heat rate are calculated. The cooling configuration values were used from the analysis presented in Section 3.4, together with the turbomachinery design data of Section 3.3.

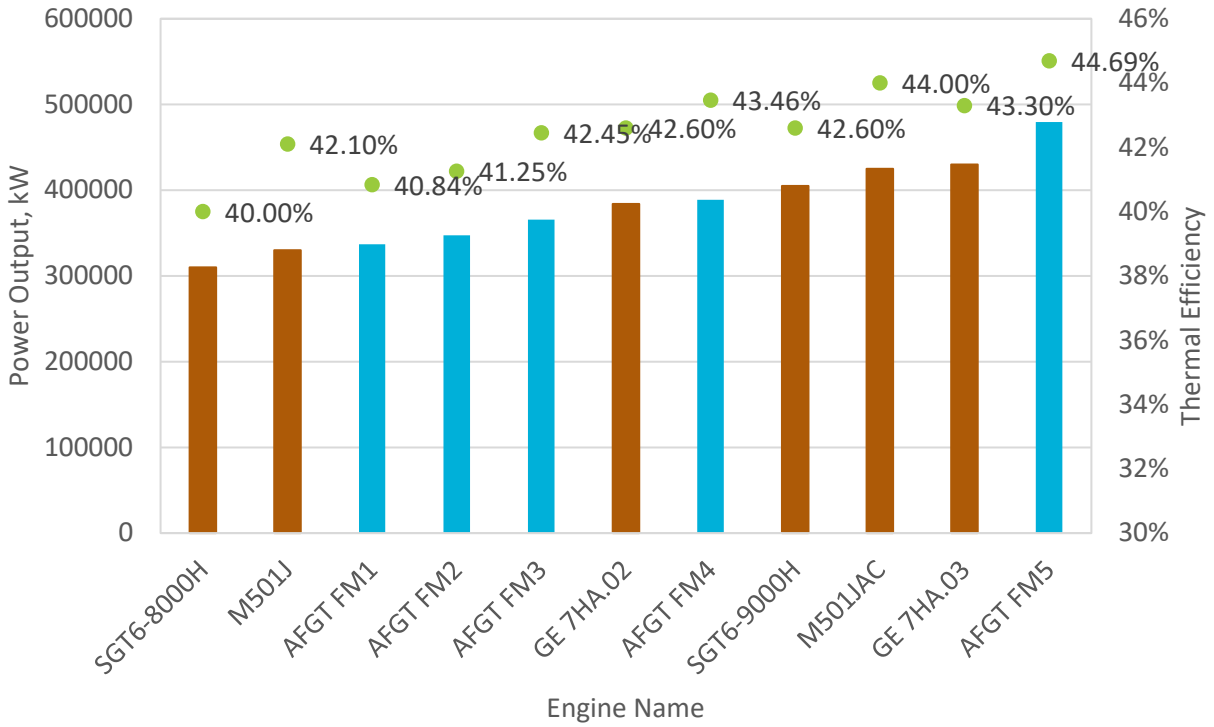
For AFGT design, power output and thermal efficiency are calculated and compared for each fuel mixture case in Exhibit 3-12.

Exhibit 3-12. Cooled gas turbine performance results of AFGT; Composition of mixes based on vol%



The performance of the ammonia fuel gas turbine is compared with several H-Class gas turbines from different vendors in Exhibit 3-13. The performance of the AFGT is comparable with current level H-Class gas turbines, which are fueled with 100% natural gas [30]. AFGT using low ammonia fraction fuels, which are mixtures 1 to 3, gives higher performance than two of the commercial H-Class gas turbines. Performance of AFGT using fuel mixture 4 is comparable to General Electric (GE) 7HA block 2 engine and Siemens' new H-Class gas turbine SGT6-9000H. AFGT using 100 percent ammonia fuel produces more power and has higher thermal efficiency than any of the current H-Class gas turbines. It should be noted that AFGT uses similar firing temperatures with the compared commercial engines and produces more power.

Exhibit 3-13. Comparison of AFGT performance with current H-Class gas turbine data [30]



The results of cooled gas turbine analysis show that to have comparable performance to H-class gas turbines, an ammonia fuel gas turbine should have at least a 2800 °F turbine inlet temperature.

The increase in the gas turbine performance (i.e., higher power output and thermal efficiency) as the ammonia fuel fraction is increased can be perplexing, as the ammonia fuel has significantly lower fuel heating values compared to natural gas and methane. Having lower fuel heating value requires the fuel flowrate to be significantly higher for ammonia fuel mixtures when compared to natural gas fuel. If the increase in the fuel flowrate cannot be balanced with the increase in the power output from the engine, then the thermal efficiency would decrease as the ammonia fraction is increased in the fuel mixture.

The unexpected trend of increased engine performance with ammonia fuel was also seen in the first engine tests made with Solar T-350 engine in 1967 by Pratt et al. [6]. In this study, the increase in the gas turbine power output and efficiency with ammonia fuel is explained with the ammonia combustion products yielding a larger enthalpy drop at the turbine, for the same turbine pressure ratio with the natural gas fuel. Even though the fuel used has lower fuel heating value, increased mass flowrate and larger enthalpy drop across the turbine leads to the engine efficiency increase. This phenomenon also explains the increase in AFGT performance when the ammonia fraction is increased in the fuel mixture. If the turbine firing temperature of AFGT design was lower, then a reduction in the engine efficiency could be seen when the ammonia fuel fraction is increased. Conversely, the increase in the engine thermal efficiency could be higher if turbine inlet temperature greater than 2800 °F is used. However, using higher

turbine inlet temperature would result in higher cooling flows and more expensive blade materials and coatings.

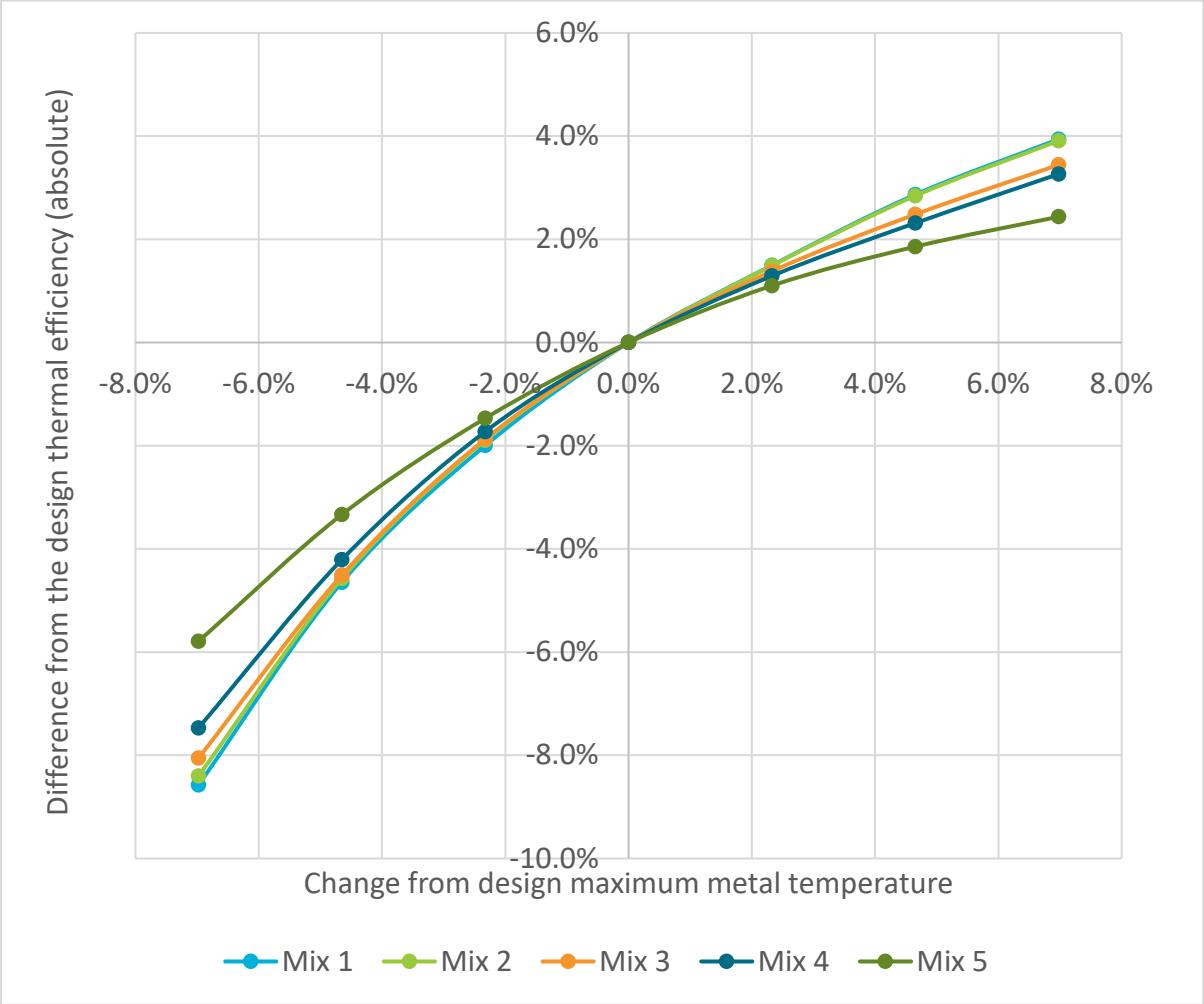
3.5.2 Sensitivity Analysis

Sensitivity analysis of gas turbine performance metrics was conducted for several turbine cooling parameters such as the maximum blade metal temperature, internal cooling effectiveness, film cooling effectiveness, and TBC performance for AFGT design. Sensitivity analysis showed how much each parameter had impact on gas turbine performance metrics. It also serves the purpose of showing the compromise on engine performance if one of the cooling design parameters, such as the material temperature limit, cannot be met due to the unavailability of the technology.

3.5.2.1 Material Temperature Limit

Selected blade material for AFGT is a common high-end material developed for land-based gas turbines. The sensitivity analysis for material temperature limits impact on gas turbine thermal efficiency is shown for all fuel mixture cases in Exhibit 3-14. If an alternate material must be used, another material with 50 degrees higher temperature limit would increase the efficiency by 1.3 percent for all mixture cases. Material temperature limit is the most impactful cooling parameter in ammonia gas turbine performance.

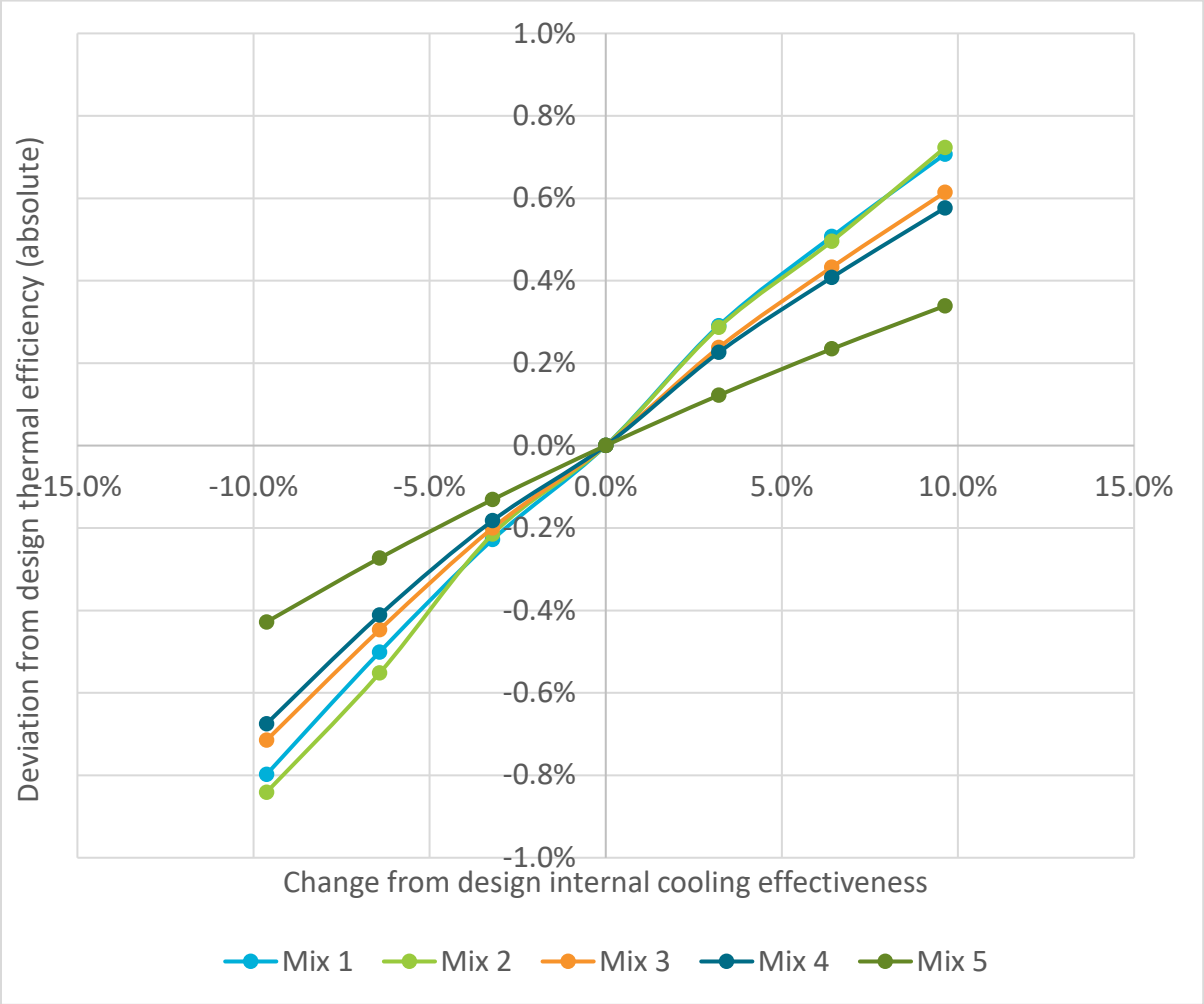
Exhibit 3-14. Sensitivity of gas turbine thermal efficiency on maximum blade metal temperature



3.5.2.2 Internal Cooling Effectiveness

By the time ammonia gas turbines go into operation, new and better internal cooling technologies than the current design might become available, especially with the advances in additive manufacturing. The sensitivity analysis for internal cooling effectiveness impact on gas turbine thermal efficiency is shown for all fuel mixture cases in Exhibit 3-15. In the internal cooling design schemes used to determine the AFGT's design point internal cooling effectiveness values, the referenced study uses more traditional internal cooling techniques. Using advanced ribs and pin-fins in earlier stages can improve internal cooling effectiveness and increase GT efficiency up to 0.7 percent (absolute) from the design values presented in Exhibit 3-12. The highest increase in the performance was observed for lower ammonia fraction fuel mixture cases.

Exhibit 3-15. Sensitivity of gas turbine thermal efficiency on internal cooling effectiveness

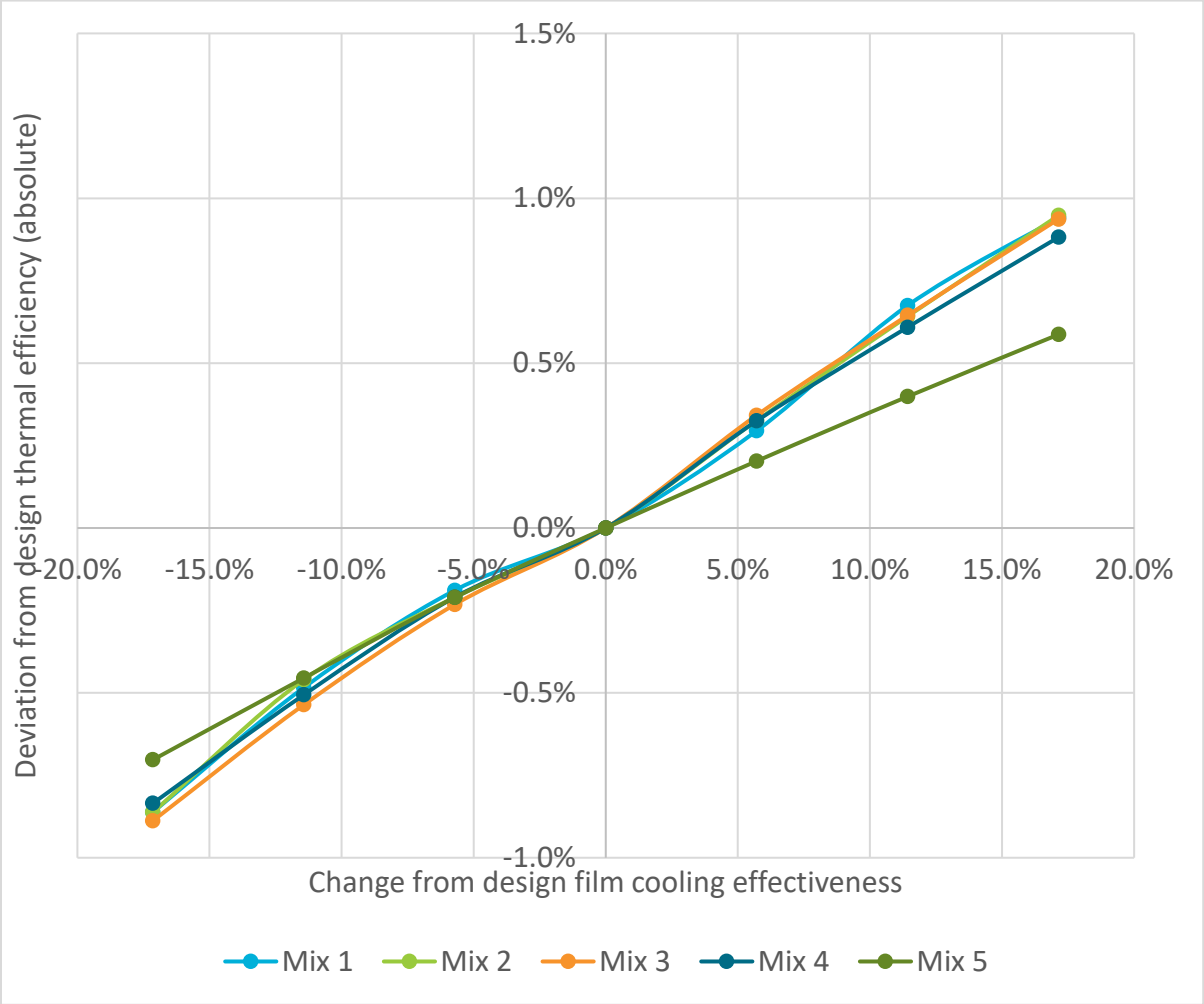


3.5.2.3 Film Cooling Effectiveness

In general, advanced film cooling techniques that use less coolant with better coolant attachment on the blade surface would increase the cooling effectiveness.

The sensitivity analysis for internal cooling effectiveness impact on gas turbine thermal efficiency is shown for all fuel mixture cases in Exhibit 3-16.

Exhibit 3-16. Sensitivity of gas turbine thermal efficiency on film cooling effectiveness

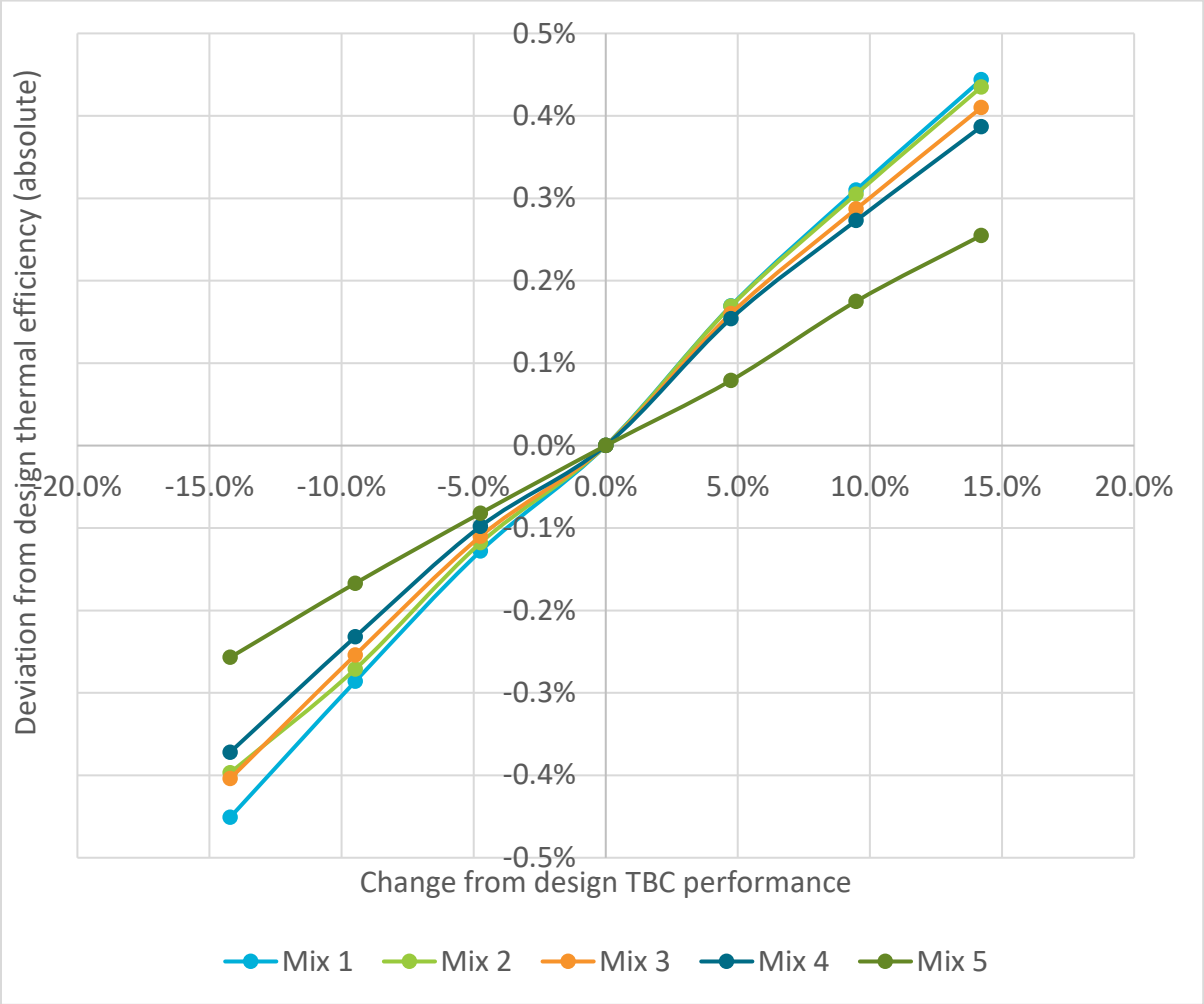


Current cooling design uses fan-shaped holes, which is a standard hole type for current advanced gas turbines. Advances in additive manufacturing could enable more advanced hole shapes with higher cooling effectiveness to be available by the time ammonia gas turbines enter service. Advanced film cooling techniques can increase AFGT efficiency up to 1 percent (absolute) from the design values of Exhibit 3-12. Higher increase in performance is observed for lower ammonia fraction fuel mixture cases.

3.5.2.4 TBC Performance

The specifics used for the TBC material of AFGT cooling design represent current level technology. Coating technologies are developing very fast; reducing the coating conductivity further might be possible in the near future. Further advancements in coating techniques will certainly improve the TBC performance. The sensitivity analysis for TBC performance impact on gas turbine thermal efficiency is shown for all fuel mixture cases in Exhibit 3-17.

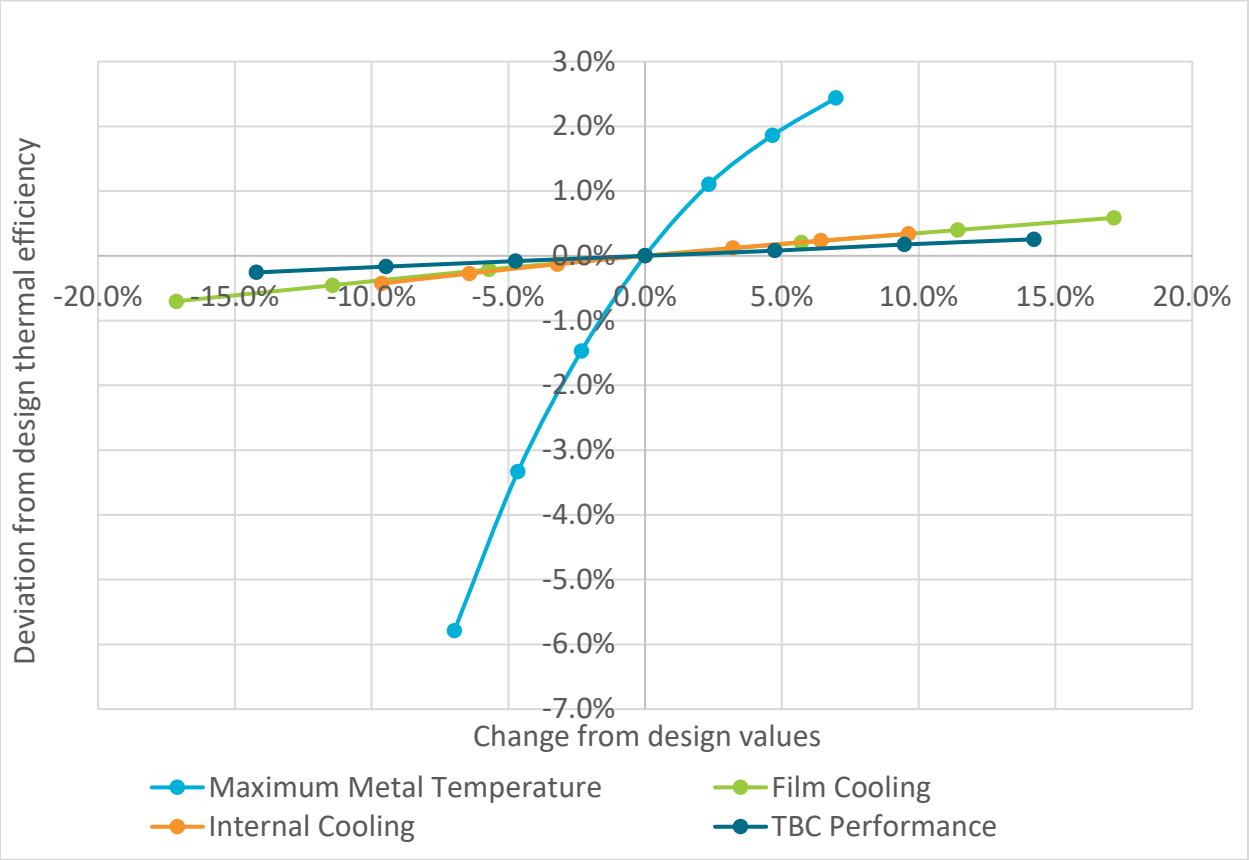
Exhibit 3-17. Sensitivity of gas turbine thermal efficiency on TBC performance



3.5.2.5 Comparison of Cooling Parameter Strengths on Ammonia Fuel Gas Turbine Efficiency

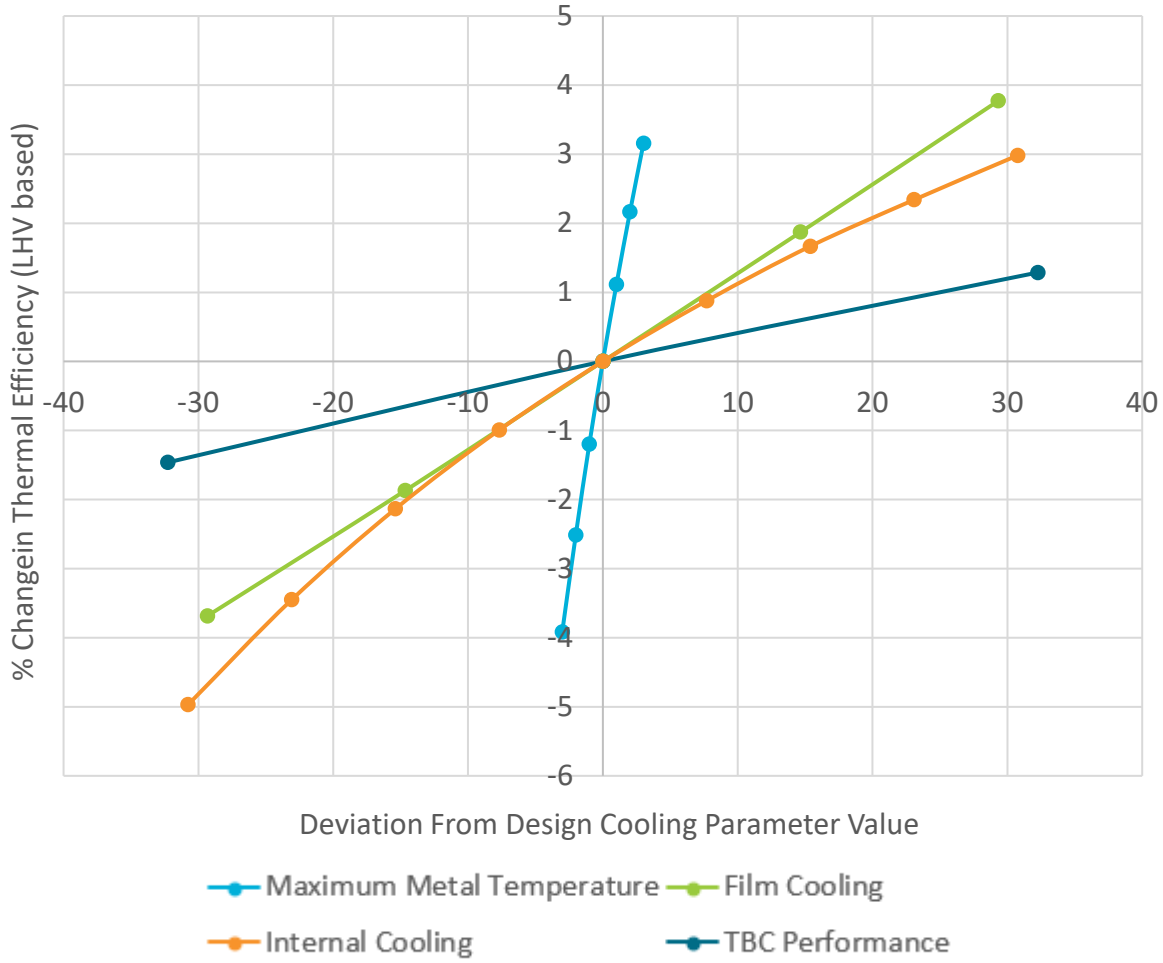
The relative strengths of each cooling technology on the gas turbine efficiency are compared for 100 percent ammonia fuel conditions in Exhibit 3-18.

Exhibit 3-18. Gas turbine efficiency sensitivity on different cooling parameters for ammonia fuel gas turbine



From the results in Exhibit 3-18, similar to natural gas turbines and hydrogen gas turbines, the metal temperature has the highest impact, followed by the film cooling effectiveness, closely followed by advances in internal cooling methods and TBC performance. However, the magnitude of the impact from cooling technologies is higher in natural gas engines compared to ammonia fuel gas turbine for the same amount of deviation from design cooling parameter value. The values for the natural gas turbine are presented in Exhibit 3-19 for comparison.

Exhibit 3-19. Gas turbine efficiency sensitivity on different cooling parameters for H-class gas turbine [19]



The main reason behind having a higher impact from the cooling technologies on gas turbine performance metrics for the natural gas turbine is due to the difference in the heat transfer rates in the turbine sections. Having higher temperature gradients in the AFGT requires bigger changes in the cooling parameters for the same amount of impact with the natural gas fuel gas turbine. For example, a 5 percent increase in the film cooling efficiency reduces the blade outer wall temperature to a lower temperature in the natural gas fuel turbine than for the flexible fuel gas turbine because of the lower heat transfer rate in the former one. For cooling the ammonia fuel gas turbines blade wall to the same temperature with the natural gas turbine case, more than a 5 percent increase in film cooling effectiveness would be required because of the higher temperature gradients.

4 AMMONIA FUEL COMBINED CYCLE PERFORMANCE ANALYSIS

For the ammonia fuel combined cycle (AFCC) analysis, the natural gas combined cycle (NGCC) revision 4 B32A ASPEN Plus model [31] was used. The gas turbine inside this model was modified to match the AFGT design specifications from Section 3. Some of the changes are listed as follows:

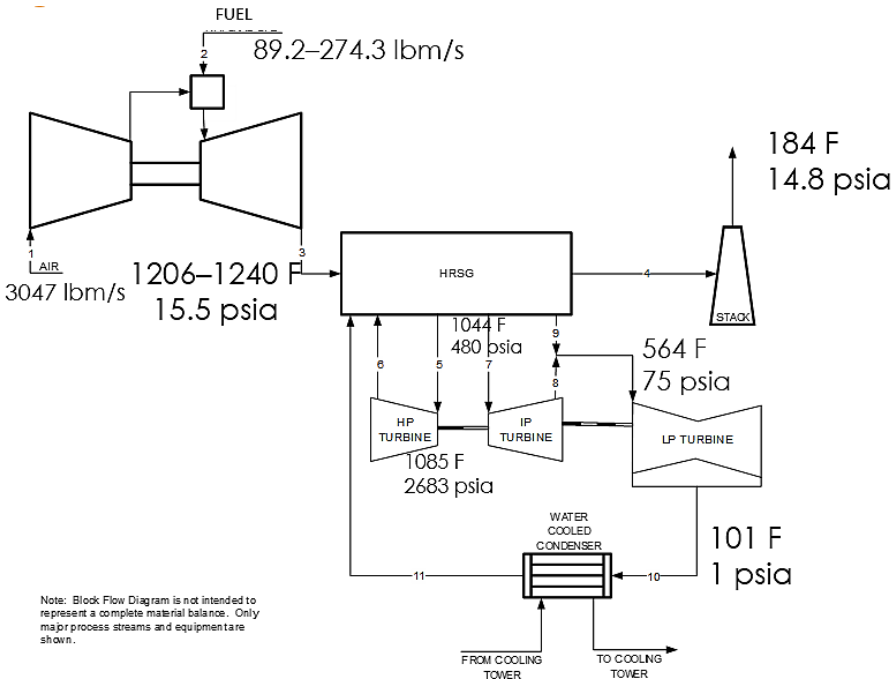
- Firing temperature was changed to 2800 °F
- Coolant flowrates were matched to AFGT design
- Compressor models pressure ratio and efficiency were matched to the compressor model with coolant extraction losses
- Turbine efficiencies were matched to cooled turbine model

The fuel type was changed from natural gas to ammonia-methane fuel mixtures defined in Section 2. Some changes were made to the steam cycle regarding the increased flue gas temperature for the AFGT cases, which is due to the increased gas turbine exhaust temperature.

4.1 STEAM CYCLE DESIGN

The steam cycle design specifics are not significantly changed from B32A values, which is for H-class gas turbine coupling. Most of the changes made in the steam cycle were to handle the increase in the flue gas temperature, which is about 40–70 °F higher in AFGT cases than the B32A configuration. Similar materials used in the heat recovery steam generator (HRSG) design for B32A can be used in AFCC. The major streams flowrates and flow states in the AFCC are presented in Exhibit 4-1. The steam cycle maximum pressure and temperatures are used from H-class levels.

Exhibit 4-1. Combined cycle configuration used for AFCC analysis



The details of each stream in Exhibit 4-1 are presented in the stream tables in Appendix A. The gas turbine exhaust temperature is the highest for Mix 1 and is lowest for Mix 5, which has the highest ammonia fuel content.

The increase in the flue gas entry temperature to HRSG will not cause changing of the duct materials, as the increase in the temperature will still be within the limits of steel materials used in the typical HRSG ducts.

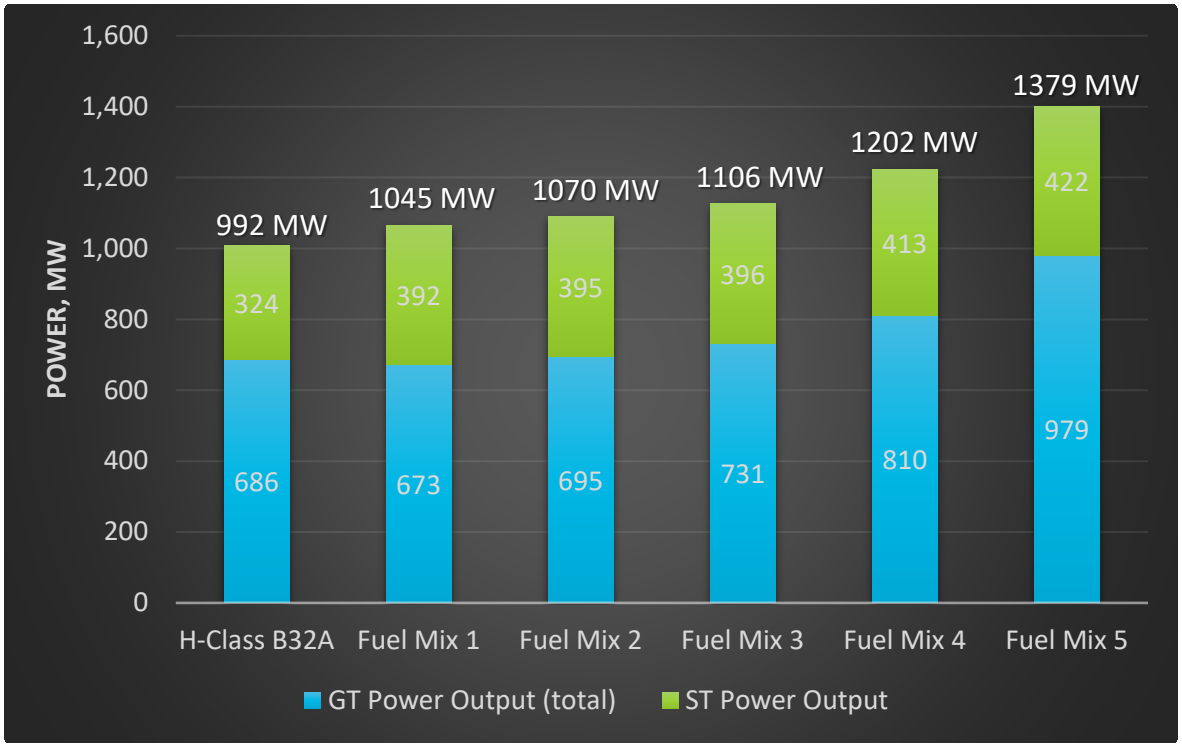
The pinch point temperature differences in low, intermediate, and high-pressure sections of the steam cycle of AFCC are very similar to the B32A values for all fuel mixture cases.

In the current study, the steam cycle specifications were used as the same from B32A NGCC values and some potential improvement areas for the steam cycle were identified for increasing the steam cycle efficiency further. If the cycle maximum temperature and pressure is increased, the steam cycle efficiency could be increased. Higher pressure ratios could increase the steam turbine power output, which eventually would increase the AFCC cycle efficiency further.

4.2 Ammonia Fuel Combined Cycle Performance Results

The net power outputs from the AFCC cases are compared with each other and to B32A NGCC levels in Exhibit 4-2.

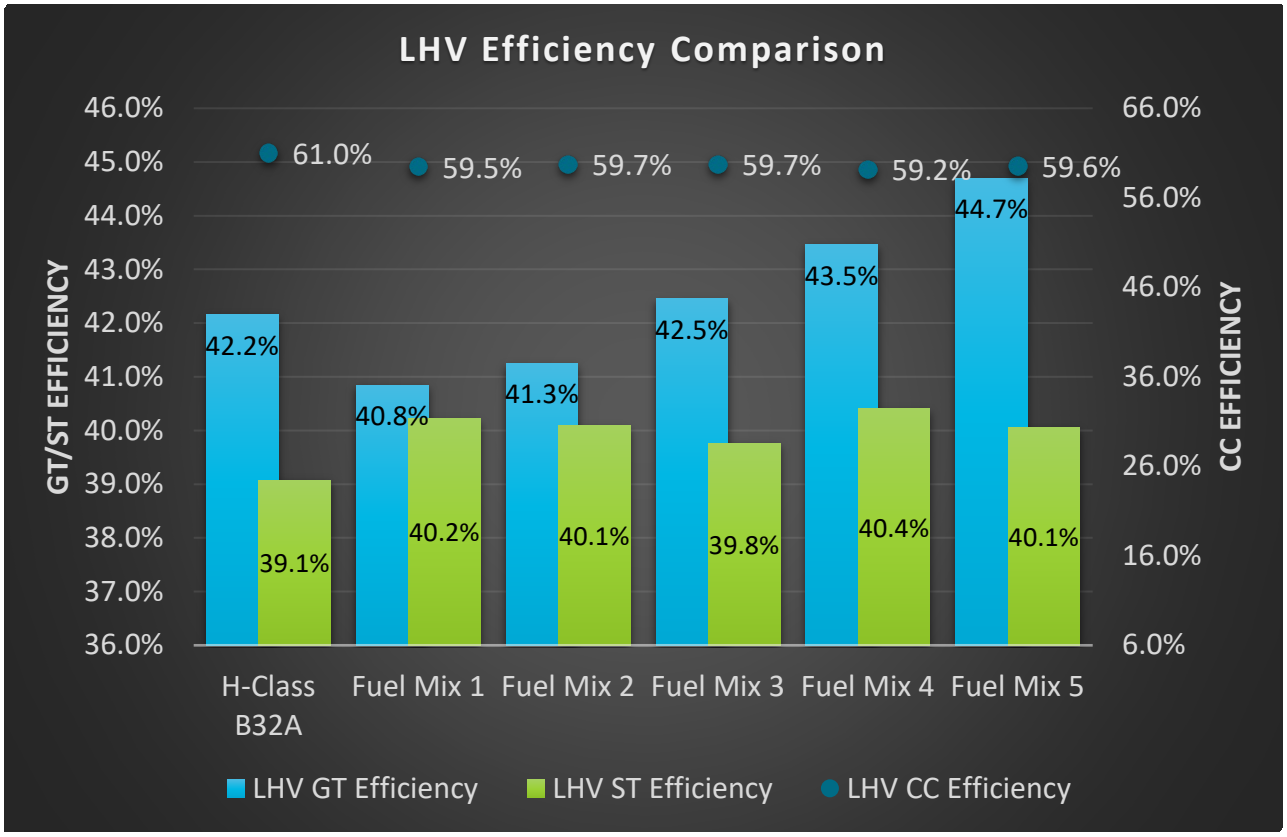
Exhibit 4-2. AFCC power output comparison with B32A levels



The power rating of the AFCC systems is 1.0–1.4 GW. It should be noted that the thermal input to the AFCC cycles is different from NGCC case. The subsequent fuel mix cases, where the ammonia fraction is increased up to 100 percent, have higher power outputs than the first case. From the power distributions, both the gas turbine and steam turbine outputs increase from fuel mix 1 to 5. The increase in the steam cycle output is due to the increase in the heat capacity of the exhaust flow.

The combined cycle efficiencies of AFCC cases are compared with each other and to B32A NGCC values in Exhibit 4-3.

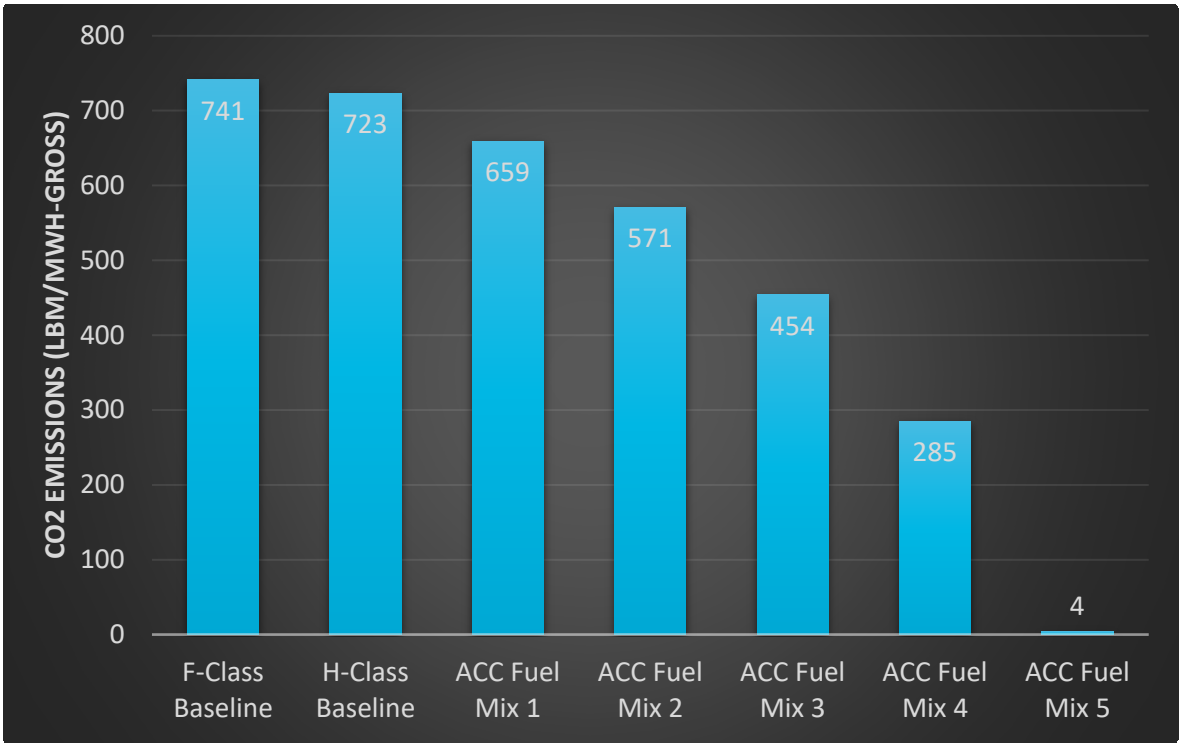
Exhibit 4-3. AFCC efficiency, gas turbine efficiency, and steam turbine efficiency comparison with B32A levels



Comparing the efficiencies with NGCC shows that ammonia combined cycle has similar combined cycle efficiency values. The main reason for having constant cycle efficiency among different fuel mixture cases is because the increase in fuel usage compensates for the increase in the steam and gas turbine cycle power output increase. The thermal input to ammonia combined cycle is comparably much higher than for NGCC, yet the flue gas entry enthalpy is significantly lower for the AFCC, making the steam cycle efficiency lower than NGCC. The steam turbine efficiency is almost constant between different fuel cases. Overall, ammonia combined cycle has lower efficiency than hydrogen combined cycle. Using a higher firing temperature than 2800 °F and having higher gas turbine performance can increase the AFCC efficiency above the NGCC levels.

The CO_2 emissions and water consumption of the AFCC are compared for each fuel mix case and to NETL baseline H- and F-class values in Exhibit 4-4.

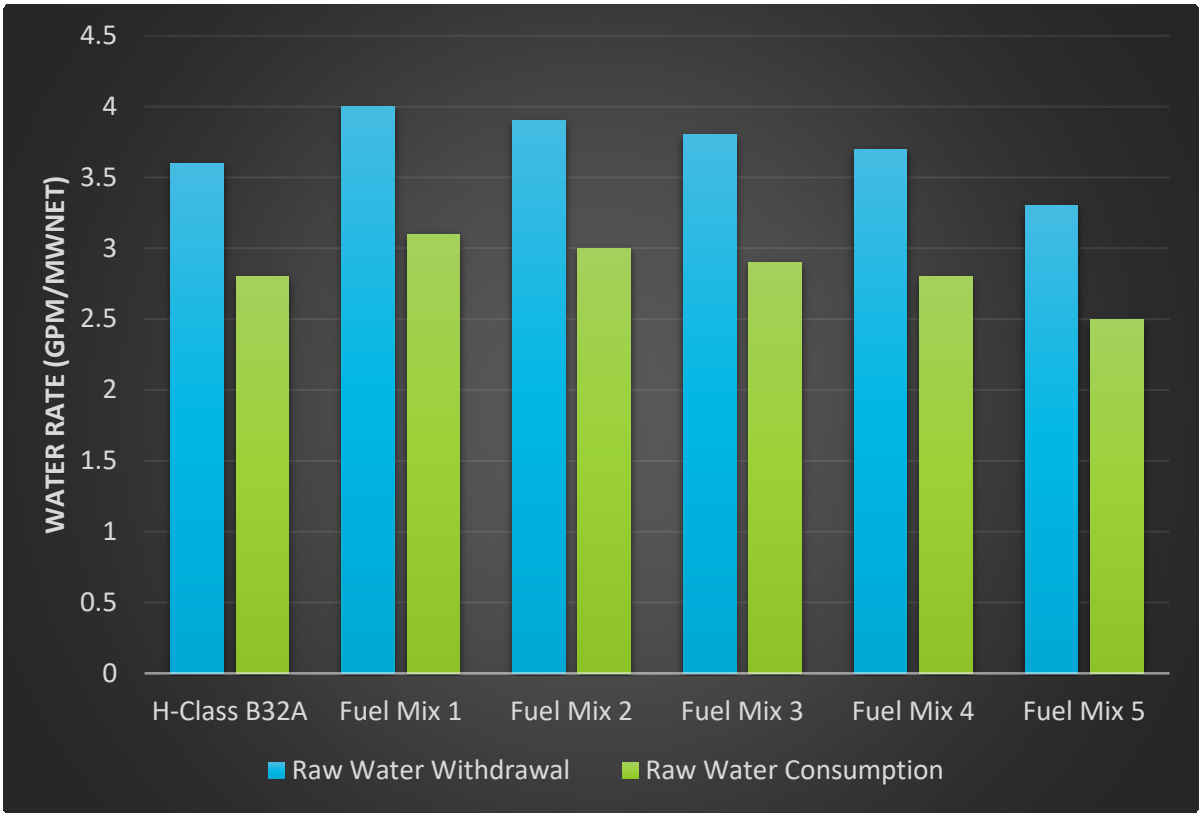
Exhibit 4-4. CO_2 emissions from AFCC cycles with B32A and B31A levels



The advantage of using ammonia in the fuel mix shows clearly for all AFCC cases. As the methane fraction in the fuel mixture is reduced, the CO_2 emissions are reduced. For the case with 100 percent ammonia fuel, the CO_2 emissions are negligible, and are comparable to NGCC with carbon capture systems. The CO_2 emission for the 100 percent ammonia case is not zero because of the CO_2 from the inlet air content. However, the 100 percent ammonia case has a net zero contribution.

Water consumption rates from the AFCC cycles are compared with H-Class (B32A) cases in Exhibit 4-5.

Exhibit 4-5. Water consumption rates from AFCC cycles with B32A and B31A levels



Water consumption of the ammonia combined cycle is slightly higher than NGCC except for the 100% ammonia case (Mix 5). This is due to having a higher flue gas temperature in the HRSG. The water usage does not change significantly between the ammonia fuel mix cases, because of having similar flue gas outlet temperatures. However, the increase in the cycle power output brings down the rate below NGCC values only for Mix 5.

The performance summaries of AFCC cycles are compared with B32A case in Exhibit 4-6. The changes in the auxiliary load items power consumption amounts for different fuel mixture cases are proportional to the changes in the water consumption rates.

Exhibit 4-6. Performance summaries of AFCC cycles compared with B32A case

	B32A	FM1	FM 2	FM 3	FM 4	FM 5
Power Summary						
Combustion Turbine Power, MWe	686	673	695	731	810	979
Steam Turbine Power, MWe	324	392	395	396	413	422
Total Gross Power, MWe	1,009	1,065	1,090	1,126	1,223	1,401
Auxiliary Load Summary						
Air Cooled Condenser Fans	0	0	0	0	0	0
Circulating Water Pumps, kWe	3,510	4,030	4,050	4,030	4,270	4,380
Combustion Turbine Auxiliaries, kWe	1,320	1,320	1,320	1,320	1,320	1,320
Condensate Pumps, kWe	180	210	210	210	220	230
Cooling Tower Fans, kWe	1,810	2,090	2,090	2,090	2,210	2,270
CO_2 Capture/Removal Auxiliaries, kWe	0	0	0	0	0	0
CO_2 Compression, kWe	0	0	0	0	0	0
Feedwater Pumps, kWe	5,760	7,380	7,520	7,760	7,760	8,040
Ground Water Pumps, kWe	330	380	380	380	400	410
Miscellaneous Balance of Plant, kWe	710	710	710	710	710	710
SCR, kWe	3	3	3	4	4	5
Steam Turbine Auxiliaries, kWe	230	230	230	230	230	230
Transformer Losses, kWe	3,070	3,240	3,320	3,420	3,720	4,250
Total Auxiliaries, MWe	17	20	20	20	21	22
Net Power, MWe	992	1,045	1,070	1,106	1,202	1,379
Performance Summary						
HHV Net Plant Efficiency, %	55.1%	53.2%	52.9%	52.1%	50.6%	49.3%
HHV Net Plant Heat Rate, kJ/kWh (Btu/kWh)	6,537 (6,196)	6,770 (6,416)	6,810 (6,454)	6,907 (6,547)	7,118 (6,747)	7,304 (6,923)
HHV Combustion Turbine Efficiency, %	38.0%	34.2%	34.3%	34.4%	34.1%	35.0%
LHV Net Plant Efficiency, %	61.0%	59.5%	59.7%	59.7%	59.2%	59.6%
LHV Net Plant Heat Rate, kJ/kWh (Btu/kWh)	5,900 (5,592)	6,052 (5,737)	6,025 (5,711)	6,026 (5,711)	6,084 (5,766)	6,045 (5,729)

	B32A	FM1	FM 2	FM 3	FM 4	FM 5
LHV Combustion Turbine Efficiency, %	42.2%	38.3%	38.8%	39.5%	39.9%	42.3%
Steam Turbine Cycle Efficiency, %	39.1%	40.2%	40.1%	39.8%	40.4%	40.1%
Steam Turbine Heat Rate, kJ/kWh (Btu/kWh)	9,213 (8,732)	8,951 (8,484)	8,980 (8,511)	9,054 (8,581)	8,910 (8,445)	8,987 (8,518)
Condenser Duty, GJ/hr (MMBtu/hr)	1,757 (1,666)	2,025 (1,920)	2,033 (1,927)	2,025 (1,919)	2,144 (2,032)	2,201 (2,086)
Fuel Gas Feed Flow, kg/hr (lb./hr)	124,025 (273,429)	145,617 (321,031)	174,225 (384,101)	216,902 (478,187)	297,336 (655,513)	448,035 (987,747)
HHV Thermal Input, kWt	1,801,631	1,965,282	2,024,116	2,122,177	2,376,696	2,797,581
LHV Thermal Input, kWt	1,626,150	1,757,071	1,790,949	1,851,277	2,031,285	2,315,295
Raw Water Withdrawal, (m^3/min)/MWnet (gpm/MWnet)	0.014 (3.6)	0.015 (4.0)	0.015 (3.9)	0.014 (3.8)	0.014 (3.7)	0.012 (3.3)
Raw Water Consumption, (m^3/min)/MWnet (gpm/MWnet)	0.011 (2.8)	0.012 (3.1)	0.011 (3.0)	0.011 (2.9)	0.011 (2.8)	0.010 (2.5)

5 COST ANALYSIS FOR AMMONIA FUEL COMBINED CYCLE

A preliminary techno-economic analysis was conducted for AFCC cases to calculate the levelized cost of electricity (LCOE), owner's costs, operating costs, and cost sensitivities on ammonia fuel price and capacity factor. The reasons that make this cost analysis preliminary and not a final or detailed one are as follows:

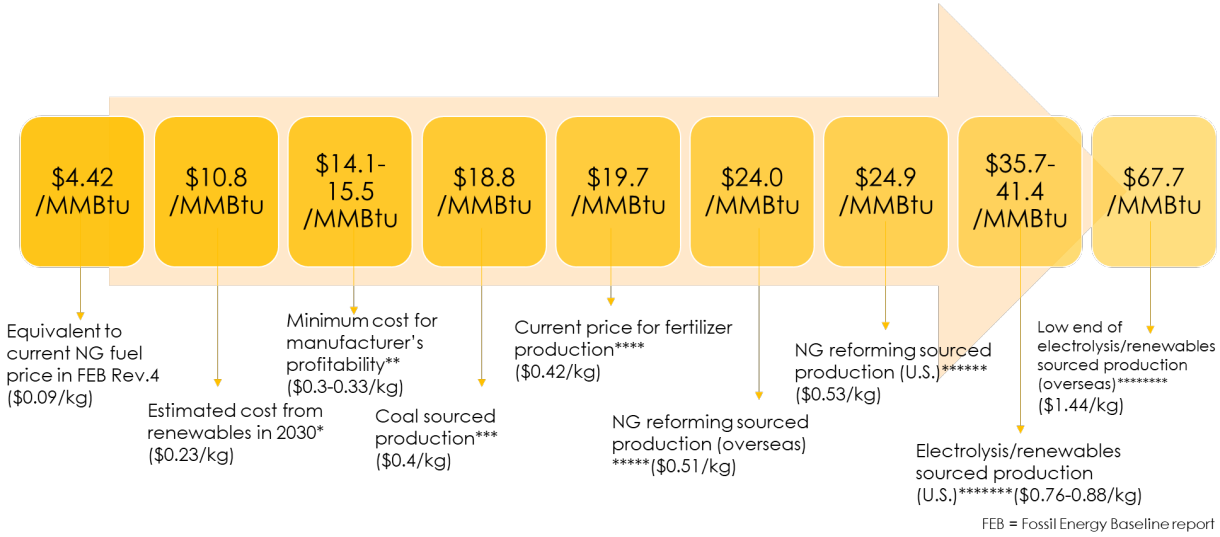
- The gas turbine cost may be higher than the estimations made with power scaling due to use of a two-stage combustor technology instead of a conventional dry low NOx (DLN) combustor, having a fifth stage in the turbine, and need for using advanced manufacturing methods to manufacture some of the cooling features used in the turbine section.
- There is uncertainty in the HRSG cost estimation. The higher gas turbine exhaust for AFGT cases can increase the HRSG capital cost if higher strength alloys (such as Inconel alloys are required.
- The ammonia fuel delivery system of the AFCC (inside plant) might require changes to the piping system (pressurization and heating) that are not included in the cost calculations and is a source of uncertainty.

The details of each calculation are provided in the following subsections. All the costs are expressed in 2018-dollar year.

5.1 AMMONIA FUEL COST

The ammonia fuel cost highly depends on how the ammonia is produced, from where it is exported, and the profitability margin for the current ammonia producers [32]. In this study, literature research was made to determine the minimum and maximum ranges for ammonia fuel cost. It should be noted that the production rates, transportation costs, and the profit margins for fuel usage will be different than for fertilizer production cases of ammonia. The data includes costs from coal, natural gas reforming and renewables-based ammonia production. The estimations gave a range of 0.1–1.44 $/kg, where the low ends and high ends of various studies differed within this range [32–39]. Some of the ammonia fuel cost values used in determining the study range are shown in Exhibit 5-1.

Exhibit 5-1. HHV-based ammonia fuel costs from literature used in determining the fuel cost range of this study (HHV of ammonia is 9,670 Btu/lb)



The study range is determined using data from open literature [32, 33, 35,36, 38, 39], NETL studies on ammonia for fuel production [34, 37] and with one special case. The low end of the current study range was extended to cover the special case of ammonia fuel cost equaling natural gas fuel cost in NETL's Bituminous Baseline -Revision 4 (Fossil Energy Baseline [FEB] Rev.4) [31], which is 0.09 $/kg (4.42 $/MMBtu-higher heating value [HHV]). For the base case comparison purposes, the NH_3 production cost is assumed to be $0.3/kg which is minimum cost for manufacturers profitability [33].

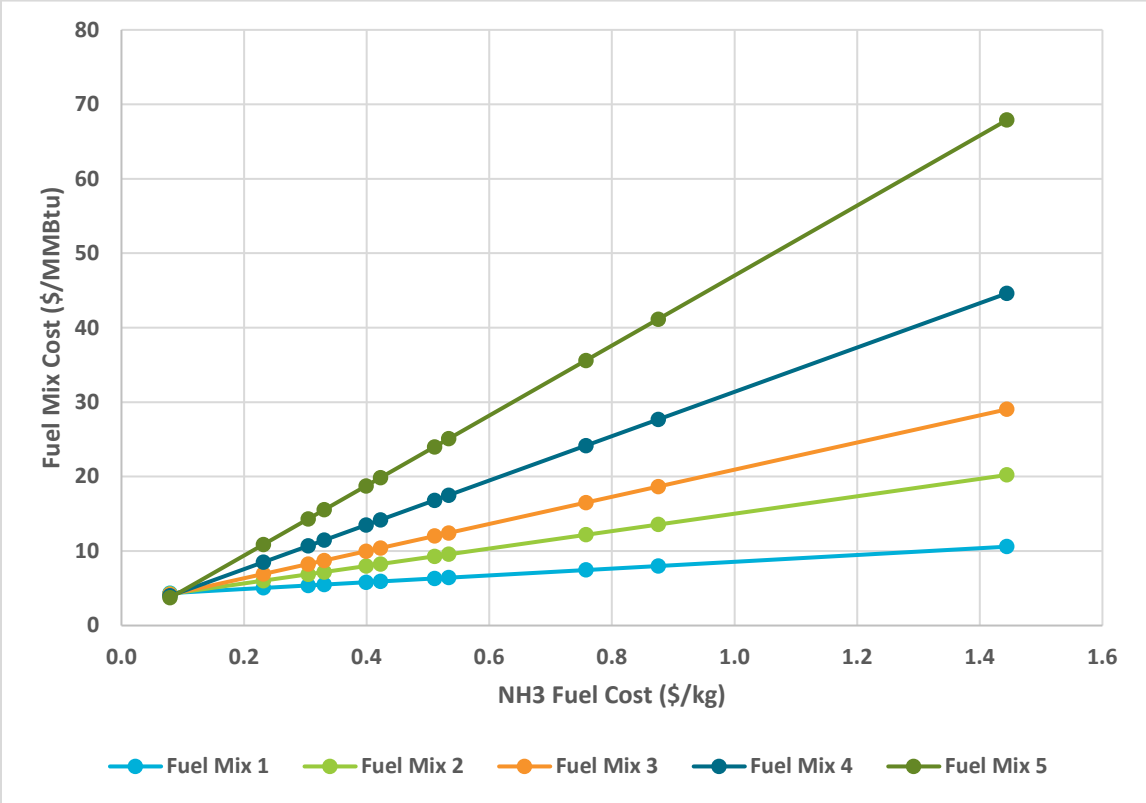
In addition to the NH_3 production price, NH_3 fuel cost should also include the transportation cost for NH_3 unless the production site is very close to the end-use. The NH_3 transportation cost depends on the mode of transportation used and transport distances. Based on literature review, the NH_3 pipeline transportation prices are in the range of $0.04 - $0.05/ton/km for long distance transportation. For the current study, the NH_3 fuel transportation price is assumed to be $0.09/kg for approximately 1,000 miles of transportation via dedicated NH_3 pipelines. Including the production and transportation costs, the baseline NH_3 fuel cost of $0.39/kg is used for rest of the report (except for NH_3 fuel price sensitivity analyses).

The fuel cost of the ammonia-methane fuel mixtures is calculated using Equation (7).

$$Fuel\ Total\ Cost = NH_3\ Energy\ Fraction \times NH_3\ Fuel\ Cost \left(\frac{\$}{MMBtu}\right) + NG\ Energy\ Fraction \times NG\ Fuel\ Cost \left(\frac{\$}{MMBtu}\right) \quad (7)$$

The dependency of the fuel cost of each fuel mixture on the ammonia fuel cost is linear. Exhibit 5-2 shows the dependency of each fuel mixtures cost on the ammonia fuel cost in $/kg basis (HHV basis).

Exhibit 5-2. Fuel mixture cost dependency on the ammonia fuel cost (HHV basis)



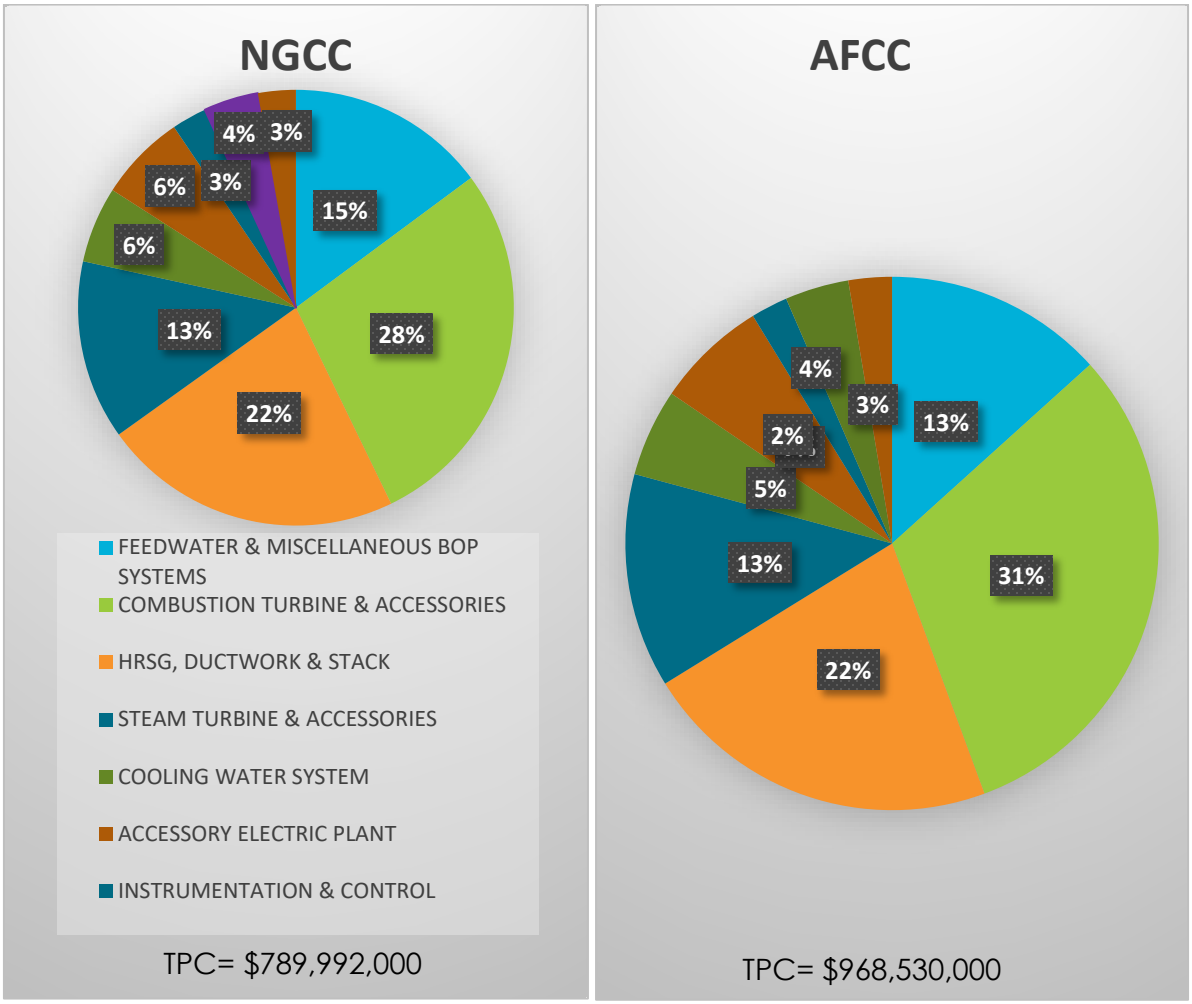
5.2 Ammonia Fuel Combined Cycle Capital Costs Calculation

A capital cost estimation analysis was run for each mixture case. The Quality Guidelines for Energy System Studies Cost Estimation Methodology for NETL Assessments of Power Plant Performance method [40] was used for cost estimation. A cost scaling was made using the Quality Guidelines for Energy System Studies Scaling Methodology [41] for the AFGT from H-class (FEB Rev.4) values. Maximum values of the capital cost items were then calculated and used in the cost calculations of AFCC, as it represents the high end of the cost range.

The reason behind using the maximum values of the capital costs estimated for AFCC items is to have a single gas turbine frame to support all of the studied fuel mixtures. Similarly, when the fuel is changed, there will be no changes in the steam cycle components. However, the steam cycle components will be capable of supporting the flue gas changes from switching between the fuel mixture operations. Therefore, there will be a single set of capital cost items for all fuel mixture cases, and the maximum values will represent the high end of the capital cost range. Hence, the gas turbine and steam cycle component costs used in LCOE, and sensitivity calculations are from the maximum values of all fuel mix cases. The capital cost values used in this study are presented in the Appendix B: Capital Costs for Ammonia Combined Cycle.

The distribution of the capital cost items in the overall power plant cost are compared for AFCC with NGCC values in Exhibit 5-3.

Exhibit 5-3. Distribution of capital cost items compared for AFCC with NGCC (w/o CCS)



The cost distributions obtained for AFCC is comparable to NGCC, except for the gas turbine and related accessories, which has 3 percent more weight (absolute) in the AFCC case compared to NGCC. The combustion turbine cost could be higher than the scaled values because of the advanced manufacturing methods usage, new combustor technology, and having a fifth turbine stage. This is mostly because of having higher capital cost for the AFGT compared to a natural gas engine. The HRSG cost could be higher than the scaled values because of the need for using advanced materials in the duct to compensate for the higher flue gas temperature.

5.3 Levelized Cost of Electricity, Owner's Costs and Operating Costs

The LCOE values calculated for AFCC cases are compared with each other and to F- and H-class FEB Rev.4 values in Exhibit 5-4. For the baseline NH_3 fuel price of $0.39/kg, the LCOE of 100% NH_3 case (ACC Fuel Mix 5) is ~3.3x that of H-class NGCC plant without carbon capture.

Exhibit 5-4. LCOE comparison of AFCC cases with NGCC without CCS for ammonia fuel cost of $0.39/kg

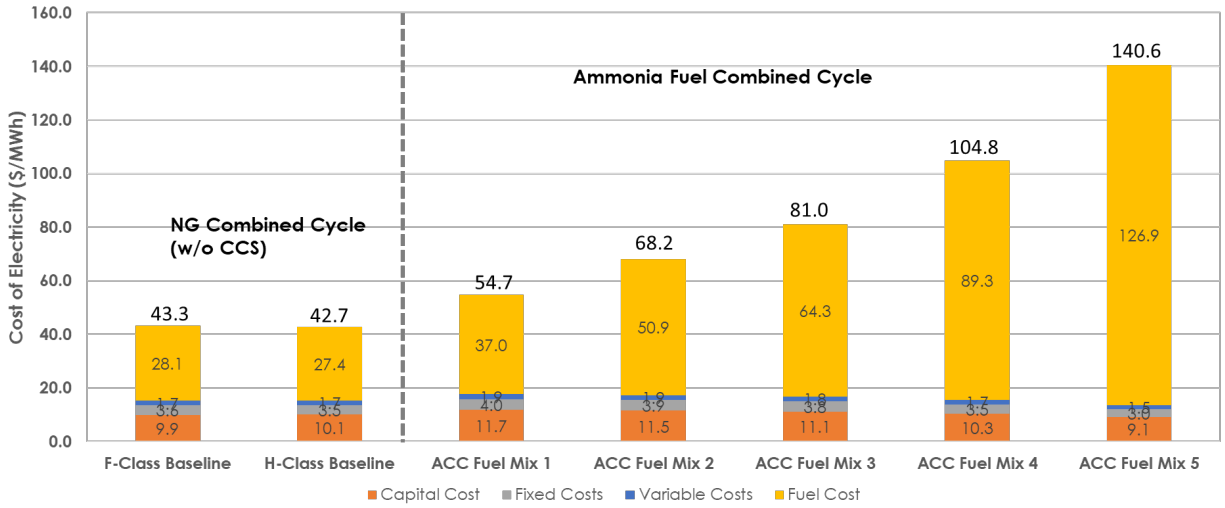
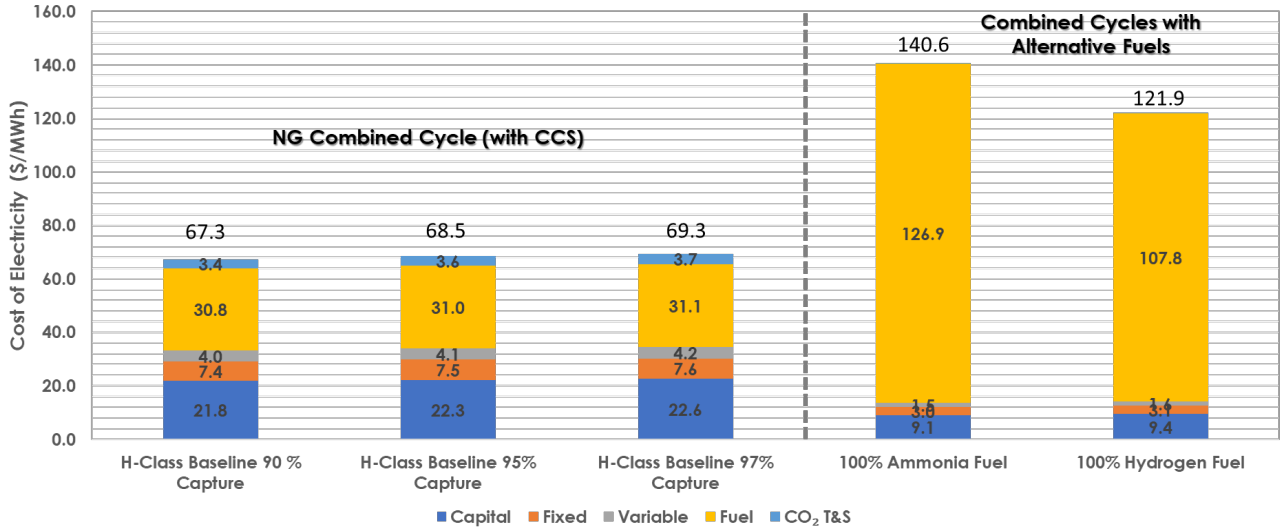


Exhibit 5-5 shows a comparison of the 100 percent ammonia fuel case LCOE compared with 90, 95, and 97 percent capture H-class NGCC cases as well as to the 100 percent hydrogen fuel case LCOE. Per the estimations, ammonia fuel cost is lower than hydrogen fuel cost but significantly higher fuel flow than hydrogen is needed for ammonia combustion, which makes ammonia combined cycle have lower efficiency than hydrogen cycle. The fraction of the fuel cost is therefore higher in AFCC, compared to HCC. All other LCOE cost components are slightly lower in AFCC than HCC, which are the operating costs and capital costs. This is mostly due to the power output of AFCC being lower than for HCC case.

Exhibit 5-5. LCOE comparison of AFCC cases with NGCC with CCS for ammonia fuel price if $0.39/kg and hydrogen fuel price of $2.4/kg



As the carbon capture rate is increased for NGCC cases, the LCOE also increases due to the higher capital and operating costs associated with capture. However, Alternative fuel combined cycles (ACC and HCC) produce negligible carbon emissions without the need for post-combustion CO_2 capture using the carbon capture equipment and chemicals. The LCOE of 100%

NH_3 fuel case (ACC Mix 5) is ~2x that of H-class NGCC plant with 97% CO_2 capture. In case of 100% H_2 fuel case, the LCOE is ~1.8x that of H-class NGCC plant with 97% CO_2 capture. For the 100 percent ammonia system to have the same LCOE with the NGCC capture cases, the ammonia fuel price needs to be as low as $9/MMBtu ($174/ton) and in case of 100 percent H_2 system, the fuel price needs to be as low as $9.2/MMBtu ($1.23/kg) in order to achieve LCOE parity with NGCC cases with capture.

The total Plant costs (TPC) and total as spent costs (TASC) are compared in Exhibit 5-6 for the AFCC cases with F- and H-class FEB Rev.4 values. The TPC is about 12–16 percent higher than NGCC levels for AFCC cases. As the ammonia fraction is increased in the HCC, the owner's costs become comparable with NGCC levels on a $/kW basis.

Fixed operating costs include annual operating labor, maintenance labor, administrative and support labor, property taxes, and insurance cost items. The operating personnel are assumed to be the same as NGCC cases in the fixed operating costs calculations. The fixed operating costs are compared in Exhibit 5-7 for the AFCC cases with F- and H-class FEB Rev.4 value.

Fixed operating costs of AFCC cases are slightly lower than F- and H-class NGCC baseline cases in $/kW basis for fuel mixtures containing ammonia fractions 80 percent and higher. The study did not include any specific tax incentives that might become available for AFCC power plants in the future. If there are such special tax reductions, the tax-related costs could be lower for AFCC.

The variable operating costs include maintenance materials, water costs, makeup and wastewater chemicals, ammonia cost, SCR catalyst cost, and disposal costs. Variable operating costs are compared in Exhibit 5-8 for the AFCC cases with F- and H-class FEB Rev.4 values. The comparison in Exhibit 5-8 shows that the variable operating costs and their distributions are similar with H-class NGCC levels without carbon capture. For the fuel mixtures containing 80 percent and higher ammonia (by mass), variable operating costs are slightly lower than for NGCC.

Exhibit 5-6. TPC and TASC comparison of AFCC cases with NGCC without CCS for ammonia fuel cost $0.39/kg

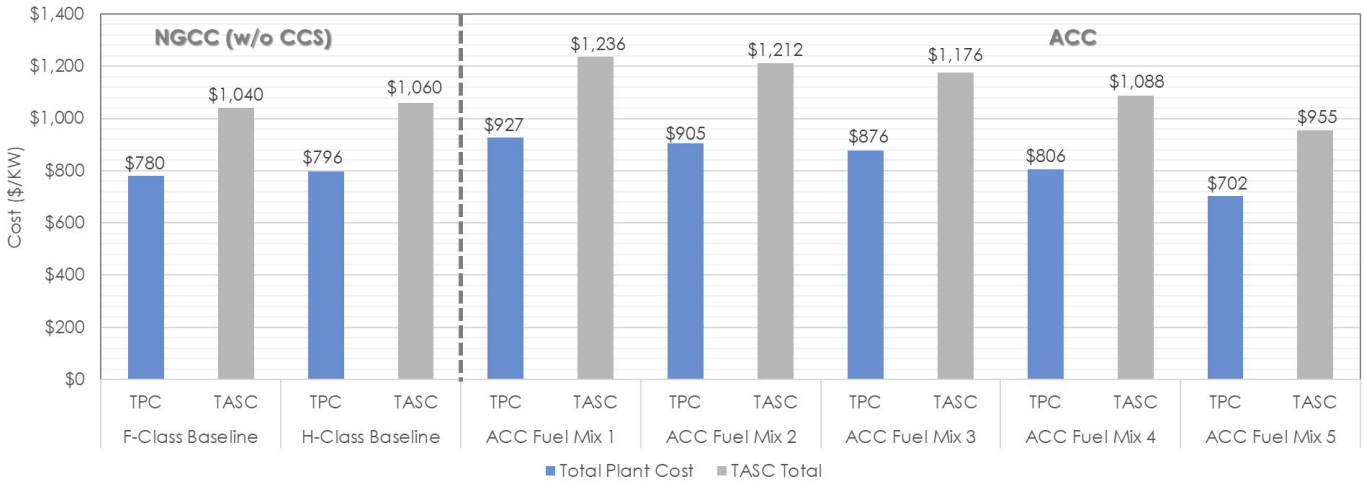


Exhibit 5-7. Fixed operating costs comparison of AFCC cases with NGCC without CCS for ammonia fuel cost $0.39/kg

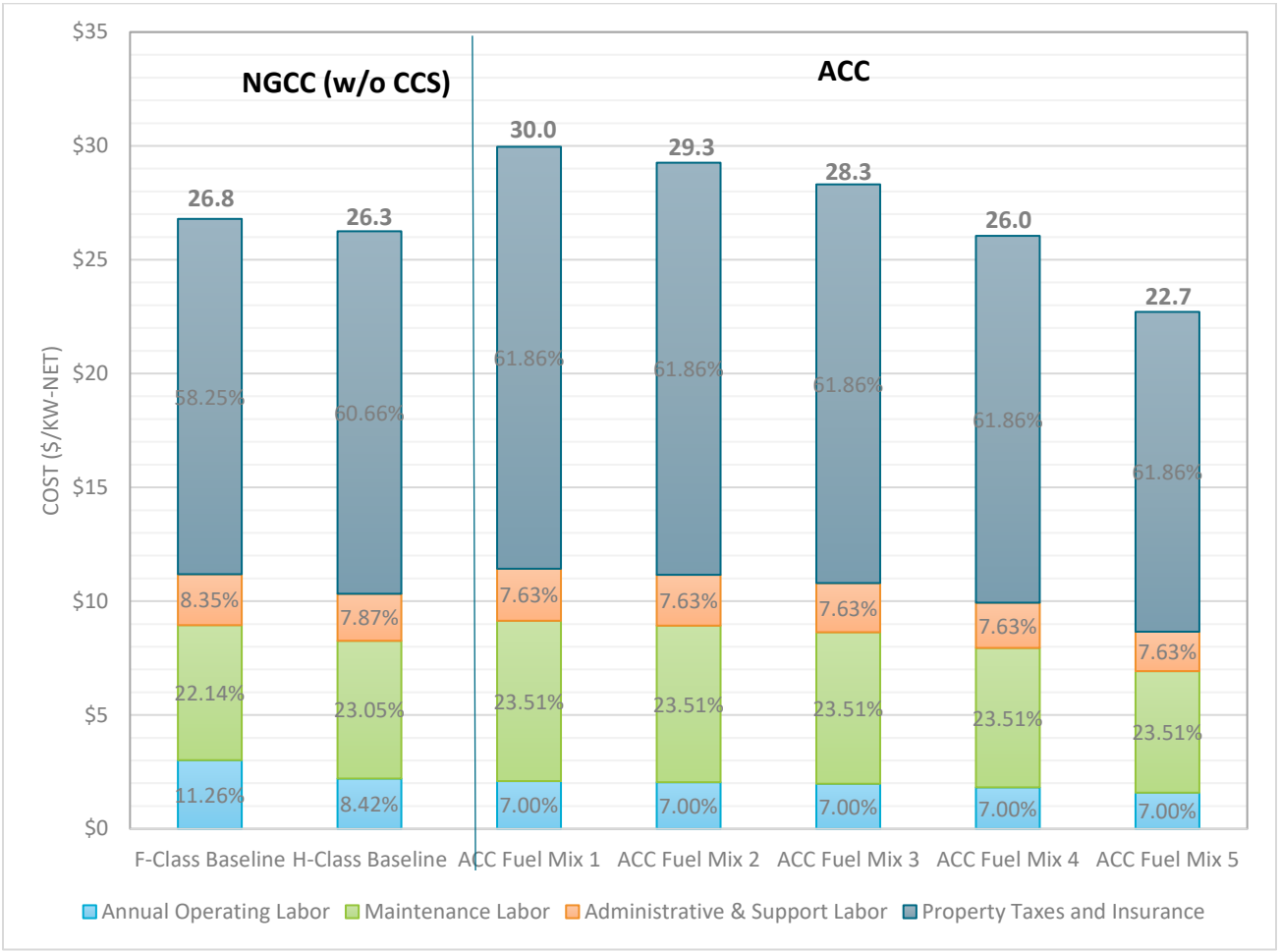
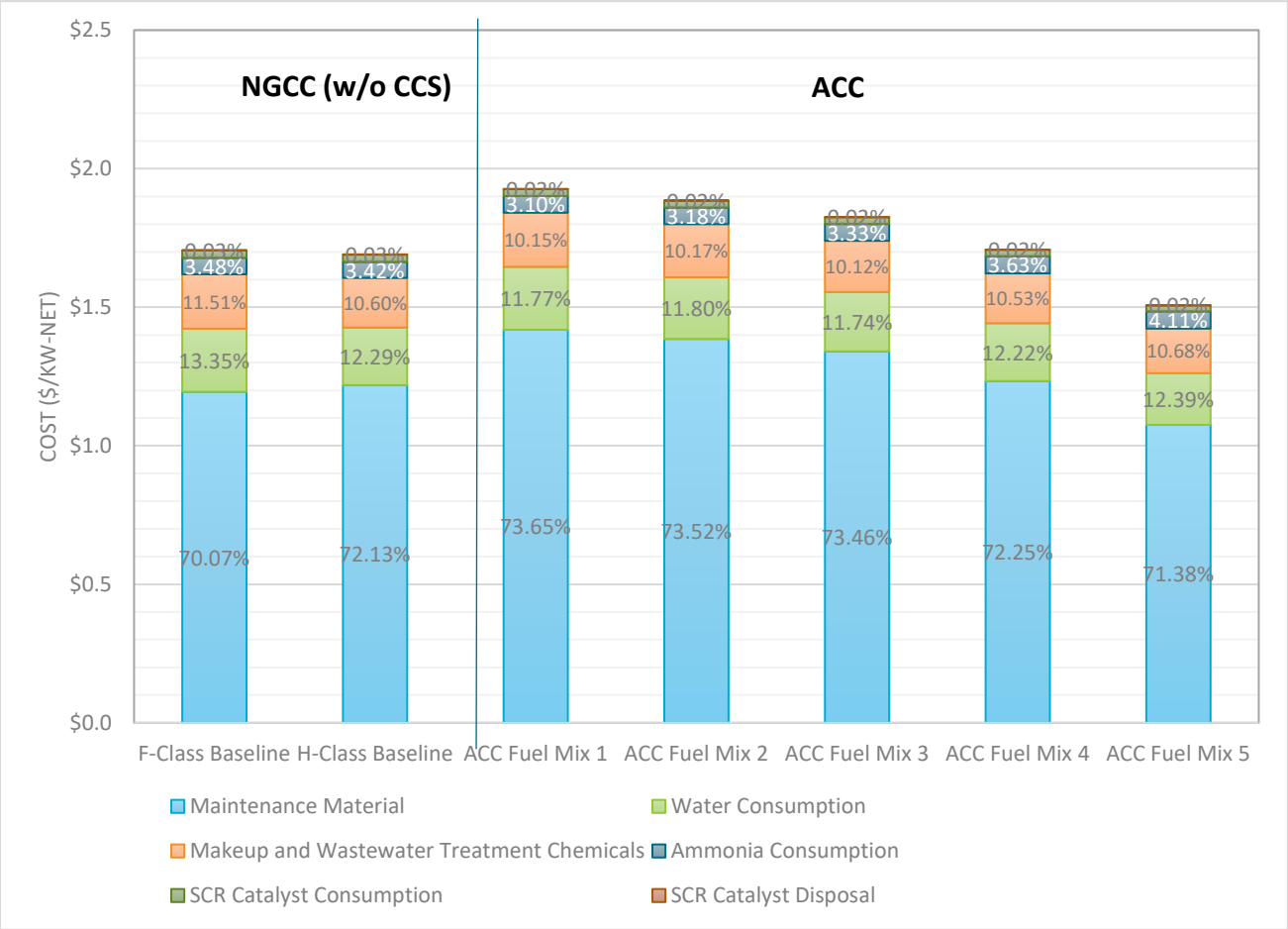


Exhibit 5-8. Variable operating costs comparison of AFCC cases with NGCC without CCS for ammonia fuel cost $0.39/kg

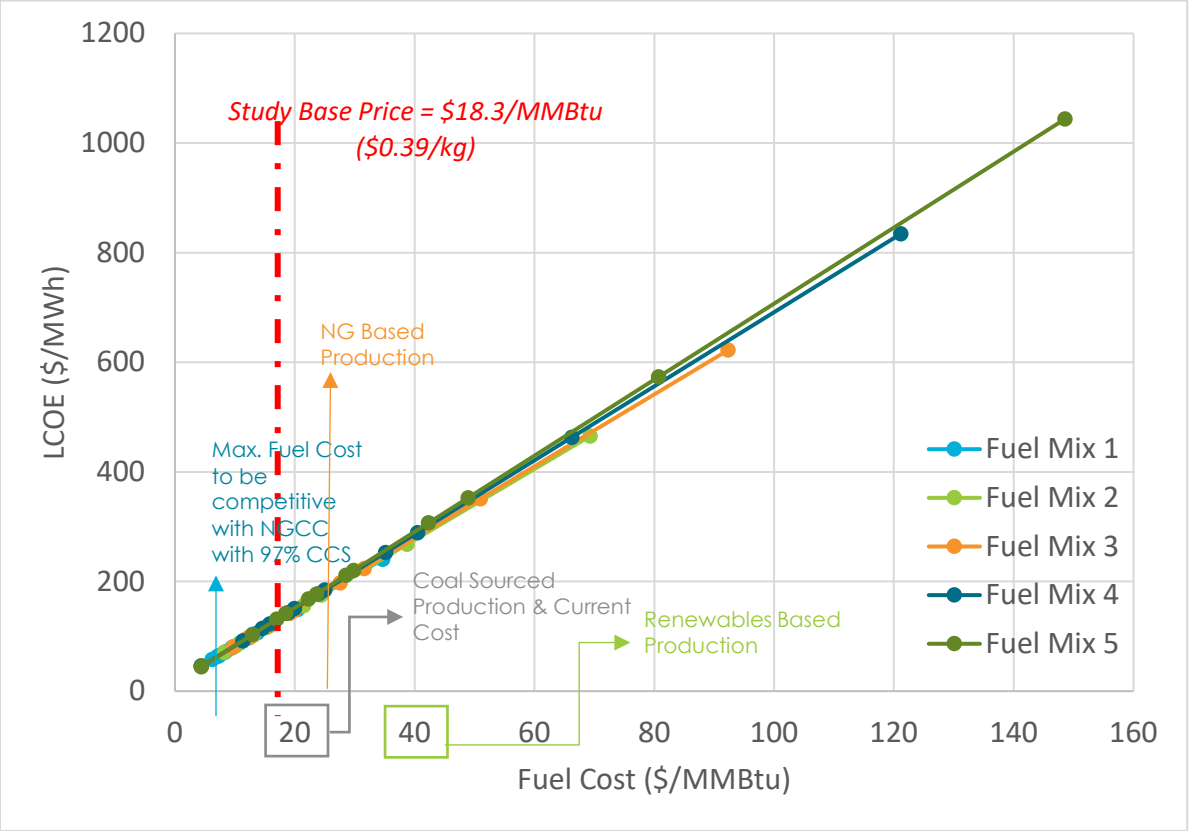


5.4 Levelized Cost of Electricity Sensitivity Analysis

5.4.1 Ammonia Fuel Cost Sensitivity

The sensitivity of the LCOE on the fuel price was studied for each fuel mixture case. In order to have the highest profit from the power plant, the cost of electricity from that plant should be impacted less from the fuel price changes; therefore, lower dependency of this sensitivity is desired. The fuel cost range varies significantly for the cases having higher ammonia content more than 60 percent (by fuel mass fraction). This is because of the wide range of ammonia fuel costs. The LCOE sensitivity curves for ammonia fuel cost for AFCC fuel mixture cases are shown in Exhibit 5-9.

Exhibit 5-9. LCOE sensitivity of AFCC on ammonia fuel cost

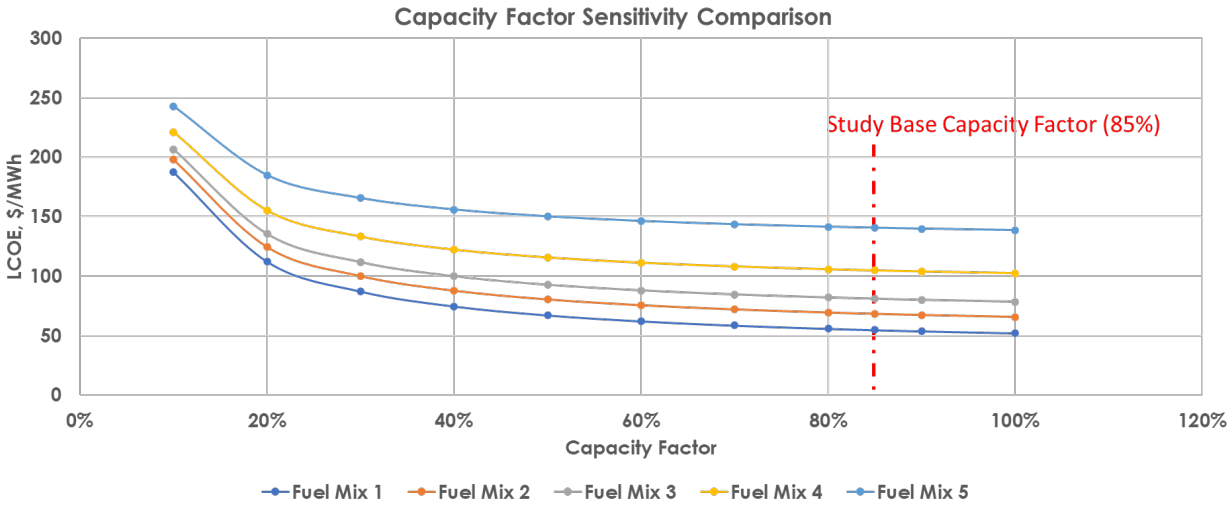


The sensitivity of the LCOE for each fuel case is compared by using the slopes of each curve. In terms of the magnitude of sensitivities, there is no significant difference among different fuel mixes. But the dependence of the LCOE on the fuel cost is lower for the cases having less ammonia content. The order for increasing LCOE sensitivity is as follows: Mix 1 (lowest), Mix 2, Mix 3, Mix 4, and Mix 5 (highest).

5.4.2 Capacity Factor Sensitivity

Another important parameter for the cost of electricity is the plant capacity factor, which is the fraction of the total electricity that would be generated if the plant operated at full load without interruption. The low end of the sensitivity range was selected as 10 percent, as the AFCC can be used in the future together with the variable renewable energy systems. The LCOE sensitivity curves for ammonia fuel cost for AFCC fuel mixture cases are shown in Exhibit 5-10.

Exhibit 5-10. LCOE sensitivity of AFCC on plant capacity factor



Comparison of this sensitivity for each fuel case shows that higher ammonia fuel content cases have lower dependency on the capacity factor changes, as compared to higher natural gas containing cases. The slopes of the curves are used to obtain the order of impact for this sensitivity. The order for increasing LCOE sensitivity is as follows: Mix 5 (lowest), Mix 4, Mix 3, Mix 2, and Mix 1 (highest).

6 CONCLUSION

In this study, a gas turbine design was made to support the flexible fuel operation for ammonia-methane fuel mixtures. The design is a slight variation of current natural gas fuel operating gas turbines, due to ammonia not requiring higher firing temperatures and to use technologies similar to current gas turbines in production and to increase the market applicability of the engine. The gas turbine design AFGT, and its turbomachinery design and cooling design were completed. Combined cycle performance analysis with the ammonia fuel mixes was performed. The cycle performance results were then used in the cost analysis, where the cost of electricity and plant costs were calculated and compared with current NGCC levels.

A combustor technology known as "two-stage combustion," which is based on RQL combustor technology was selected for this study to reduce the NOx emissions and to eliminate unburned ammonia in the gas turbine exhaust. The RQL combustor design is a proven technology and can reduce the NOx emissions to the current SCR technology limits. A simple combustion analysis was performed with the two-stage combustor model developed at NETL and the combustor design details for minimum NOx emissions were determined.

Gas turbine performance analysis showed that AFGT has comparable and, in some cases, higher performance than most of the current H-Class engines. The results from the gas turbine performance analysis show that ammonia gas turbine can be an easier step to carbon-free fuels before hydrogen because of having a similar gas turbine design to current natural gas engine systems, current level technology materials and coatings technologies could be used in ammonia gas turbine and ammonia being readily available in commercial scale.

Cooling analysis showed that AFGT has the potential to reach 47 percent gas turbine efficiency with 100 percent ammonia fuel (by fuel mass fraction). A sensitivity analysis on cooling parameters showed that the order of impact strengths of cooling design parameters on performance of an NH_3 fuel GT is the same for natural gas (NG) and H_2 fuel GTs, where the blade material temperature limit has the highest impact, followed by film cooling, internal cooling, and TBC performance.

The ammonia combined cycle performance analysis showed that the steam turbine power output increases from fuel mixture 1 to 5, which is due to having higher steam content in the gas turbine exhaust. However, the increase in the gas turbine power output and steam turbine output are compensated with the increased fuel usage, which resulted in almost constant combined cycle efficiency for all ammonia fuel fractions. However, ammonia combined cycle LHV efficiency, which is 60 percent, is comparable with current level NGCC's using F-Class gas turbines.

The preliminary cost analysis showed that the LCOE of 100% NH_3 fired combined cycle case is ~2x that of H-class NGCC plant with 97% CO_2 capture, assuming that the NH_3 fuel cost is $0.39/kg (which includes $0.3/kg for production and $0.09/kg for transportation). To achieve LCOE parity with NGCC (97% CCS), ammonia fuel cost should be less than $150/ton ($7.77/MMBtu) and to achieve LCOE parity with NGCC without CCS, ammonia fuel cost should be less than $83/ton ($4.31/MMBtu). The results may differ if the gas turbine and HRSG costs are changed significantly, beyond the Quality Guidelines for Energy System Studies (QGESS)

standard scaling estimations used in this study. One of the major outcomes of this study is that significant research and development is needed to reduce the ammonia fuel cost to 1/3 of its current level values (14.0–20.0 $/MMBtu), for ammonia to be a feasible fuel option for large frame gas turbines and combined cycle systems.

Potential future work ideas include a gas turbine design with higher firing temperature and higher power output. There might be some improvements in combined cycle performance metrics for this case because the current design gives combined cycle efficiencies on the same level as current NGCC technologies. In this study, the steam cycle specifics were used as the same from B32A NGCC values and some potential improvement areas for the combined cycle were identified for increasing the cycle efficiency further. If the steam cycle maximum temperature and pressure is increased, the steam cycle efficiency could be further increased for AFCC cases. Higher pressure ratios could increase the steam turbine power output, which eventually would increase the maximum AFCC cycle efficiency above 60 percent. A detailed cost analysis for all gas turbine sub-systems can be done for AFGT design to improve the accuracy of the cost analysis calculations.

7 REFERENCES

[1] Karabeyoğlu A. and Evans B., (2013), "Ammonia based Fuels for Environmentally Friendly Power Generation," Presentation for NH_3 Fuel Conference 2013, Sacramento, CA

[2] NH_3 Fuel Association, "Comparisons-The Logical Path Forward," retrieved from https://nh3fuelassociation.org/comparisons/ in May 2022

[3] Okafor E., Hayakawa A., and Kobayashi H. et al., (2019), "Pure Ammonia Combustion Micro-Gas Turbine System," Presentation at AICHE 2019, Orlando, FL

[4] Kurata O., Iki N., Inoue T. et al., (2018), "Development of Low-NOx Combustor of Micro Gas Turbine Firing Ammonia Gas," Presentation at AICHE 2018, Pittsburgh, PA

[5] Uchida M., Ito S., Suda T., and Fujimori T., (2019), "Performance of Ammonia/Natural Gas Co-Fired Gas Turbine with Two Stage Combustor," Presentation at AICHE 2019, Orlando, FL

[6] Pratt D.T., (1967), "Performance of Ammonia Fired Gas Turbine Combustors," Technical Report TS-67-5, University of California- Berkeley

[7] Valerie-Medina A., Bowen P. and Pugh D., (2018), "Ammonia-Hydrogen Power for Combustion Engines," Presentation at 2018 Ammonia Fuel Conference, Pittsburgh, PA

[8] Okafor E.C., Hayakawa A., and Kobayashi H., (2019), "Pure Ammonia Combustion for Micro Turbine System," Presentation at 2019 AIChe Annual Meeting, Orlando, FL

[9] Uchida M., Ito S., Suda T., and Fujimori T., (2019), "Performance of Ammonia/Natural Gas Co-Fired Gas Turbine with Two Stage Combustor," Presentation at 2019 AIChe Annual Meeting, Orlando, FL

[10] Patel S., (2021), "Mitsubishi Power Developing 100% Ammonia Capable Gas Turbine," Power Magazine, retrieved on May 13, 2022, from https://www.powermag.com/mitsubishi-power-developing-100-ammonia-capable-gas-turbine/

[11] SBIR-STTR Project, DOE Award Number DESC00290903, retrieved from https://www.sbir.gov/node/1834409

[12] DOE Office of Fossil Energy and Carbon Management, Additional Selections for Funding Opportunity Announcement 2400: Fossil Energy Based Production, Storage, Transport and Utilization of Hydrogen Approaching Net-Zero or Net-Negative Carbon Emissions, retrieved from https://www.energy.gov/fecm/articles/additional-selections-funding-opportunity-announcement-2400-fossil-energy-based

[13] Miller J.A., Smooke M.D., Green R.M. and Kee R.J., (1983), "Kinetic Modeling of the Oxidation of Ammonia in Flames," Combust. Sci. Technol., Vol. 34, pp. 149–176

[14] Kobayashi H., Hayakawa A., Kunkuma K.D., Somarathne A. and Okafor E.C., (2019), "Science and technology of ammonia combustion," Proceedings of the Combustion Institute, Vol. 37, pp.109-133

[15] K.D.K.A. Somarathne, S. Hatakeyama , A. Hayakawa , H. Kobayashi, (2017), " Numerical study of a low emission gas turbine like combustor for turbulent ammonia/air premixed swirl flames with a secondary air injection at high pressure," Int. J. Hydrogen Energy, Vol. 42 pp. 27388–27399

[16] Samuelsen S., (2006), "Rich Burn, Quick Mix, Lean Burn (RQL) Combustors," NETL Gas Turbine Handbook, NETL, Pittsburgh, PA

[17] Bedick C., (2022), Python Code for Two-Stage Combustor Analysis, NETL, Pittsburgh, PA

[18] Li Z. and Li S., (2021), "Kinetics Modelling of NOx Emissions Characteristics of a NH3/H2 Fueled Gas Turbine Combustor," International Journal of Hydrogen Energy, Vol. 46, Elsevier Inc., pp. 4526–4537

[19] Uysal S.C., (2017), "Analytical Modelling of the Effects of Different Gas Turbine Cooling Techniques on Engine Performance," Ph.D. Thesis, West Virginia University, ProQuest Publishing, Ann Harbor, MI

[20] Burnes D. and Camou A., (2019), "Impact of Fuel Composition on Gas Turbine Engine Performance," Journal of Engineering for Gas Turbines and Power, Vol. 141, p. 101006

[21] Siemens Energy Inc., (2015), "Advanced Hydrogen Turbine Development-Final Report for DOE Award DE-FC26-05NT42644," DOE-SEI-42644, Orlando, FL

[22] GE Power and Water, (2015), "Advanced IGCC/Hydrogen Gas Turbine Development-Final Report for DOE Award DE-FC26-05NT-42643," Schenectady, NY

[23] Siemens Power Generation Inc., (2007), "Advanced Hydrogen Turbine Development-Phase 1 Report for DOE Award DE-FC26-05NT42644," Orlando, FL

[24] Lee K.N., (2007), "Chapter 4.4.2-Protective Coatings for Gas Turbines," in NETL Gas Turbine Handbook, Morgantown, WV

[25] Pint B. and Kane K.A., (2021), "Next Generation Environmental Barrier Coatings (FEAA121)," Presentation for UTSR 2021 Meeting, retrieved in December 2021 from https://netl.doe.gov/sites/default/files/netl-file/21UTSR_Pint.pdf

[26] Chiesa P., Lozza G. and Mazzocchi L., (2005), "Using Hydrogen as Gas Turbine Fuel," Journal of Engineering for Gas Turbines and Power, Vol. 127, pp. 73–80

[27] ASPENTech Inc., (2017) "ASPEN Plus v10," Bedford, MA

[28] Wahl J. and Harris K., (2015), "Recent Advances in Cast SX Superalloys," Cannon-Muskegan Corporation Presentation at TMS 2015 Conference, Orlando, FL

[29] Gibbons T.B. and Wright I.G., (2009), "A Review of Materials for Gas Turbines Firing Syngas Fuels," ORNL/TM-2009/137, Oak Ridge, TN

[30] Gas Turbine World Magazine, (2020), "2020 Gas Turbine World Performance Specifications," Pequot Publishing, Fairfield, CT

[31] James, R., Zoelle, A., Keairns, D., Turner, M., Woods, M., Kuehn, N., Shah, V., Chou, V. and Pinkerton, L., (2022), "Cost and Performance Baseline for Fossil Energy Plants Volume 1: Bituminous Coal and Natural Gas to Electricity," DOE/NETL-2018/1885

[32] International Energy Agency, (2021), "The role of low-carbon fuels in the clean energy transitions of the power sector," Paris, France, p. 116

[33] Kawakami Y, Endo S, Hirai H, (2019) "A feasibility study on the supply chain of CO2-free ammonia with CCS and EOR," IEEJ Report, The Institute of Energy Economics, Japan, p.27

[34] Steele A.H., Zaremsky C., Charlton C., Chukwunenye K., Shirley P., Clahane L., Kumar Y., Newby R., and Pickenpaugh G., (2021), "Syngas Products from Coal Markets Analysis," NETL Report DOE/NETL-2021-2694, NETL, Pittsburgh, PA

[35] Tullo A T (2020) Yara plans to make green ammonia in Norway. Available from: https://cen.acs.org/business/petrochemicals/Yara-plans-make-green-ammonia/98/web/2020/12 last accessed in November 2022

[36] Hiraoka K, Fujimura Y, Watanabe Y, Kai M, Sakata K, Ishimoto Y, Mizuno Y, (2018), "Cost Evaluation Study on Low Carbon Ammonia and Coal Co-Fired Power Generation," NH3 Fuel Conference 2018, Pittsburgh, PA

[37] McNaul S. and White C.W.W, (2022), "Ammonia from Natural Gas Techno-Economic Analysis," NETL-Internal Report, NETL, Pittsburgh, PA

[38] Patonia A, Poudineh R, (2020), "Ammonia as a storage solution for future decarbonized energy systems," OIES Paper: EL 42., Oxford, UK, Oxford Institute for Energy Studies (OIES), p.44

[39] Argus Media Group, (2020), "Green shift to create 1 billion tonne 'green ammonia' market?", Whitepaper by Argus Media Group LLC, London, UK retrieved from: "Argus White Paper - Green Ammonia.pdf (argusmedia.com)"

[40] Gerdes K., Summers W.M. and Wimer J., (2011), "Cost Estimation Methodology for NETL Assessments of Power Plant Performance," DOE/NETL-2011/1455

[41] Turner M.J., Zoelle A. and Pinkerton L.L., (2019), "Capital Cost Scaling Methodology," DOE/NETL-PUB-2253

APPENDIX A: STREAM TABLE FOR 100% AMMONIA FUEL CASE

The main streams properties and state data for 100 percent ammonia fuel case (Mix 5) of ammonia combined cycle (AFCC) are presented in Exhibit A-1.

Exhibit A-1. AFCC stream Table for 100% Ammonia fuel case

Hierarchy Name					H-STMCYC	H-STMCYC	H-STMCYC	H-STMCYC	H-STMCYC	H-STMCYC	H-STMCYC
Stream Name	AIR-CT1	NG-1	CT-9	STKGAS-3	ST-MAIN3	HPS-1	HPS-8	IPS-1	HRS-LP3	LPS-COND	CN-PUMP
	CONVEN	CONVEN	CONVEN	CONVEN	CONVEN	CONVEN	CONVEN	CONVEN	CONVEN	CONVEN	CONVEN
Property Method	PENG-ROB	PENG-ROB	PENG-ROB	PENG-ROB	STEAM NBS	STEAM NBS	STEAM NBS	STEAM NBS	STEAM NBS	STEAM NBS	STEAM NBS
Stream Number	**1**	**2**	**3**	**4**	**5**	**6**	**7**	**8**	**9**	**10**	**11**
V-L Mole Fraction											
Ar	0.0092	0.0000	0.0078	0.0078	0.0000	0.0000	0.0000	0.0000	0.0000	0.0000	0.0000
CH_4	0.0000	0.0000	0.0000	0.0000	0.0000	0.0000	0.0000	0.0000	0.0000	0.0000	0.0000
CH_4S	0.0000	0.0000	0.0000	0.0000	0.0000	0.0000	0.0000	0.0000	0.0000	0.0000	0.0000
C_2H_6	0.0000	0.0000	0.0000	0.0000	0.0000	0.0000	0.0000	0.0000	0.0000	0.0000	0.0000
C_3H_8	0.0000	0.0000	0.0000	0.0000	0.0000	0.0000	0.0000	0.0000	0.0000	0.0000	0.0000
C_4H_{10}	0.0000	0.0000	0.0000	0.0000	0.0000	0.0000	0.0000	0.0000	0.0000	0.0000	0.0000
CO_2	0.0003	0.0000	0.0003	0.0003	0.0000	0.0000	0.0000	0.0000	0.0000	0.0000	0.0000
H_2O	0.0099	0.0000	0.1963	0.1963	1.0000	1.0000	1.0000	1.0000	1.0000	1.0000	1.0000
N_2	0.7732	0.0000	0.7147	0.7147	0.0000	0.0000	0.0000	0.0000	0.0000	0.0000	0.0000
O_2	0.2074	0.0000	0.0809	0.0809	0.0000	0.0000	0.0000	0.0000	0.0000	0.0000	0.0000
SO_2	0.0000	0.0000	0.0000	0.0000	0.0000	0.0000	0.0000	0.0000	0.0000	0.0000	0.0000
NH_3	0.0000	1.0000	0.0000	0.0000	0.0000	0.0000	0.0000	0.0000	0.0000	0.0000	0.0000

Total	1.0000	1.0000	1.0000	1.0000	1.0000	1.0000	1.0000	1.0000	1.0000	1.0000	1.0000
Flowrates (SI Units)											
V-L Flowrate (kg_{mole}/hr)	177,074	26,308	209,958	209,958	44,703	44,703	50,273	50,273	5,287	55,560	55,614
V-L Flowrate (kg/hr)	5,109,811	448,035	5,557,845	5,557,845	805,344	805,344	905,674	905,674	95,254	1,000,928	1,001,901
Solids Flowrate (kg/hr)	0	0	0	0	0	0	0	0	0	0	0
Thermodynamic State Data (SI Units)											
Temperature (°C)	15	27	653	85	585	336	562	296	287	38	38
Pressure (MPa, abs)	0.10	3.79	0.11	0.10	18.50	3.62	3.31	0.52	0.51	0.01	0.01
Steam Table Enthalpy (kJ/kg)*	30.23	-3,928.62	1,112.78	430.60	3,509.09	3,066.29	3,593.90	3,054.93	3,037.05	2,360.12	160.78
AspenPlus Enthalpy (kJ/kg)**	-97.58	-3,928.62	-1,046.76	-1,728.94	-12,471.21	-12,914.01	-12,386.39	-12,925.37	-12,943.24	-13,620.17	-15,819.51
Density (kg/m^3)	1.2	599.5	0.4	0.9	51.8	13.9	8.7	2.0	2.0	0.1	992.8
V-L Molecular Weight	28.857	17.031	26.471	26.471	18.015	18.015	18.015	18.015	18.015	18.015	18.015
Flowrates (English Units)											
V-L Flowrate (lb_{mole}/hr)	390,381	57,999	462,879	462,879	98,554	98,554	110,832	110,832	11,657	122,489	122,608
V-L Flowrate (lb/hr)	11,265,204	987,747	12,252,951	12,252,951	1,775,480	1,775,480	1,996,668	1,996,668	210,000	2,206,668	2,208,814
Solids Flowrate (lb/hr)	0	0	0	0	0	0	0	0	0	0	0
Thermodynamic State Data (English Units)											

Temperature (°F)	59	80	1,207	186	1,085	637	1,044	565	549	101	101
Pressure (psia)	14.7	550.0	15.5	14.8	2,683.2	525.0	479.8	75.0	73.5	1.0	1.0
Steam Table Enthalpy (Btu/lb)[A]	13.0	-1,689.0	478.4	185.1	1,508.6	1,318.3	1,545.1	1,313.4	1,305.7	1,014.7	69.1
AspenPlus Enthalpy (Btu/lb)[B]	-42.0	-1,689.0	-450.0	-743.3	-5,361.7	-5,552.0	-5,325.2	-5,556.9	-5,564.6	-5,855.6	-6,801.2
Density (lb/ft^3)	0.076	37.423	0.023	0.056	3.233	0.869	0.546	0.125	0.124	0.003	61.977
	[A] Steam Table Reference conditions are 32.02 °F & 0.089 psia										
	[B] AspenPlus thermodynamic reference state is the component's constituent elements in an ideal gas state at 25°C and 1 atm.										

APPENDIX B: CAPITAL COSTS FOR AMMONIA COMBINED CYCLE

The capital costs calculated for ammonia combined cycle (AFCC) are presented in Exhibit B-1.

Exhibit B-1. Capital costs calculated for AFCC cases

Case:	AFCC					Estimate Type:			Conceptual	
Plant Size (MW, net):	1379					Cost Base:			Dec-18	
Description	Equipment Cost	Material Cost	Labor		Bare Erected Cost	Eng'g CM H.O.& Fee	Contingencies		Total Plant Cost	
			Direct	Indirect			Process	Project	$/1,000	$/kW (net)
3	FEEDWATER & MISCELLANEOUS BOP SYSTEMS									
Feedwater System	$2,441	$4,185	$2,092	$0	$8,718	$1,744	$0	$1,569	$12,031	$9
Water Makeup & Pretreating	$5,186	$519	$2,939	$0	$8,644	$1,729	$0	$2,075	$12,447	$9
Other Feedwater Subsystems	$1,389	$455	$433	$0	$2,277	$455	$0	$410	$3,142	$2
Service Water Systems	$1,574	$3,005	$9,729	$0	$14,308	$2,862	$0	$3,434	$20,603	$15
Other Boiler Plant Systems	$286	$104	$260	$0	$649	$130	$0	$117	$895	$1
Natural Gas Pipeline and Start-Up System	$12,341	$531	$398	$0	$13,270	$2,654	$0	$2,389	$18,312	$13
Waste Water Treatment Equipment	$6,841	$0	$4,193	$0	$11,034	$2,207	$0	$2,648	$15,889	$12
Open	$0	$0	$0	$0	$0	$0	$0	$0	$0	$0
Miscellaneous Plant Equipment	$18,904	$2,479	$9,607	$0	$30,991	$6,198	$0	$7,438	$44,626	$32
Subtotal	$48,962	$11,277	$29,651	$0	$89,889	$17,978	$0	$20,079	$127,946	$93
6	COMBUSTION TURBINE & ACCESSORIES									
Combustion Turbine Generator	$197,511	$0	$12,019	$0	$209,531	$41,906	$0	$37,716	$289,153	$210
Open	$0	$0	$0	$0	$0	$0	$0	$0	$0	$0
Combustion Turbine Accessories	$4,812	$0	$293	$0	$5,104	$1,021	$0	$919	$7,044	$5
Compressed Air Piping	$0	$1,589	$360	$0	$1,948	$390	$0	$351	$2,689	$2
Combustion Turbine Foundations	$0	$1,301	$1,407	$0	$2,708	$542	$0	$650	$3,900	$3
Subtotal	$202,323	$2,890	$14,078	$0	$219,292	$43,858	$0	$39,635	$302,785	$220
7	HRSG, DUCTWORK & STACK									
Heat Recovery Steam Generator	$76,189	$0	$19,047	$0	$95,236	$19,047	$0	$17,142	$131,426	$95
Heat Recovery Steam Generator Accessories	$28,574	$0	$5,288	$0	$33,862	$6,772	$0	$6,095	$46,729	$34
Ductwork	$0	$1,371	$953	$0	$2,324	$465	$0	$418	$3,207	$2
Stack	$13,115	$0	$2,427	$0	$15,542	$3,108	$0	$2,798	$21,448	$16
Heat Recovery Steam Generator, Ductwork & Stack Foundations	$0	$974	$914	$0	$1,887	$377	$0	$453	$2,718	$2
Selective Catalytic Reduction System	$1,971	$828	$1,155	$0	$3,955	$791	$0	$712	$5,458	$4
Subtotal	$119,849	$3,173	$29,783	$0	$152,805	$30,561	$0	$27,618	$210,985	$153

Case:	AFCC					Estimate Type:			Conceptual	
Plant Size (MW, net):	1379					Cost Base:			Dec-18	
Description	Equipment Cost	Material Cost	Labor		Bare Erected Cost	Eng'g CM H.O.& Fee	Contingencies		Total Plant Cost	
			Direct	Indirect			Process	Project	$/1,000	$/kW (net)
8	STEAM TURBINE & ACCESSORIES									
Steam Turbine Generator & Accessories	$47,259	$0	$6,921	$0	$54,180	$10,836	$0	$9,752	$74,768	$54
Steam Turbine Plant Auxiliaries	$206	$0	$470	$0	$676	$135	$0	$122	$933	$1
Condenser & Auxiliaries	$11,109	$0	$5,330	$0	$16,439	$3,288	$0	$2,959	$22,686	$16
Steam Piping	$10,971	$0	$4,446	$0	$15,417	$3,083	$0	$2,775	$21,275	$15
Turbine Generator Foundations	$0	$1,769	$2,922	$0	$4,690	$938	$0	$1,126	$6,754	$5
Subtotal	$69,545	$1,769	$20,088	$0	$91,402	$18,280	$0	$16,734	$126,416	$92
9	COOLING WATER SYSTEM									
Cooling Towers	$11,290	$0	$3,444	$0	$14,734	$2,947	$0	$2,652	$20,333	$15
Circulating Water Pumps	$1,479	$0	$87	$0	$1,566	$313	$0	$282	$2,162	$2
Circulating Water System Auxiliaries	$10,168	$0	$1,342	$0	$11,510	$2,302	$0	$2,072	$15,883	$12
Circulating Water Piping	$0	$3,014	$2,730	$0	$5,744	$1,149	$0	$1,034	$7,927	$6
Make-up Water System	$354	$0	$454	$0	$808	$162	$0	$145	$1,115	$1
Component Cooling Water System	$444	$0	$341	$0	$785	$157	$0	$141	$1,084	$1
Circulating Water System Foundations	$0	$697	$1,158	$0	$1,855	$371	$0	$445	$2,672	$2
Subtotal	$23,735	$3,712	$9,556	$0	$37,002	$7,400	$0	$6,772	$51,174	$37
11	ACCESSORY ELECTRIC PLANT									
Generator Equipment	$3,717	$0	$2,804	$0	$6,521	$1,304	$0	$1,174	$8,998	$7
Station Service Equipment	$3,994	$0	$343	$0	$4,336	$867	$0	$781	$5,984	$4
Switchgear & Motor Control	$5,702	$0	$989	$0	$6,692	$1,338	$0	$1,204	$9,234	$7
Conduit & Cable Tray	$0	$1,378	$3,971	$0	$5,349	$1,070	$0	$963	$7,382	$5
Wire & Cable	$0	$2,057	$3,677	$0	$5,734	$1,147	$0	$1,032	$7,913	$6
Protective Equipment	$175	$0	$609	$0	$784	$157	$0	$141	$1,082	$1
Standby Equipment	$877	$0	$810	$0	$1,687	$337	$0	$304	$2,329	$2
Main Power Transformers	$15,515	$0	$317	$0	$15,832	$3,166	$0	$2,850	$21,848	$16
Electrical Foundations	$0	$145	$368	$0	$513	$103	$0	$123	$738	$1
Subtotal	$29,980	$3,580	$13,888	$0	$47,448	$9,490	$0	$8,571	$65,509	$48
12	INSTRUMENTATION & CONTROL									
Natural Gas Combined Cycle Control Equipment	$239	$0	$152	$0	$392	$78	$0	$71	$541	$0
Combustion Turbine Control Equipment	$492	$0	$313	$0	$805	$161	$0	$145	$1,112	$1
Steam Turbine Control Equipment	$384	$0	$244	$0	$628	$126	$0	$113	$867	$1
Other Major Component Control Equipment	$597	$0	$380	$0	$977	$195	$0	$176	$1,349	$1

Case:	AFCC					Estimate Type:			Conceptual	
Plant Size (MW, net):	1379					Cost Base:			Dec-18	
Description	Equipment Cost	Material Cost	Labor		Bare Erected Cost	Eng'g CM H.O.& Fee	Contingencies		Total Plant Cost	
			Direct	Indirect			Process	Project	$/1,000	$/kW (net)
Signal Processing Equipment	$537	$0	$16	$0	$553	$111	$0	$100	$763	$1
Control Boards, Panels & Racks	$132	$0	$80	$0	$212	$42	$0	$38	$293	$0
Distributed Control System Equipment	$7,317	$0	$223	$0	$7,539	$1,508	$0	$1,357	$10,404	$8
Instrument Wiring & Tubing	$604	$483	$1,933	$0	$3,020	$604	$0	$544	$4,168	$3
Other Instrumentation & Controls Equipment	$418	$0	$969	$0	$1,387	$277	$0	$250	$1,914	$1
Subtotal	$10,720	$483	$4,311	$0	$15,514	$3,103	$0	$2,793	$21,410	$16
13	IMPROVEMENTS TO SITE									
Site Preparation	$0	$714	$15,152	$0	$15,866	$3,173	$0	$3,808	$22,847	$17
Site Improvements	$0	$2,296	$3,032	$0	$5,328	$1,066	$0	$1,279	$7,673	$6
Site Facilities	$2,203	$0	$2,311	$0	$4,514	$903	$0	$1,083	$6,500	$5
Subtotal	$2,203	$3,010	$20,495	$0	$25,708	$5,142	$0	$6,170	$37,020	$27
14	BUILDINGS & STRUCTURES									
Combustion Turbine Area	$0	$497	$262	$0	$759	$152	$0	$137	$1,048	$1
Open	$0	$0	$0	$0	$0	$0	$0	$0	$0	$0
Steam Turbine Building	$0	$4,631	$6,160	$0	$10,790	$2,158	$0	$1,942	$14,891	$11
Administration Building	$0	$457	$310	$0	$767	$153	$0	$138	$1,058	$1
Circulation Water Pumphouse	$0	$80	$40	$0	$120	$24	$0	$22	$165	$0
Water Treatment Buildings	$0	$418	$381	$0	$799	$160	$0	$144	$1,103	$1
Machine Shop	$0	$688	$440	$0	$1,128	$226	$0	$203	$1,557	$1
Warehouse	$0	$528	$319	$0	$848	$170	$0	$153	$1,170	$1
Other Buildings & Structures	$0	$366	$266	$0	$631	$126	$0	$114	$871	$1
Waste Treating Building & Structures	$0	$891	$1,589	$0	$2,481	$496	$0	$447	$3,424	$2
Subtotal	$0	$8,556	$9,766	$0	$18,323	$3,665	$0	$3,298	$25,286	$18
Total	**$507,317**	**$38,450**	**$151,617**	**$0**	**$697,384**	**$139,477**	**$0**	**$131,669**	**$968,530**	**$702**

www.netl.doe.gov
Albany, OR • Anchorage, AK • Morgantown, WV • Pittsburgh, PA • Sugar Land, TX
(800) 553-7681

